PhD Program in Translational and Molecular Medicine

DIMET

(XXIX cycle, academic year 2015/2016)

University of Milano-Bicocca
School of Medicine and Faculty of Science

BAFF RECEPTOR (BAFF-R) CAR-REDIRECTED T CELLS: A NOVEL TOOL TO TREAT HIGH RISK B-CELL ACUTE LYMPHOBLASTIC LEUKEMIA (B-ALL)

Dr. Nice Turazzi

Matr. No. 744699

TABLE of CONTENTS

Chapter 1

General Introduction

1. ACUTE LYMPHOBLASTIC LEUKEMIA

The term acute lymphoblastic leukemia (ALL) comprises heterogeneous malignant disorders in which lymphoblasts, originating from B- (B cell precursor, BCP-ALL) or T- (T-ALL) progenitors, aberrantly proliferate within the Bone Marrow (BM), peripheral blood and other organs [1].

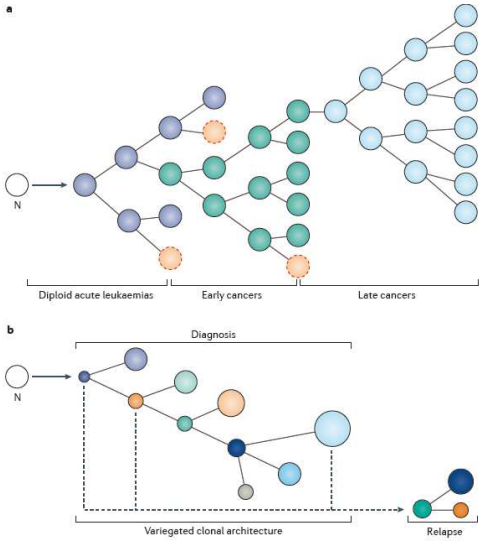

Figure 1. The clonal evolution model. a. Nowel's clonal evolution model proposed in the paper published in 1976. He suggested the presence of a linear succession with sequential round of selection in ALL. **b**. More recently, clonal studies on ALL has revealed more branched and complex architecture where relapse could potentially emerge from every subclone [2].

In the 1950's the accepted idea was that cancers frequently origin from a single transformed cell. Nowell re-elaborated this idea in the 1970's postulating his *clonal evolution model* in which the single cell of origin produces a progeny that acquires genetic variability and instability due to selective pressures (tissue ecosystems, immune

system and therapy) [3,4]. These pressures lead to a sequential selection of more aggressive or drug-resistant sub-clones. Therefore, Nowell's model suggests that disease progression comprises the sub-clonal selection of clones with higher fitness advantages [5].

Leukemias are neoplasms that, for their intrinsic characteristics, lend themselves to multiplexed single-cell analysis and single-cell whole-genome sequencing approaches [6,7]. Thanks to these recently developed techniques, it becomes possible to backtrack leukemia evolution from relapse to sub-clones that were present in diagnostic sample, providing a detailed timing sequence and genetic architecture of the disease (Figure 2). However, pre-leukemic and earliest events may be lost during leukemia progression [8]. The PCR-based analysis of neonatal blood spots or stored cord blood of monozygotic monochorionic twins with concordant leukemia supplies a unique occasion to comprehend the cancer history and to identify possible *in utero* pre-leukemic lesions that could predispose to disease onset. Indeed, in monozygotic twins with monochorionic placenta, genetic lesions (e.g. ETV6-RUNX1) originating during fetal development of one twin are shared via vascular anastomoses to the second twin, but post-natal events are independent. Consequently, studying twins with concordant ALL helped researchers to identify pre-leukemic events and to distinguish between *in utero* and post-natal mutational events uncovering, in this way, the timeline of mutations that contributed to clonal evolution of the disease [9,10]. Also in other hematological disorder, such as the Acute Myeloid

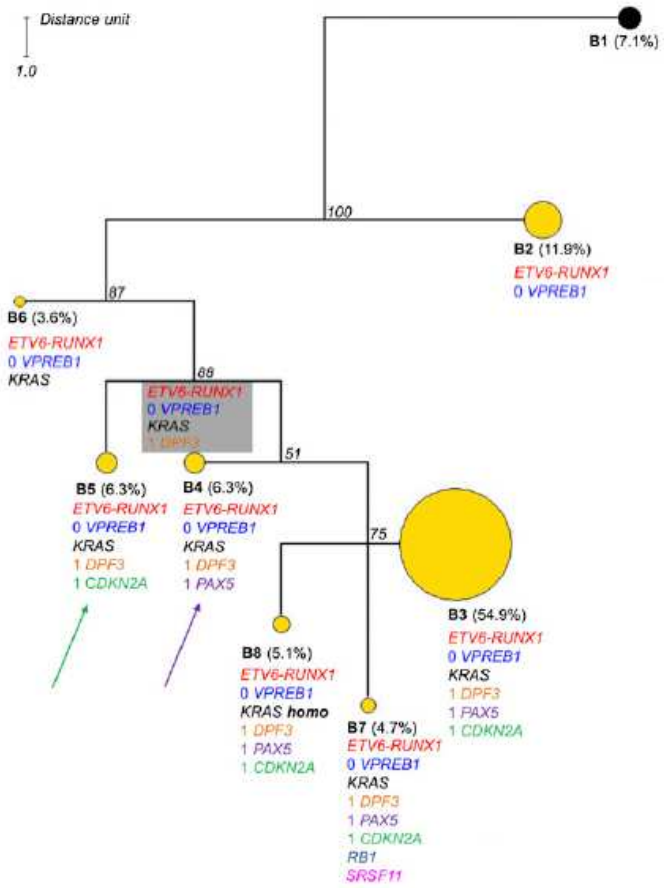

Figure 2. Example of multiplexed single-cell analysis applied to a B-ALL patient. The clone of interest was indicated by a yellow circle. The size of circle reflected the frequency of the clone within sample analyzed. Adapted from Potter *et al.* 2013 [6].

Leukemia (AML), pre-leukemic clones and their precursor lesions have been identified [11]. Furthermore, it has been demonstrated that these ancestral lesions in ALL and AML, despite being rare populations, survive to chemotherapy providing a cellular resource which may drive later relapses [12,13].

The rare population hypothesized to be responsible of the relapse is called Leukemia Stem Cells (LSCs). Since LSCs are derived from stem or progenitor cell undergoing mutation, they share many characteristics with normal Hematopoietic Stem Cells (HSCs), including quiescence, multipotency and self-renewal [14]. Quiescence of these cells is the main reason of ALL multidrug resistance, being chemotherapeutic drugs active on proliferating cells. Another mechanism responsible of chemoresistance is represented by the presence of pumps on LSC's membrane which efficiently efflux drugs form cells protecting them from chemotherapeutic agents [15]. Bonnet and Dick in 1997 elegantly demonstrated that, in the AML context, only LSCs within the CD34+CD38- compartment are responsible of leukemia support [16]. On the contrary, in patients with ALL LSCs with different genetical and functional characteristics have been reported. Currently, in the ALL context, the debate about LSC's features is still open. [4,17]

Like healthy HSCs, LSCs are thoughts to reside in a leukemic niche [18]. Here, thanks to the interactions with BM niche components, LSCs are protected from chemotherapy, survive and acquire drug-resistance [19]. LSCs in turn can induce reversible changes in the BM microenvironment, promoting the survival of leukemic cells and the suppression of normal hematopoiesis [20,21].

2. B-CELL PRECURSOR ALL

2.1. EPIDEMIOLOGY

BCP-ALL is the most common type of leukemia in children with an incidence of 3-4 cases per 100,000 each year. Otherwise, the annual incidence is approximately 1 case per 100,000 in adults. Outcomes for patients with BCP-ALL have greatly improved over the past decades, reaching an overall survival rate of 85% for children and 45% for adults [1].

2.2. RISK FACTORS

The onset of BCP-ALL is believed to be multi-factorial, comprehending genetic predisposition and exogenous factors. The exogenous factors, such as genotoxic exposures, infections, diet and exercise, modifies the tissue microenvironment (hormones levels, inflammatory response, metabolism) and, directly, the cancer cells. Very few data are available about risk factors for ALL.

As evidenced by the consequences observed in 1945 in Japan after the atomic bomb [22], ionising radiation is a well established cause of ALL, as well as infections and specific genetic syndromes.

Infections remain, nowadays, the strongest candidate as risk factor for ALL [23]. The hypothesis, supported by epidemiological data, proposes that ALL results from an abnormal or dysregulated immune response to a common infection (viral or bacterial) in a subject with a genetic susceptibility [23,24].

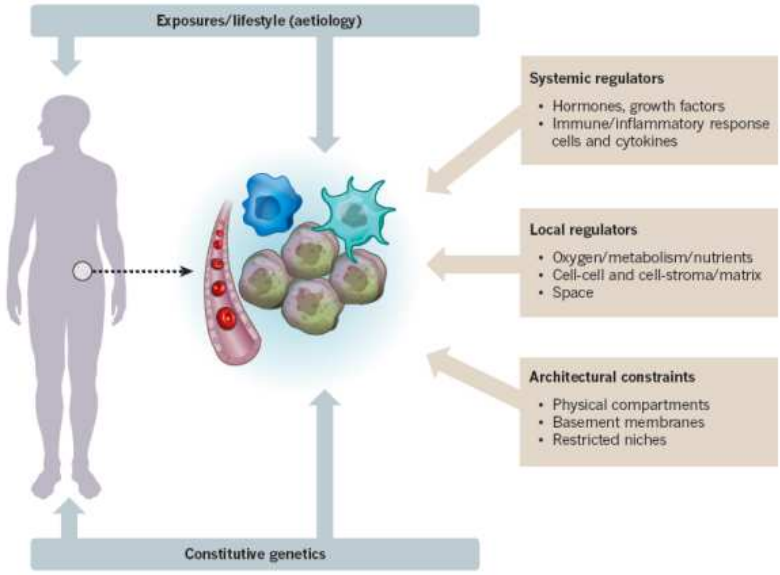

Figure 3. Tissue Ecosystem [5].

Infants born with Down Syndrome have ~20-fold higher risk to develop ALL, suggesting the involvement of genes on chromosome 21 in predisposition to leukemic transformation [25]. The identification of a "Down Syndrome Critical Region" which includes candidate genes such as RUNX1, ERG and ETS2 has been derived from the analysis of patients with partial trisomy 21 [26]. Other genetic conditions, including neurofibromatosis, Shwachman syndrome and Klinefelter syndrome, are associated with an increased risk of developing ALL [27].

2.3. PATHOBIOLOGY AND GENETIC ALTERATIONS

Clinically, at diagnosis individuals affected by ALL present anemia, bleeding, fever with infections, bone pain, headache, detectable

blast-cells (usually >90% within the BM) and less than 10% have central nervous system (CNS) involvement. Symptoms reported by patients at the onset are mainly due to deleterious effects of the expanding blast population on bone marrow and on secondary infiltrated organs [28,29].

For correct diagnosis of ALL, the morphological identification of blasts, the determination of lineage commitment and stage of differentiation by immunophenotype are necessary.

Recurrent chromosomal abnormalities represent a hallmark of ALL. For this reason, cytogenetic analysis plays a fundamental role in the initial work-up.

Numerical abnormalities such as hyperdiploidy (presence of more than 46 chromosome) and hypodiploidy are common in B-ALL patients. Generally, hyperdiploidy is associated with good prognosis particularly in co-presence with trisomies of chromosomes 4, 10 and 17. On the other hand hypodiploidy is associated with poor outcome [30,31].

The most frequent cytogenetic abnormality in childhood B-ALL (15-25% of ALL patients) is the t(12;21)(p13;q22), encoding ETV6-RUNX1 (TEL-AML1). The translocation generates the TEL-AML1 fusion gene where the helix-loop-helix domain of TEL is fused with the DNA-binding and transactivation domain of AML1. Both genes are essential in normal hematopoiesis [32]. The presence of this translocation in neonatal blood spots has been demonstrated, providing evidence that most TEL-AML1 fusions originate *in utero* and represent the initial somatic event in this type of leukemia [31].

However, this initial event is not sufficient for a full leukemic transformation. This hypothesis is supported by the observation that 1% of newborns possess the fusion gene but only a fraction of them will develop ALL [33]. Patients with TEL-AML1 expression demonstrate a favorable outcome with event-free survival of 90% [34].

The t(1;19)(q23;p13) translocation fuses the transactivation domain of E2A transcription factor on chromosome 19, which have a role in lymphocyte development, to the homeobox gene PBX1 on chromosome 1. The formation of chimeric transcription factor E2A-PBX1 blocks the expression of HOX genes and of the E2A targets. Patients with this translocation show favourable prognosis [35].

The most common translocation in adult B-ALL is t(9;22)(q34;q11) which represents the 2-4% of childhood ALL and generates the Philadelphia (Ph) chromosome, encoding the BCR-ABL1 fusion protein, a tyrosine kinase constitutively activated [36]. Recently, a new subgroup has been identified and named Ph-like, which exhibits a gene expression profile similar to Ph+ ALL with aberrant activation of intracellular kinase, but are BCR-ABL1 negative. Ph-like subgroup showed several types of kinase alteration, including *Ikaros* (IKZF1), CRLF2 and JAK2. Both Ph+ ALL and Ph-like ALL are associated with poor prognosis [37].

In patients younger than 1 year, 90% harbor rearrangements of mixed-lineage leukemia (MLL) gene on chromosome 11 such as t(4;11), and t(11;19) with an event-free survival around 50%. All translocations generate a fusion protein which posses the NH2-terminus of MLL fused to COOH-terminus of the fusion partner

(actually more than 70 MLL fusion genes have been reported) [38,39]. This gene is even involved in a rare subgroup of acute leukemia which expresses simultaneously the myeloid and lymphoid markers named mixed phenotype leukemia [40]. Rearrangements of MLL gene have been found also in AML patients with ages between 30 and 50 years, but were more commonly seen in AML cases originated from previous exposure to chemotherapy (named therapy-related AML) [41]. Another novel subtype of ALL have cytokine receptor-like factor 2 (CRLF2) rearrangement at the pseudo-autosomal region 1 (PAR1) of the sex chromosomes. The rearrangement leads to over-expression of CRLF2 and is commonly associated with JAK1/2 mutation resulting in an activation of JAK-STAT signaling pathway. CRLF2 rearrangement occurs in 5% of B-ALL and approximately in 50% of B-ALL associated with Down syndrome and is often associated with a gene expression profile typical of Ph-like subgroup [42,43].

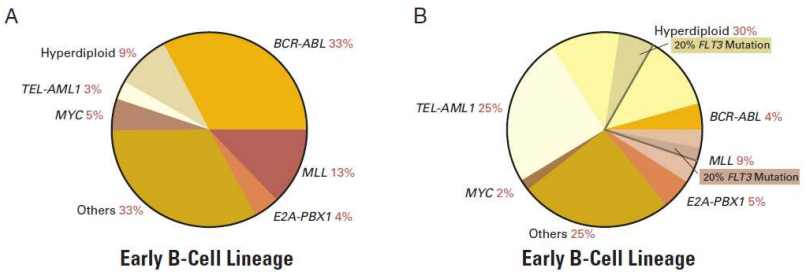

Figure 4. Frequency of chromosomal abnormalities found in B-ALL respectively for adults (A) and children (B). Modified from Armstrong *et al.* 2005 [30].

2.4. CLASSIFICATION

Prior to 2008, the used classification systems were proposed by the Frech-American-British (FAB) Cooperative Working Group and the European Group for Immunological Characterization of Leukemia (EGIL). FAB system classified subgroups of ALL on the basis of morphology, the major criterion for primary diagnosis, as:

ALL-L1 characterized by small cells, no nucleoli with scanty cytoplasm, and it occurs in approximately 25-30% of ALL cases;

ALL-L2 characterized by large heterogeneous cells, presence of nucleoli, irregular nuclear shape and it occurs most frequently in adult (65-70%);

ALL-L3 constitutes only 5-10%, generally with large and homogeneous blast, prominent nucleolus and vacuolated cytoplasm [44,45].

Guidelines given by EGIL have provided a more precise characterization of ALL subgroups as reported in Table 1 [46].

B Lineage
Pro-B
CD19+, CD22+, CD79a+
Pre-B
CD19+, CD22+, CD79a+, CD10+, cIg
Mature
CD10+, sIg, CD19+, CD22+, CD79a+, CD20 (+/-)

Table 1. Immunological classification of B-ALL proposed by EGIL group. Adapted from Al Ustwani et al. 2015 [47].

Nowadays, the classification of neoplasms of the hematopoietic and lymphoid tissues published in 2001 and updated in 2008 by World Health Organization, in collaboration with the Society for Hematopathology and the European Association of Haematopathology, represents a landmark for the diagnosis of these tumors.

The major principle of the classification is the recognition of distinct diseases, by integrating cell type and immunophenotype with molecular, genetic, and clinical features. In this way, the different disease entities are better classified and stratified for an adequate therapeutic treatment [48].

B lymphoblastic leukemia/lymphoma
B lymphoblastic leukemia/lymphoma, NOS
B lymphoblastic leukemia/lymphoma with recurrent genetic abnormalities
B lymphoblastic leukemia/lymphoma with t(9;22)(q34;q11.2);*BCR-ABL 1*
B lymphoblastic leukemia/lymphoma with t(v;11q23);*MLL* rearranged
B lymphoblastic leukemia/lymphoma with t(12;21)(p13;q22) *TEL-AML1* (*ETV6-RUNX1*)
B lymphoblastic leukemia/lymphoma with hyperdiploidy
B lymphoblastic leukemia/lymphoma with hypodiploidy
B lymphoblastic leukemia/lymphoma with t(5;14)(q31;q32) *IL3-IGH*
B lymphoblastic leukemia/lymphoma with t(1;19)(q23;p13.3);*TCF3-PBX1*

Table 2. Who Classification modified from Vardiman *et al.* 2009 [48].

2.5. THERAPY

The standard treatment for ALL consists of 4 phases: remission/induction phase, consolidation/intensification phase, re-induction phase and continuation/maintenance therapy to eliminate residual disease.

The remission/induction therapy has the aim to eradicate the initial leukemic cell burden and to restore normal hemopoiesis. The chemotherapy agents commonly used during this phase include a glucocorticoid, prednisone or dexamethasone, vincristine, and L-asparaginase. Patients are treated also with anthracycline (doxorubicin, daunorubicin) during this phase.

After the restoration of normal haemopoiesis and body function, patients receive consolidation/intensification therapy in order to eradicate residual drug-resistant leukemic cells and reduce the risk of relapse. In this phase, commonly used agents are high-dose methotrexate, frequently accompanied with mercaptopurine, vincristine and asparaginase.

Re-induction phase intensifies the therapeutic effect of the previous treatment. Patients are treated with the same drugs used in induction phase and are administered 5-7 months after the diagnosis increasing the healing percentage.

Prolonged maintenance treatment is necessary to prevent relapse by suppressing the re-emergence of a drug-resistant clone by continuously reducing the pool of residual leukemic cells. Therapy consists of daily mercaptopurine and weekly methotrexate with or without vincristine and dexamethasone. During maintenance treatment, drugs doses are adjusted according to absolute leukocyte or neutrophil count and platelet count [49,50].

An important phase of B-ALL standard therapy is the control of CNS involvement. To effectively control disease on this site, prophylactic cranial irradiation (12-18Gy) was administered. More recently, this

prophylactic treatment has been replaced by methotrexate for all newly diagnosed patients. Cranial irradiation is nowadays used only in patients with absolute leukocyte count ≥100,000/µL at the onset. The CNS prophylaxis has reduced the neurotoxicity, neurocognitive deficits, secondary malignancies and mortality [51].

2.6. RISK ASSIGNMENT

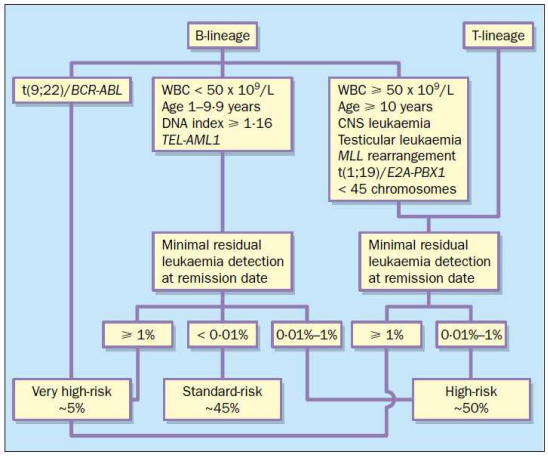

Figure 5. Risk-classification system based on age and leukocyte count proposed by St. Jude Children Research Hospital. Estimated proportions of patients classified to each of the three risk groups are shown in their respective boxes [52].

An accurate assessment of relapse's risk is fundamental to direct patients to a risk-adapted therapy, ensuring that very intensive treatment is given only to high risk cases and spearing patients at lower risk from excessive toxic effects. Risk factors for relapse has been initially identified in the 1980s and included age and leukocyte count at diagnosis and response to therapy [53]. Nowadays, with

increasing information about disease biology, commonly used factors in risk stratification can be grouped into three categories: patient's clinical features, disease's biological factors and early response to induction therapy.

Clinical Factors: age at diagnosis has a strong prognostic impact. Pui *et al* has reported a 5-year event-free survival of 44% for infants younger than 12 months, 88% for children aged 1-9 years, 73% for adolescents aged 10-15 years and 69% form patients older than 15 years. In adult patients, the outcome worsens with increasing age [54]. It remains an open question whether adolescents have to be treated with pediatric or adult regimens. In this regards, some clinical trials demonstrated a superior outcome of adolescents and young adults treated with pediatric regimens instead of adult protocols [55,56].

Leukocyte count at diagnosis represents an important prognostic variable. Indeed, an high leukocyte count confers a poor outcome [57]. Patients with a severe hyperleucocytosis (>400x10^9/L) are at high risk for complications such as CNS hemorrhage [58].

The worse outcome observed in black and Hispanic patients has been linked to socioeconomic factors and to differences in genomic alterations. Over-expression of somatic CRLF2 rearrangements was reported in children with a Hispanic genetic background. Black people have an higher incidence of t(1;19) which is well known to be associated with dismal prognosis [59].

Biological factors: Genetic abnormalities provide essential prognostic information. Patients with hyperdiploidy (>50 chromosomes), trisomy 4, 10, 17 and TEL-AML1 fusion have the most favourable

outcome, whereas those with the BCR-ABL fusion, hypodiploidy or MLL rearrangements have a dismal prognosis. In adults, the high frequency of unfavorable genetic abnormalities partially explains their inferior overall survival [47,54].

Response to treatment: an important prognostic factor which predicts the risk of relapse is represented by the degree of reduction of leukemic bulk population after induction therapy. Patients who fail to achieve clinical remission by the accepted morphological standard (with 1% or more leukemic cells at the end of induction therapy) exhibit a poor prognosis, whereas people who achieve remission (<0,01% leukemic cells) have an excellent outcome [60].

In AIEOP-BFM 2000 study prednisone response measured at 8 and 15 days after induction therapy has been reported as critical factor in risk assignment. In this protocol, minimal residual disease (MRD) measurements were carried out at the end of induction (day 33) and the end of consolidation (day 78) phases. Patients who had MRD levels $>10^{-3}$ at day 78, as well as those with a prednisone poor response, induction failure, or with t(4;11) or t(9:22) chromosomal translocations, were allocated to the high-risk group, receiving intensified blocks of post-consolidation therapy. By MRD risk assignment alone, the Event Free Survival (EFS) at 5 years was 91% in the standard-risk group compared with 77% in the intermediate-risk group and 50% in the high-risk group [61].

2.7. HEMATOPIETIC STEM CELLS TRANSPLANT (HSCT)

Historically, HSCT has been developed and used with the purpose to provide an anti-tumor immune response. HSCT is considered the first developed strategy of Adoptive Cell Therapy (ACT) which has revolutionized the treatment of leukemias and lymphomas. HSCT can be distinguished, according to the relationship between patient and donor, in autologous and allogeneic. In the autologous setting, hematopoietic stem cells are harvested from patient and reinfused after a myeloablative treatment. On the contrary, the infused stem cells derived from an HLA-matched healthy donor in the allogenic transplant. The demonstration of the ability of the immune system in fighting tumor cells derives from the observation of the Graft Versus Leukemia effect (GVL). The existence of an anti-leukemic activity exerted by donor cells was first suggested by Barnes and collaborators in 1956 who reported the elimination of leukemia in transplanted mice [62]. The same effect was then demonstrated in leukemic patients by the Seattle group in 1979 which described a significative reduction of relapses in the transplanted group [63]. The most important side effect observed after allogenic HSCT is the elevated treatment-related mortality due to the development of Graft versus Host Disease (GvHD) or other complications. GvHD occurs in 40% of patients undergoing allogenic HSCT and it is a multisystem syndrome with predominant involvement of skin, upper gastrointestinal tract, oral mucosa, liver, bones and tendons [64]. Despite this important side effect, HSCT remains the treatment of

choice for patients with very high-risk ALL or persistent disease. At present, optimized HSCT protocols have allowed the reduction of relapse-related mortality, therapy-related toxicity and infections. GvHD could be prevented by T-cell depletion of the donor graft. However, this method led to a higher rates of relapses, being T cells the mainly responsible of the GvL effect [65].

2.8. RELAPSED LEUKEMIA

In the last few years remarkable advances have been achieved in the treatment of ALL. Thanks to optimal use of anti-leukemic agents and a stringent application of prognostic factors for risk-directed therapy, current treatment strategy results in a long-term remission for nearly 80% of children with ALL. Despite that, 20% of patient relapse, especially those with high-risk disease features, and resistant form of the disease still represents a leading cause of cancer-related mortality. Cure rate after relapse is approximately 25% to 40% [66]. Bone marrow is the most frequent site of relapse, although the CNS, testes and other extramedullary localization may be interested. Isolated relapse in extramedullary localization (CNS or testis) show a better prognosis than relapses isolated to bone marrow, while a mixed relapse localization, has intermediate prognosis [67].

Clearly, novel strategies are needed to improve the outcome of patients with relapsed or refractory ALL. The remarkable advantages in understanding molecular pathway underlying the pathogenesis of ALL should lead to personalized treatment with targeted agents,

resulting in more effective and less toxic treatments for patients. Such drugs are considered “smart” since they selectively target cancer signaling pathways or expression of genes specifically over-expressed in cancerous and not healthy cells. Examples are the use of imatinib mesylate and second-generation ABL kinase inhibitors, which act as signal transduction inhibitors, target enzymes over-expressed by malignant tumors involved in uncontrolled cell proliferation, inhibition of apoptosis, and cell adhesion [68,69]. Treatment with tyrosine kinase inhibitors (TKI) resulted in improvement of 3- year event-free survival of pediatric patients with Ph+ ALL, from 35% of the historical control to 80% with no increased toxicity [70]. Other important molecules are represented by FLT3 inhibitor, DNA methyltransferase inhibitor, γ-secretase inhibitor, epigenetic drugs and novel agent in early phase of clinical testing [71–73]. Besides this, major resources are now applied to find novel HSCT strategies, more potent for improving GvL, such as haplo-identical transplants, possibly limiting the incidence of GvHD and the toxicities related to transplant itself.

3. IMMUNOTHERAPEUTIC STRATEGIES FOR B-ALL TREATMENT

Cancer immunotherapy is based on strategies which improve the anti-cancer immune response through either promoting components of the immune system that mediate an effective immune response or by suppressing inhibitory factors. There are two types of immunotherapy: active and passive.

3.1. ACTIVE IMMUNOTHERAPY

Active immunotherapy represents a strategy aimed at restoring patient's immune system toward tumor cells with tumor-specific vaccines. Vaccines were designed to generate a response against a specific antigen through the formation of an anti-tumor immunological memory able to control and eliminate the disease.

Different approaches have been developed in attempt to stimulate the immune response of T cells, including vaccines composed of tumor-specific peptides, dendritic cells (DCs) pulsed *in vitro* with peptides, and whole tumor cells.

The major disadvantage of active immunotherapy is that the presence of patient's residual immunocompetence is necessary. Unfortunately, this subjects are commonly immunocompromised by many cycles of immunosuppressive therapies.

3.2. PASSIVE IMMUNOTHERAPY

Passive immunotherapy does not rely on the patient's immune system but it is based on the transfer of immune effector molecules, such as monoclonal antibodies, or immune cells generated *ex vivo* (ACT) which are able to exert a powerful anti-tumor action bypassing patient's immunocompromised state.

3.2.1. Monoclonal Antibodies (mAbs)

The use of mAbs for B-ALL treatment, especially in combination with chemotherapy, is a highly promising approach. MAbs acts through numerous mechanisms: antibody-dependent-cellular cytotoxicity (ADCC), stimulation of complement-dependent cytotoxicity (CDC), inhibition of cellular proliferation signals or direct induction of apoptosis. To potentiate their anti-tumor responses, antibodies could be conjugated with potent cytotoxins in case the target is internalized following the binding. Early generations of mAbs were of murine origin or chimeric. Recent generations are humanized or fully human with the aim of decreasing their antigenicity [74,75].

The expression of target antigen on at least 20% of leukemic blasts is generally required as a prerequisite for an effective mAbs immunotherapeutic approach [76]. To date, several targets have been investigated in B-ALL including CD20, CD22 and CD19. Initial success has been achieved with the anti-CD20 mAb rituximab which is currently part of the standard of care for lymphomas [77,78]. Rituximab is also used in combination with chemotherapy in aggressive

lymphomas, CLL and CD20-positive ALL [79,80]. The second generation fully humanized anti-CD20 mAb ofatumumab is more potent than rituximab in promoting CDC *in vitro*. Furthermore, it has been recently demonstrated the safety and efficacy of ofatumumab in patients with *de novo* ALL with an encouraging 1-year overall survival of 95% [81,82]. Inotuzumab ozogamicin is an humanized conjugated antibody directed against CD22. The antibody is linked to calicheamicin, a potent cytotoxic agent that, once internalized, causes double-stranded DNA breaks, inducing apoptosis of malignant cells [83]. In a recent study at MD Anderson Cancer Center, 49 refractory/relapsed ALL patients were treated with Inotuzumab ozogamicin and an overall response of 57% has been observed [84].

The last frontier in humoral immunotherapy are bispecific T-cell engagers mAbs (BiTEs). BiTEs are fusion proteins composed of two single chain antibodies able to recruit patient's cytotoxic T cells and to induce a transient synapse between T cells and tumor cells. Therefore, cytotoxic T cells became activated and induce tumor cell death via a perforin and granzyme system. The ***B lin***eage-specific ***a***nti-***tu***mor ***mo***use ***m***onoclonal ***a***nti***b***ody Blinatumomab is a CD3/CD19 bispecific antibody [85]. Blinatumomab is a 55-kDa fusion protein composed of CD19-specific variable domains joined to CD3-specific variable domains with a short non immunogenic linker sequence [86]. Based on the short half-life, blinatumomab requires continuous intravenous infusion. In patients with relapsed/refractory B-ALL blinatumomab showed an overall response rate of 69% with a

median overall survival of 9.8 months (the follow-up was of 12.1 months) [87].

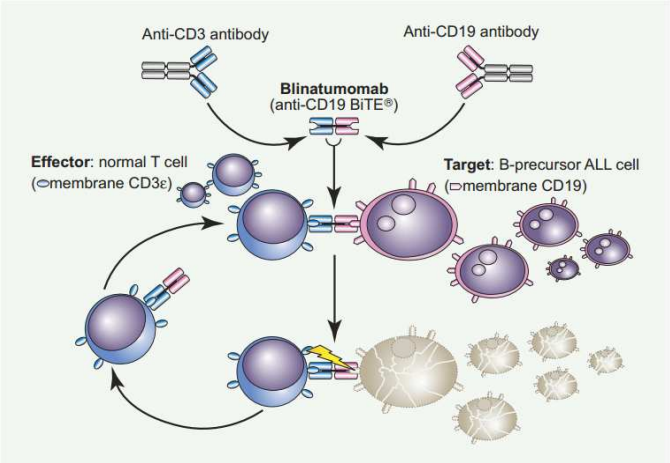

Figure 6. BiTE mechanism. Blinatumomab mediate the interaction between normal CD3+ T-cells and CD19+ ALL cells, followed by activation of T-cell cytotoxicity exerted towards CD19+ blast T-cells [88].

3.2.2. Adoptive Cell Therapy (ACT)

ACT consists in isolation and subsequent infusion into patients of *ex vivo* expanded autologous or allogenic cells [89].

The clinical problems of HSCT due to establishment of severe GvHD could be circumvented by temporally separating T cell depleting graft from the subsequent donor lymphocyte infusion (DLI). The first evidence of the potency of the DLI as therapeutic tools came from the observation that T cells infusion after HSCT in chronic myeloid leukemia (CML) patients could be used to generate an immune

response against tumor with the achievement of complete molecular remission [90]. The best response rate of DLI has been observed in the context of myeloid hematological diseases, followed by lymphomas, multiple myeloma, with limited efficacy in ALL. Clinical response is most effective when tumor burden is reduced through chemotherapy induction and/or when lymphodepletion is provided, to help the expansion of donor T cells after being infused into the recipient [91]. Complications described in patients that undergoes DLI comprises GvHD in about 50-60% of patients and aplasia in 20-40% of patients with an overall mortality of about 5% caused by infections and bleeding [92,93].

Tumor Infiltrating Lymphocytes (TIL) ACT strategy consists in the collection of tumor-specific T cells from fresh biopsies, *ex vivo* expansion using high doses of interleukin (IL)-2 and subsequent reinfusion into the patient [94]. Thanks to the great feasibility in generating TIL in melanoma patients compared to other tumor types, this strategy has been applied almost exclusively in this context by Rosenberg and colleagues reporting 60% of response rate [95]. However, the isolation and expansion of tumor specific T cells is time and labor intensive, moreover the lack of T cells with high affinity for tumor antigens, due to T-cell tolerance and tumor immune-escape mechanisms, hamper the activity and persistence of these patient derived T cells.

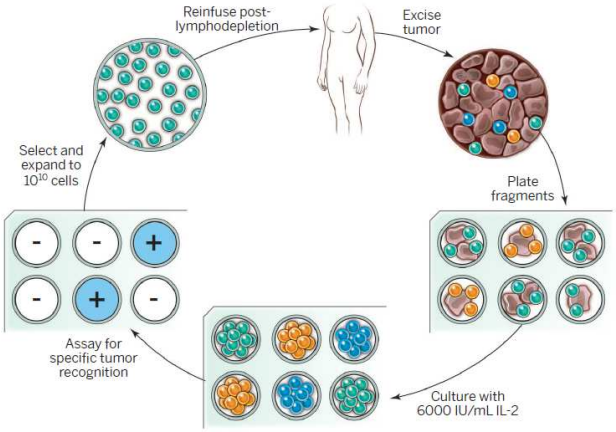

Figure 7. Adoptive cell transfer using autologous tumor specific TILs. The biopsy is digested to obtain a single-cell suspension. Every cell is grown singularly in IL-2. After 2-3 weeks the single cell generate a pure culture that will be tested for reactivity towards tumor cells. The selected cultures is then expanded and reinfused into patient [95].

Significant advances in gene transfer technology have been obtained in the last decade offering new tools to exploit T cells. T lymphocytes can be genetically modified to generate a high number of engineered T cells able to react against tumor cells resulting in a significant reduction of GVHD rates without affecting GVL effect. Actually, the most promising approaches in this field are T-cells engineered to express artificial T-cell receptors (TCRs) or Chimeric Antigen Receptors (CARs).

4. CYTOKINE-INDUCED KILLER (CIK) CELLS

The main obstacle of ACT is the clinical applicability represented by the difficulty to obtain an adequate number of effector cells with a selective and powerful anti-tumor activity *in vivo*. In the early 1990's Lu and Negrin have optimized an innovative protocol to generate *ex vivo* a population of effector cells with high cytotoxic activity, named CIK [96]. CIK cells, also known as natural killer-like T-cells, represent an extremely heterogeneous population of cytotoxic T cells enriched in CD3+CD56+ cells and composed by a large amount of T-CD8+ and a share of T-CD4+. CIK cells are present in very low percentage in the peripheral blood (1-5% of mononucleated cells) and can be efficiently generated *in vitro* starting from healthy donor peripheral blood mononuclear cells (PBMCs). These cells are able to expand up to 1000 times in 14-21 days by sequentially stimulating with IFN-γ, which drives the expansion of CD56-positive T-cells, the anti-CD3 mAb OKT-3 triggering the T-cell receptor (TCR) and IL-2 [97]. At the end of the differentiation, the obtained population is extremely heterogeneous and enriched in CD3+/CD56+ cells with the highest cytotoxic potential. Most of these cells also express the α and β chains of the TCR, CD8, CD45, CD95, CD161 whereas a minor fraction retains CD4 expression [98]. Moreover, in addition to the TCR-dependent activity, CIK cells are able to mediate *in vitro* a MHC-unrestricted cytotoxicity towards a variety of tumor targets and do not require a previous target contact or the exogenous administration of IL-2 to become activated [99,100]. Despite the

molecular mechanism which mediates tumor killing is currently not completely understood, previous studies indicate that it is principally exerted through the activation of both the TCR/CD3 signaling and the MHC-unrestricted NKG2D (Natural Killer Group 2 member D) receptor. Upon stimulation, CIK cells respond with granule exocytosis, cytokine secretion, and cytotoxicity. NKG2D also triggers IL-2 activated cells, inducing calcium flux, cytokine release and cytotoxicity [101].

Another aspect that makes these cells so interesting is their ability to migrate to the tumor site where they exert GVL without affecting healthy tissues and causing minimal GVHD [102]. This capacity to dissociate the immune response against the tumor from the one against the host can be attributed to a reduced expression of molecules involved in homing markers and chemokine receptors such as α4β7, CCr9, E-selectin, CXCR3 and CCR5.

Furthermore, the reduced secretion of pro-inflammatory cytokines in the GVHD site and the production of large amounts of IFN-γ, which seems to have a protective role against GvHD in this context, contribute to the reported feature [103]. Moreover, Mase *et al.* demonstrated, concurrently to the activity on tumor cells, the elimination of dendritic cells by CIK cells in the host, which represent the most important cells in initiating GvHD reaction [104].

Normally, circulating CIK cells are responsible, *in vivo*, of various immune responses, including control of microbial infections, tumor immune surveillance, induction of tolerance and suppression of GvHD after HSCT and are widely distributed throughout the body, in

bone marrow, lymph nodes, lungs, liver and spleen. Their peculiar distribution within the most frequently infiltrated organs which is preserved in cells expanded *in vitro*, makes CIK cells particularly attractive for therapy of hematologic malignancies. Indeed, CIK cells express specific receptors for adhesion molecules such as CD49d and CD11a, which are present on bone marrow and endothelium, and CXCL12, CCL19, CCL20 and CCL21, which allow homing to the bone marrow and to extra-lymphoid tissues [105].

In order to collect and evaluate data obtained in clinical trials using CIK cells, an International Registry on CIK Cells (IRCC) has been created (http://www.cik-info.org/index.php?kat=ircc---international-registry-on-cik-cells). Actually, the database gather 45 clinical trials testing 22 different kind of tumors and include a number of 2729 total patients enrolled. Current data indicate absence of severe side effects and a prolonged overall survival and progression free survival, after treatment with CIK cells, with a general improvement in the quality of life [106]. Among these trials, our group also participated with a phase I study in which allogenic CIK cells have been infused into 11 patients with relapsed hematological malignancies, obtaining complete remission in 3 patients and the stabilization of the disease in 1 patient [107]. Data obtained from phase II study has been presented at the ASH congress this year. Here they demonstrate the feasibility of CIK cells administration in patients relapsed after HSCT observing minimal GvHD. Among the seventy-four patients enrolled 24 died, 18 showed no response, 1 had stable disease, 21 obtained complete remission while 6 had partial remission. In 4 patients the

clinical response could not be evaluated. GvHD was observed only in 11 patients [108]. Overall, CIK cell immunotherapy rises as an attractive approach in cancer therapy thanks to their great manageability, their ability to expand *ex vivo* in few days and to reach tumor infiltrating sites.

Table 3. Summary of clinical studies applying CIK cells (A.O. Papa Giovanni XXIII)

Reference	N° of patients	Disease	% CR	% PR	% NR	% DP	% SD	Median follow-up	Toxicity
Introna (2007)	11	AML (n=4), HD (n=3), ALL (n=1), CMML (n=1), MDS (n=2)	27%	/	54%	9%	9%	1 year	aGVHD (n=2), cGVHD (n=2)
Lussana (2016)*	74	AML (n=41), HD (n=3), ALL (n=20), NHL (n=2), MM (n=4), MPN (n=4)	28%	8%	24%	32%	1%	3 years	aGVHD (n=11), cGVHD (n=8)

Abbreviations: CR, complete remission; PR, partial remission; NR, non responder; DP, disease progression; SD, stable disease; AML, acute myeloid leukemia; HD, Hodgkin's disease; ALL, acute lymphoblastic leukemia; CMML, chronic myelomonocitic leukemia; MDS, myelodisplastic syndrome; NHL, non-Hodgkin lymphoma; MM, multiple myeloma; MPN, myeloproliferative neoplasm; aGVHD, acute graft versus host disease; cGVHD, chronic graft versus host disease. **ASH meeting 2016, abstract number 1160.*

5. CHIMERIC ANTIGEN RECEPTORS (CARs)

CARs are artificial receptors able to redirect T-cell specificity and killing/effector activity towards virtually any tumor-associated antigen (TAA) of interest in a non MHC-restricted manner [109]. The CAR molecule combines an antigen-binding domain and one or more intracellular signaling domains. The extracellular domain most often consists of variable chains obtained from a specific monoclonal antibody. Variable chains, light (VL) and heavy (VH) are joined by a flexible linker peptide (usually consisting of a serine/glycine rich motif) to form a single chain Fragment variable (scFv). This structure can be directly connected to the intracellular transduction domain or separated by a spacer region which provides greater flexibility and

different orientations of the binding domain. Examples of spacer regions are the constant heavy chain domains CH2-CH3 derived from the Fc portion of IgG, and the Ig-like domains derived from extracellular regions of CD8 or CD4 [110,111].

The intracellular transduction domain is responsible for transmitting the signal within the cell and it is most commonly constituted by the CD3-ζ chain of the TCR complex that is sufficient to initiate the cascade of activation signal. The ζ chain is a non-glycosylated protein which forms homodimers with the other components of the TCR complex through disulfide bridges. Each ζ chain contains three activation motifs composed by tyrosine and plays a key role in signal transduction [112].

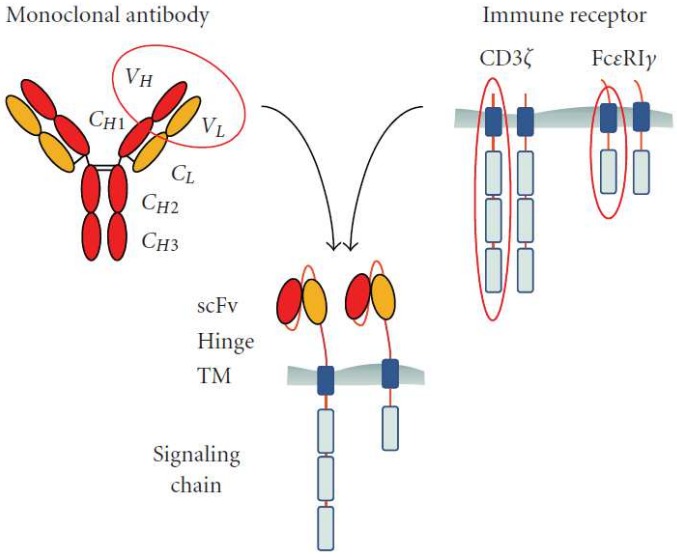

Figure 8. CAR architecture. CARs are composed by a binding domain, an extracellular spacer domain (hinge), a transmembrane region (TM), and an intracellular transduction domain. Usually the antigen-binding domain is derived from a tumor-specific monoclonal antibody (scFv) [111].

The main advantage of the CAR approach is the possibility to make a universal receptor directed to a specific molecule which is recognized in a MHC-unrestricted manner. The CAR approach allows to efficiently overcome the most common immune evasion system in cancer: the down-regulation of MHC molecules. Secondly, it can potentially be used to treat all patients, in contrast to the transgenic TCR for which the recognition is limited to a single MHC haplotype [113]. Moreover, the range of antigens that can be recognized by CARs is not limited to protein antigens, but also to antigens derived from glycolipids and carbohydrates. Therefore, all TAAs on cell surface virtually represent potential targets [114].

CAR approach enables to overcome the hypo-responsiveness of T cells modified with transgenic TCR. Indeed, the repetitive stimulation of TCR by the tumor-specific antigen inevitably causes a hypo-responsiveness of the cells that become terminally differentiated. This condition greatly reduces their therapeutic efficacy caused by an alteration in synapse formation at the level of the endogenous TCR complex. Although terminally differentiated T cells are mainly hypo-responsive, recruitment of CAR molecules allows to mediate effector functions with the same efficiency. The CD3-ζ chain of the CAR enables to bypass this problem by starting the signal transduction downstream and restoring a functional response of T cells [115].

First generation CAR contains a single signal unit derived in most cases from the ζ chain of CD3 or the γ chain of FcεRI [112]. Once introduced into T cells, first generation CARs can produce optimal antitumor cytotoxic response. However, signals transmitted through

the CD3ζ alone induce a transient T-cell division and a sub-optimal cytokine secretion, not allowing polyclonal prolonged expansions and sustained anti-tumor responses *in vivo*.

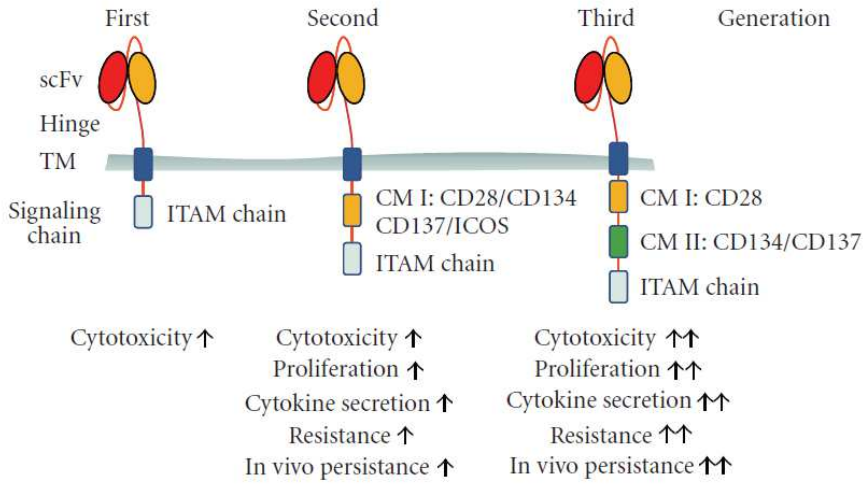

Figure 9. CARs evolution. First generation CARs transmit activation signals solely through ITAM. Second generation CARs contain an additional co-stimulatory domain, generally represented by the CD28 and 4-1BB, which allows an increase of proliferation and secretion of cytokines. Finally, cells transduced with a third-generation CAR seems to have superior qualities regarding effector functions and *in vivo* persistence [111].

Subsequent studies have defined that full activation and proliferation of T cells require the presence of a co-stimulatory signal, as through CD28-B7 interaction. The addition of CD28 in second generation CARs results in intense proliferation and secretion of greater quantities of IL-2 and interferon (IFN)-γ [116].

Afterwards, other co-stimulatory molecules including ICOS (inducible costimulatory), OX40 (CD134), 4-1BB (CD137), CD27, DAP10 or 2B4 (CD244) were tested in CAR context. In the context of second

generation CARs, more recent studies demonstrated the superiority of CAR 4-1BB compared to CD28. Indeed, CAR-T cells containing 4-1BB domain express lower levels of markers of exhaustion and show a better persistence *in vivo* [117]. Constructs with more than one additional costimulatory molecule are known as "third generation" CARs. Commonly, in third generation CARs, CD28 and 4-1BB or CD28 and OX40 domains have been combined [118,119]. An interesting co-stimulatory molecule appears to be OX40 (CD134), for which various studies have shown that its signal can increase the CD28-activated T-cell response by increasing proliferation, survival and cytokine secretion [111].

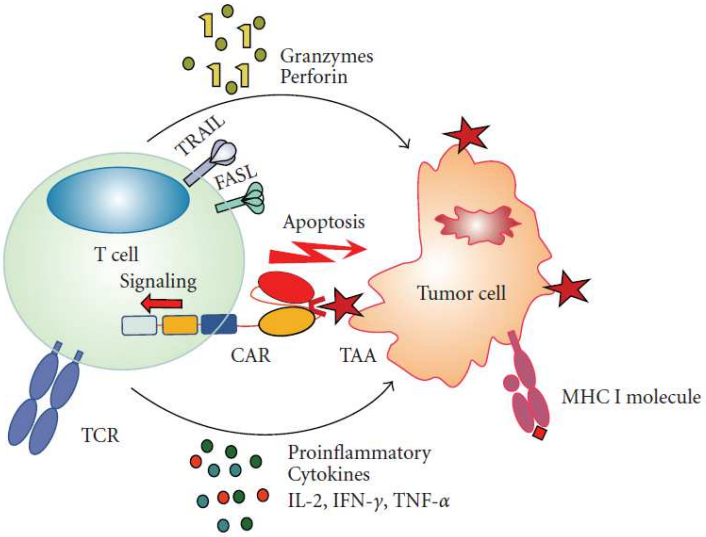

Figure 10. Antitumor effects mediated by CAR-modified T cells. The recognition of cancer cells by engineered T cells is mediated by CAR molecule which binds to the TAA. Consequently, T cells are activated and efficiently eliminate tumor cells through the secretion of perforin, granzymes and the expression of FasL and TRAIL (TNF-Related Apoptosis Indicing Ligand). Moreover, thanks to the secretion of various pro-inflammatory cytokines, immune system's cells are recruited [111].

The effectiveness of CAR strategy was confirmed in a phase I clinical trial conducted by Pule *et al.* in patients with neuroblastoma [120]. In this study, patients were treated with cytotoxic T lymphocytes specific for the Epstein Barr virus (EBV-CTLs) and engineered to express a CAR against diasialoganglioside G(D2a) which is over-expressed by human neuroblastoma cells. Pule and colleagues reported a prolonged survival of EBV-CTLs and the regression or necrosis of the tumor mass in 50% of the treated subjects [120].

Kochenderfer *et al*. in 2010 used a second-generation anti-CD19 CAR. CD19 antigen is expressed by tumor B cells, mature B cells, B-cell precursors and plasma cells. In this trial, two patients partially responded and one underwent complete remission. Toxicities observed were hypotension, fever, and the complete elimination of B-cell lines, also known as B-cell aplasia, from blood and bone marrow (manageable by intravenous immunoglobulin infusion) [121].

In the field of CAR many advances have been made in the clinic reinforcing pre-clinical data and revolutionizing cancer treatment during the last decade. Clinical advances and side effects of this approach will be addressed in more detail later in this chapter.

5.1. SAFETY ISSUES OF CAR TECHNOLOGY

Despite the initial success associated to CAR approach, various obstacles and concerns should be considered, including the risk of "on-target, off-tumor" toxicities and the cytokine release syndrome (CRS).

In 2010 Morgan *et al*. reported the case of one patient suffering from colon cancer with lung and liver metastases that was treated with T lymphocytes modified with a third-generation CAR specific for ERBB2, antigen over-expressed by tumor cells, but also expressed at low levels by lung epithelial cells. The administration of modified T cells led to an immediate pulmonary toxicity causing patient's death. Post-mortem analysis revealed the presence of high levels of pro-inflammatory cytokines (IFN-γ, TNF-α, IL-6 and IL-10). The authors hypothesized that the low levels of ERBB2 on lung epithelial cells were sufficient to activate infused T cells, unleashing a lethal systemic inflammatory reaction as "on-target, off-tumor" toxicity [122].

The release of high levels of cytokines, named CRS, is a phenomenon already observed in several clinical settings, including GVHD after HSCT, and monoclonal antibody/BiTE therapy or in presence of severe bacterial/viral infections [123–128]. CRS represents a dreadful side effect within CAR therapy. The most common symptoms found in patients who experience CRS are nausea, headache, tachycardia, hypotension and rash. This disorder is caused by an excessive immune response with a massive release of inflammatory cytokines and chemokines which results in endothelial and organ damage [129]. Possible life-threatening complications of CRS are represented by cardiac dysfunction, respiratory distress syndrome, neurologic toxicity, renal and hepatic failure. CRS is almost always associated to the macrophage activation syndrome (MAS) which is characterized by IL-6 release and symptoms partially overlapping CRS comprising fever, hepatosplenomegaly, coagulopathy, hyperferritinemia,

cytopenia, and high levels of triglycerides, transaminases and conjugated bilirubin [130]. Very recently the diagnostic criteria for CRS in CAR immunotherapy have been defined [131]. Symptoms rises 5-21 days after CAR T-cell infusion and the severity seems to be proportional to the amount of the leukemic bulk and it correlates to the efficacy of the immunotherapeutic treatment [132,133].

Criteria for sCRS
Fevers for at least three consecutive days
Two cytokine max fold changes of at least 75 or one cytokine max fold change of at least 250
At least one clinical sign of toxicity such as hypotension (requiring at least one intravenous vasoactive pressor) or,
Hypoxia (PO_2 < 90%) or,
Neurologic disorders (including mental status changes, obtundation, and seizures)

Table 4. Diagnostic criteria suggested by Davila *et al*. for CRS developed after treatment with CAR T cells[131].

Severe CRS-associated toxicities are managed with vasoactive pressors, mechanical ventilation, antiepileptics, corticosteroids, antipyretics and the administration of the IL-6 receptor-blocking monoclonal antibody Tocilizumab and the anti-IL-6 monoclonal antibody Siltuximab [131].

Another important complication to be considered in CAR therapy is the tumor lysis syndrome which arises about one month after CAR T-cell infusion. The syndrome is due to the rapid release of intracellular metabolites such as DNA, phosphate, potassium, uric acid, xanthine

and cytokines by lysed tumor cells. Common manifestations are hyperuricemia, hyperkalemia, hyperphosphatemia, hypocalcemia, hypotension and kidney failure [129].

5.2. CAR DESIGN IMPLEMENTATION: LENGTH OF THE SPACER AND EFFECTOR-TARGET DISTANCE

The spacer moiety connects the scFv to the transduction domain. Recently, a large amount of data has been reported about the importance of the CAR design and, in particular, of the length and composition of the spacer domain for an optimal *in vitro* and *in vivo* activity. Indeed, the characteristics of the spacer domain seem to influence the effector-target interaction and, consequently, the signal transduction. The importance of the inclusion of a spacer region within the CAR structure to optimize the antigen binding and cytotoxic activity of CAR-expressing T cells was first suggested by Moritz et al [134].

Guest and collaborators in 2005 demonstrated how the interaction between CAR and its antigen is influenced by the location of the recognized epitope and its distance from cell surface. In this comparative study, four scFvs have been used, directed towards carcinoembryonic antigen (CEA), neural cell adhesion molecule (NCAM), the oncofetal antigen 5T4, and the B-cell antigen CD19. Anti-5T4 and anti-NCAM CARs, which recognize epitopes located near the cell membrane, show an optimal activity only when a spacer region is present. On the other hand, anti-CEA and anti-CD19 CARs

demonstrate an enhanced cytotoxic activity only in absence of the spacer domain because the recognized epitope is distant from the cell membrane. Consequently, for optimal effector-target recognition, the length of the spacer region should be modified depending on the targeted epitope [135]. More recently, further attention is gained in defining how the length of the spacer should be optimized and how this region influences CAR-expressing T-cell performances. Investigators tested various lengths and defined that the spacer region plays an important role in activation and proliferation of T cells [136,137].

The inclusion of a spacer derived from Fc portion of IgG1 or IgG4 can exhibit detrimental side effects because of the maintained partial ability of this region to interact with FcγR receptors. In presence of $FcγR^+$ cells (monocytes and natural killer cells), these interactions can potentially result in an unspecific activation of CAR T cells, followed by activation-induced cell death (AICD). At the same time, $FcγR^+$ cells can be activated, initiating innate immune responses. In the mice model, this potential side effect inhibits the efficacy of CAR T cells and contributes to a premature CAR T-cell clearance *in vivo* [138,139]. In order to reduce this off-tumor effect, Fc-derived spacer regions are engineered to disrupt sequences responsible of their binding ability to the corresponding Fc receptor. Avoiding off-target CAR T-cell activation may increase persistence *in vivo* and anti-tumor potency [137,138].

In conclusion, the distance between effector and target cells is crucial for optimal cytotoxic activity. Therefore, the length and flexibility of

the spacer should be modulated depending on the target epitope localization and accessibility.

6. CAR-MODIFIED T CELLS GENERATION

Stable introduction of therapeutic transgenes into human cells can be accomplished using viral and non-viral approaches.

6.1. VIRAL VECTORS

In the past two decades, recombinant viral vectors have constituted a valuable tool for successful gene therapy thanks to their efficacy in mediating stable gene transfer into primary cells with standardized GMP-grade process and overall safety in modifying differentiated immune cells [140,141]. To date, the most commonly used viral vectors in clinical setting include retroviral (gamma-retroviral or lentiviral) vectors, adenovirus, and adeno-associated virus (AAV).

Viral vectors are the most popular approach, having been used in approximately two-thirds of trials preformed up to 2012 [142]. Although viral vectors are superior in terms of efficient delivery of genetic material into cells *in vivo*, many hurdles remain to be overcome. Adenovirus vectors are the most widely used in gene therapy clinical trials (23.3%), but they have shown a strong propensity to elicit an abnormal immune response against vector and/or transgene product [142]. The recruitment of macrophages, neutrophils, and NK cells at the injection site cause the rapid elimination of transgene expression [143,144]. Actually, lentiviral and AAV vectors do not seem to induce

inflammatory responses against viral proteins, but T cell responses can still be elicited against the expressed transgene product. Pre-existing humoral immunity to parental wild-type viruses is another obstacle that affect all classes of viral vector. Circulating virus-neutralizing antibodies can preclude efficient viral vector transduction [145]. An important downside of retroviral and lentiviral vectors is represented by the ability of this vector to preferentially integrate in high-expressed regions and near to promoters of the transcriptional active genes [146]. However, this safety issue is mainly restricted to the modification of stem cells. Conversely, integrating viral vectors have been proved secure in modifying differentiated immune cells for adoptive T-cell therapy clinical trials [141]. Finally, viral vectors are also limited by production costs and restricted cargo capacity accepting transgenes only up to 8 Kb [147].

6.2. NON-VIRAL VECTORS

The non-viral methods have recently emerged for the advantages offered in terms of cost and production time, as well as for the lower risk of insertional mutagenesis, that characterizes some of these systems, and for the absence of immunogenicity [147]. In this case the integration efficiency is inferior than viral methods, but more recently developed strategies show comparable efficiency to viral vectors [148]. Non-viral methods include systems based on transposons, mobile genetic elements that can be inserted into the genome without the need of sequence homology, such as the "Sleeping

Beauty" system. This strategy allows the introduction of genes up to 11 Kb delivered by transposon plasmid. The cargo gene is preceded and followed by specific inverted repeated sequences (IRs), inside which there are two shorter direct repeated sequences (DRs). These IR/DR sequences are recognized by transposase enzyme (named SB10X, SB11X, SB100X, etc. depending on the increasing enzymatic activity) that mediates a cut-and-paste transfer of the cargo gene from the transposon directly into the genome of the host cell ensuring stable expression [148–150].

Optimal ratio of transposase to transposon and genetic cargo size are hallmarks required for highest transposition rates. Preferred molecular ratio of transposon to transposase should be 1:4 for maximal rates of transposition. If the transposase concentration exceeds this ratio occurs a phenomenon known as “overproduction inhibition”. Two-part transposon system, in which transposase acts in trans, allows to modulate the transposon/transposase ratio, and to overcome the limit of overproduction inhibition [151]. Similar to other transposable elements, the efficiency of SB transposase decreases with the increase of cargo size [152]. In this field our group recently developed a clinical-grade protocol to obtain CAR-modified CIK cells using the SB transposon system[153].

7. CD19 CAR T CELLS: PROMISES AND CHALLENGES

7.1. CLINICAL TRIALS USING CD19 CAR T CELLS

The CD19 antigen has been widely used in immunotherapeutic approaches for B-cell neoplasms. The CD19 antigen is a 95 kd transmembrane glycoprotein classified as a type I transmembrane protein, with a single transmembrane domain, a C-terminus cytoplasmic domain, and a N-terminus extracellular domain. Despite only two transcript isoforms have been isolated *in vivo*, there are more mRNA transcripts. CD19 is also called "pan-B" antigen since it is expressed in each B-cell differentiation stage. CD19 functions as the dominant player in a multimolecular complex with the complement receptor CD21, and the tetraspanin membrane protein CD81 (TAPA-1), as well as the CD225. Modulating both B-cell receptor (BCR) dependent and independent signaling, CD19 has an important role in establishing intrinsic B-cell signaling thresholds. Moreover, CD19 transgenic and knockout mouse models revealed the fundamental role of CD19 in maintaining the balance between humoral, antigen-induced response and tolerance induction [154]. Moreover, CD19 represent an ideal target being expressed at high level in more than 95% of B-cell neoplasms. Furthermore, the "on-target, off-tumor" toxicity is limited to B-cell aplasia which is easily manageable with intravenous administration of immunoglobulins [155].

The first clinical success obtained with an anti-CD19 CAR has been reported in 2010 in the context of refractory lymphoma. Subsequently, it has rapidly expanded to other cancers including

relapsed B-ALL [156]. The first clinical trials were conducted in 2013 by researchers of the Memorial Sloane Kettering and the University of Pennsylvania [157]. In the study of Grupp *et al.*, two pediatric ALL patients were treated and achieved complete remissions. Nevertheless, one of them developed a CD19-negative relapse two months after treatment. More recently, Maude *et al.*, in a larger cohort of patients comprising Blinatumomab and HSCT resistant patients, observed 90% of complete remissions at one month. In this setting, the proliferation and persistence of CAR T cells seems to correlate to a durable response, with an event free survival (EFS) of 67% at 6 months after treatment [158]. It has also been reported the ability of T cells modified with anti-CD19 CAR to infiltrate and control the disease in the CNS [159].

7.2. CD19-NEGATIVE ESCAPE

Despite the success of CD19-targeting approaches, some challenges remain to be solved. In particular, a significant subset of patients, after achieving initial response, develop relapses characterized by the apparent loss of CD19 [158,160,161]. The incidence of CD19-negative relapse in CD19-targeting strategies is about 30% after Blinatumomab and 60% after CART-cell therapy [162]. In the previously mentioned work by Maude and collegues, despite no residual disease detection by flow cytometry at day 23 after treatment, high throughput DNA sequencing of the IGH locus reveals the presence of the malignant clone. Furthermore, sequencing of DNA isolated from

blasts at the relapse shows that the CD45+CD34+CD19− cells are clonally related to the initial dominant CD45+CD34+CD19+ leukemia. The potent selective pressure of the redirected CAR T cells drives the specific escape mechanism causing CD19-negative relapse [158].

Sotillo and colleagues have revealed the mechanism underneath the CD19-negative relapse. The epitope recognized by the CAR is frequently removed as a result of alternative exon splicing forms of the CD19 gene where exon 2 was spliced out. This mechanism makes B-ALL blasts invisible to immunotherapeutic approaches targeting CD19 antigen, and CD19-negative when assessed by cytofluorimetric methods. Moreover, the alternative CD19 isoform is predominantly cytoplasmatic and untreatable by CART. Furthermore, the authors confirmed that the Serine/Arginine-Rich Splicing Factor (SRSF3), normally involved in splicing regulation, was the only responsible of Δex2 isoform accumulation. Indeed, downregulation of SRSF3 resulted in increased concentrations of Δex2 isoform [163].

Subsequently, Gardner and collaborators reported the case of an additional mechanism of escape from CD19-targeting CAR T cells. Two out seven patients with MLL gene rearrangement relapsed with a myeloid phenotype and loss of B lymphoid antigens after CAR T-cell treatment. Both relapses were clonally related to the initial disease. For the first patient, the underlying mechanism suggested by the authors is the reprogramming/de-differentiation of a committed B lymphoid progenitor because of the retention of the IGH rearrangement. In the second patient the IGH rearrangement is absent, suggesting a possible myeloid differentiation of a non-

committed precursor or selection of a pre-existing myeloid clone by CAR T-cell treatment [164]. A similar event was observed in a case of infant B-ALL with MLL-AFF1 rearrangement treated with blinatumomab and relapsed with an AML phenotype [165]. The transition from a lymphoid to myeloid phenotype or *vice versa* represents a rare event previously reported only after intensive chemotherapy and HSCT. Thus, the selective pressure exerted by CD19-targeted therapies can led to reprogramming events or eventually promote the growth of a pre-existing minor CD19-negative clone. Furthermore, this event occurs more frequently in subtypes of B-ALL that have a genetic background characterized by innate plasticity such as mixed phenotype leukemia [166].

More recently, a newly identified resistance mechanism has been published by Braig *et al*. Despite the wild-type sequence of CD19 gene and the detection of CD19 mRNA in the relapsed leukemia, the analyzed patient showed a complete antigen-loss at the cell membrane level, as demonstrated using CD19 antibodies with different epitope recognition in flow cytometry. This observation suggests an evasive mechanism based on post-translational altered regulation. This patient also displayed negative surface expression for CD21 and CD81. Since CD81 is involved in maturation and transport of CD19 to the cell surface, the absence of this protein seriously impairs CD19 trafficking [167].

Table 5. Clinical studies applying CD19 CART

Reference	Center	Disease (median age)	Patiens (n)	CAR design	CAR gene transfer	T cell origin	Cell dose range	Persistence of CAR T cells	Adverse events	Outcomes
Jensen (2010)	City of Hope	NHL	2	FMC63 anti-CD19 scFv-CD3ζ (1st generation)	DNA electroporation	Autologous	100-200 x 10^7/m² total T cells	< 1 week	Lymphopenia	No responses
Kochenderfer (2010) Kochenderfer (2012)	National Institute of Health	NHL, CLL, SMZL (55)	8	FMC63 anti-CD19 scFv-CD28+CD3ζ (2nd generation)	Retroviral	Autologous	0.3-3 x 10^7 CAR+ T cells/kg	Up to 6 months	B cell aplasia CRS	6 PR, 1 CR, 1 NR
Savoldo (2011)	Baylor College of Medicine	DLBCL, NHL (55)	6	FMC63 anti-CD19 scFv - CD3 ζ and anti-CD19 scFv-CD28-CD3ζ (1st and 2nd generation)	Retroviral	Autologous	2-200 x 10^7/m² total T cells	Up to 6 weeks	None	2 SD, 4 NR
Porter (2011) Kalos (2011) Porter (2015)	University of Pennsylvania	CLL (66)	14	FMC63 anti-CD19 scFv-41BB-CD3ζ (2nd generation)	Lentiviral	Autologous	1.4-113 x 10^7 CAR+ T cells	Up to 49 months	B cell aplasia. CRS, TLS, neutropenia	4 CR, 4 PR
Brentjens (2011)	Memorial Sloan Kettering Cancer Center	CLL, ALL (60)	9	SJ25C1 anti-CD19 scFv-CD28-CD3ζ (2nd generation)	Retroviral	Autologous	0.4-3 x 10^7 CAR+ T cells/kg	Up to 6 weeks	B cell aplasia, fever, hypotension, death	1 PR, 2 SD, 1 cCR, 4 NR, 1 death
Brentjens (2013) Davila (2014)	Memorial Sloan Kettering Cancer Center	ALL (50)	16 (4 post allo-SCT)	SJ25C1 anti-CD19 scFv-CD28-CD3ζ (2nd generation)	Retroviral	Autologous	0.14-0.3 x 10^7 CAR+ T cells/kg	Up to 4 months	Severe CRS	14 CR, 12 MRD negative
Kochenderfer (2013) Brudno (2016)	National Institute of Health	CLL, NHL (48)	20 (all post allo-SCT)	FMC63 anti-CD19 scFv-CD28+CD3ζ (2nd generation)	Retroviral	Allogenic	0.04-0.8 x 10^7 CAR+ T cells/kg	Up to 4 weeks	B cell aplasia, CRS, hypotension, TLS	2 PR, 6 CR, 8 SD, 4 PD
Grupp (2013) Maude (2014)	University of Pennsylvania	ALL (14)	30 (18 post allo-SCT)	FMC63 anti-CD19 scFv-41BB-CD3ζ (2nd generation)	Lentiviral	Autologous	0.2-1.2 x 10^7 CAR+ T cells/kg	Up to 26 weeks	CRS, CNS toxicity	27 CR, 22 MRD negative
Cruz (2013)	Baylor College	ALL, CLL (39)	8	FMC63 anti-CD19 scFv-CD28+CD3ζ (2nd generation)	Retroviral	Allogenic	1.9-11 x 10^7	Up to 3 months	none	1 CR, 1 PR, 1 SD, 2 cCR, 3 NR
Kochenderfer (2014)	National Institute of Health	NHL (56)	15	FMC63 anti-CD19 scFv-CD28+CD3ζ (2nd generation)	Retroviral	Autologous	0.1-0.5 2 x 10^7 CAR+ T cells/kg	Up to 11 weeks	B cell aplasia, CRS, infectious complications	8 CR, 4 PR, 1 SD
Lee (2014)	National Institute of Health	ALL, NHL	21 (8 post allo-SCT)	FMC63 anti-CD19 scFv-CD28+CD3ζ (2nd generation)	Retroviral	Autologous	0.003-0.3 2 x 10^7 CAR+ T cells/kg	Up to 7-8 weeks	CRS, B cell aplasia	14 CR, 13 MRD negative
Kebriaei (2016)	MD Anderson	DLBCL, MCL, ALL (40)	26	FMC63 anti-CD19 scFv-CD28+CD3ζ (2nd generation)	Electroporation with SB Transposon	Autologous (n=7) and Allogenic (n=19)	10^8-5 x 10^9 T cells/m²	201 and 57 days after infusion	GVHD in 3/19 patients treated with allogenic protocol	15 CR after HSCT, 3 SD, 5 DP, 2 died in remission, 1 CR2

Abbreviations: CR, complete remission; PR, partial remission; NR, non responder; DP, disease progression; SD, stable disease; NHL, non-Hodgkin lymphoma; CLL, cronic lymphocytic leukemia; SMZL, splenic marginal zone lymphoma; DLBCL, diffuse large B-cell lymphoma, ALL, acute lymphoblastic leukemia; MCL, mantle cell lymphoma; SB, sleeping beauty; CRS, cytokine release syndrome; TLS, tumor lysis syndrome; CNS, central nervous system; GVHD, graft versus host disease; MRD, minimal residual disease; HSCT, hematopoietic stem cell transplantation.

7.3. ADDITIONAL TARGETS

Other target antigens have been proposed for treatment of refractory/relapsed B-ALL comprising CD22, CD20, CD123 and the thymic stromal lymphopoietin (TSLP) receptor. The ability of CD123-specific CAR T cells of eradicating CD19-negative blasts in preclinical mouse models has been recently demonstrated by Ruella and collegues [162]. Currently, there are 3 clinical trials ongoing with CART22 for B-ALL in which also CD19-negative relapsed patients reached complete remission after treatment [168–170]. Nonetheless, the single antigen targeting strategy could again lead to the same antigen-loss escape observed for CD19. For this reason, various groups propose the targeting of more than one antigen expressed on B-ALL blasts as a successful strategy to avoid tumor evasion. For example, in glioblastoma preclinical models it has been demonstrated that T cells expressing both anti-HER2 CAR and anti-IL-3Rα2 zetakine are able to avoid tumor escape. Anurathapan *et al*. demonstrates a reduction of antigen escape in prostate cancers with pooled CAR T cells specific for MUC1 and PSCA [171]. Moreover, dualCAR (CAR structures were distinctly co-expressed by T-cell) and TanCAR (two scFv specific for two different antigens built in tandem on a single CAR structure) layouts show higher anti-tumor activity than pooled CAR T cells [172,173]. Similarly, Ruella *et al*. establishes that anti-CD19 and anti-CD123 dualCAR T cells are efficacious in preventing antigen loss in preclinical xenograft models [162].

8. THE B-CELL ACTIVATING FACTOR (BAFF) SYSTEM

8.1. BAFF AND ITS RECEPTORS

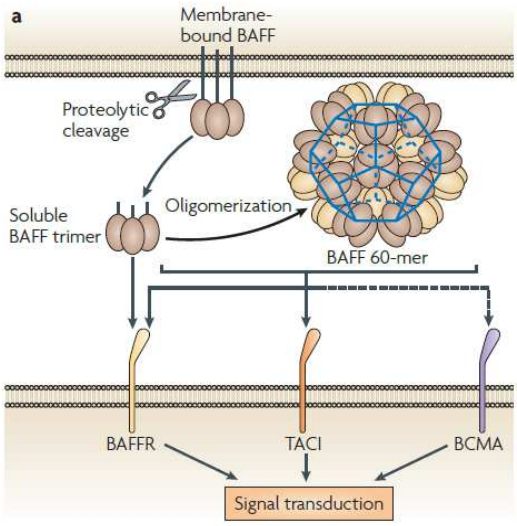

Figure 11. BAFF signaling. Schematic representation of BAFF forms. The membrane-bound form could be cleaved and released as soluble form. BAFF could also be found in the periphery as a 60-mer oligoprotein. The signal transduction is activated by interaction of the cytokine and three receptors: BAFF-R, TACI and BCMA. Image adapted from Mackay *et al*. 2009 [174].

BAFF, also known as BLyS, TNFSF13B, THANK, zTNF4 or TALL-1, belongs to the tumor necrosis factor (TNF) ligand superfamily and plays a fundamental role in B-cell survival. BAFF, discovered in 1999 in the context of autoimmunity, can be found as membrane-bound homotrimer or released in a soluble form after cleavage mediated by furin-type proteases. The soluble form can be assembled as homotrimer or as virus-like capsid composed of 20 trimers (60-mer)

[175,176]. BAFF is produced by monocytes, neutrophilis and dendritic cells upon activation of the Toll-like receptors or in response to pro-inflammatory cytokines such as IFN-γ, IL-10 and G-CSF [174]. Moreover, also several cells of non-hematopoeitic origin, such as splenic radiation-resistant stromal cells, astrocytes, fibroblast-like synoviocytes, nurse-like cells, osteoclasts and ductal epithelial cells, express BAFF [177]. Soluble BAFF binds to three different receptors: BCMA (*B-cell maturation antigen*), TACI (*Transmembrane Activator and Cyclophilin ligand interactor*), BAFF-R (*BAFF Receptor*). The differential distribution of these three receptors through maturative stages allows the cytokine to support the homeostasis of B cells [178].

BCMA is expressed on antibody-producing cells (plasmablasts, plasma cells, germinal centre B cells) and plays a critical role in their long term survival [179,180]. BCMA-deficient mice do not show abnormalities in B-cell development, suggesting that BCMA is dispensable for humoral immune response and has a presumable redundant role [181]. The factors regulating the expression of BCMA are still unknown.

TACI is highly expressed by marginal zone B cells, transitional type 2 (T2) B cells and B1 B cells. TACI-deficient mice are characterized by an increased number of peripheral B cells and the development of autoimmune disorders, revealing an inhibitory/regulatory effect of the signaling through TACI on B-cell homeostasis. TACI demonstrates an important role in the immune tolerance by down-regulation of B cell-proliferation [182,183].

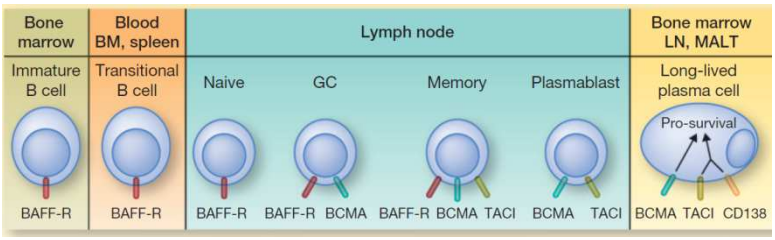

Figure 12. Expression of BAFF Receptors BCMA, TACI and BAFF-R during B-cell developmental stages.

BAFF-R, a type III transmembrane protein, is the receptor with the highest affinity for BAFF (~16nM) and is expressed starting from immature B cells upon acquiring a functional B cell receptor (BCR) [184,185]. Tussiwand and collaborators elegantly described the expression of BAFF-R through B-cell developmental stages in mouse and in humans by cytofluorimeter analysis. The receptor is absent on pro-B and pre-B cells (CD19+ B220+ IgM-) and its expression occurs starting from immature B cells (CD19+ B220+ IgM+) upon acquiring a functional BCR. The absence of BAFF-R expression on normal B-cell precursors represent an important advantage if the antigen is considered for a immunotherapeutic treatment. Indeed, this aspect is a basic requirement in the case of these approaches because normal cells could be spared. In addition, the authors hypothesized that the expression of a functional BCR in conjunction with the up-regulation of BAFF-R allows B cells to overcome the activation threshold necessary to guarantee survival of the developing B cell and achievement of complete cell maturation. Furthermore, BAFF-R is

expressed on all splenic B-cell subsets: T1 (CD19+ CD93+ CD21- CD23-), T2/3 (CD19+ CD93+ CD21+ CD23+), follicular (CD19+ CD93- CD21+ CD23+), marginal zone B cells (CD19+ CD93- CD21+ CD23-). Moreover, the receptor is expressed on all mature B cells in the BM and in the periphery with the exception of plasma cells [186]. The BAFF/BAFF-R axis plays a fundamental role during transition from Transitional type 1 (T1) to T2 B cells and in sustaining maturation and long-term survival of mature B cells. This role has been confirmed in BAFF- and BAFF-R-deficient mice which show B-cell lymphopenia and antibody deficiency and lack a mature B-cell compartment because B-cell maturation is impaired at the transition from T1 to T2 stages, except for peritoneal cavity B1 cells that do not require BAFF and BAFF-R to survive. BAFF-R deficiency in humans causes an arrested B-cell development at the stage of transitional B cells, a severely reduced number of all subsequent B-cell stages and is associated with an adult-onset antibody deficiency syndrome [187]. On the contrary, B-cell precursor populations within the bone marrow remain unaffected. This findings from knock-out mice indicated that BAFF-R is responsible of the survival and maturation of B cells [188,189].

The binding of BAFF to BAFF-R results in signaling initiation which involves trimeric intracellular proteins named *TNF receptor associated factors* (TRAF). BAFF-R recruits and degrades TRAF3, inducing a potent activation of the alternative pathway of *nuclear factor kappa light chain enhancer of activated B cells* (NF-kB) and a weakly activation of the classical pathway. NF-kB activation leads to the transcription of anti-apoptotic proteins (Bcl-2 and Bcl-xL) and to

the promotion of glycolysis, protein synthesis and cell growth through the PI3K-AKT1-mTOR pathways. A direct target of the classical NF-kB pathway is MYC which is responsible for the regulation of genes involved in metabolism, B-cell growth and resistance to atrophy [175,190].

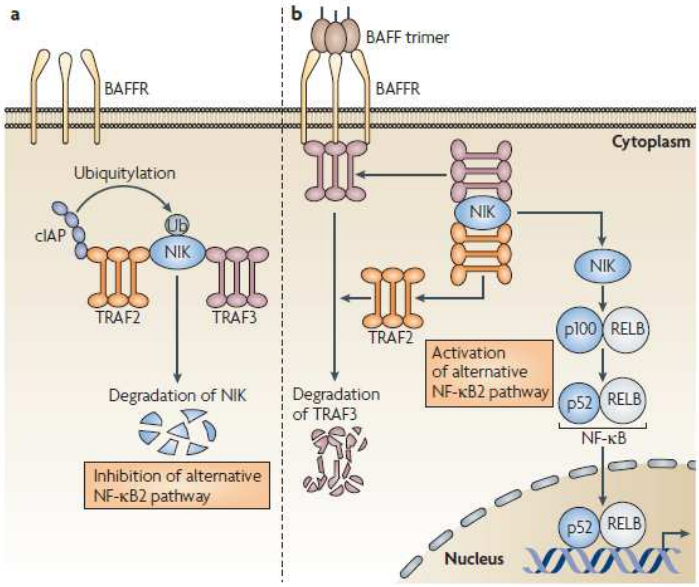

Figure 13: Signaling pathway of BAFF through BAFF-R. Image adapted from Mackay *et al*. 2009 [175].

8.2. THE ROLE OF BAFF/BAFF-R AXIS IN PATHOLOGICAL CONDITIONS

As mentioned before, BAFF/BAFF-R axis is essential for maturation and survival of B cells starting from the T1 B cells. Hence, physiological concentrations of BAFF enable, through BAFF-R, transitional B cells to offset apoptotic stimuli induced by the BCR and to continue to the subsequent maturation step [191]. B-cell immune tolerance is granted by the elimination of autoreactive B-cells upon strong death signals from BCR-autoantigen interaction which is not overcome by physiological levels of BAFF [192]. However, an excessive production of BAFF can result in autoimmune symptoms. Studying BAFF-transgenic mice researchers observed elevated serum levels of immunoglobulins IgM, IgG, IgA, IgE and B-cell hyperplasia, particularly affecting the T2 and Marginal Zone B cells, suggesting a defect in self-reactive B-cell negative selection during maturation. In addition, histological analysis showed expanded B-cell follicles and marginal zone B-cell areas with an increasing in germinal centers number [176]. An excess of BAFF, indeed, can bypass death signals derived from autoantigens through the BCR. As a consequence, low-affinity self-reactive B cells survive and expand, leading to the development of autoimmune symptoms similar to Systemic Lupus Erythematosus (SLE) and Sjögren's Syndrome (SS) [193]. The finding that large amount of circulating BAFF were found also in patients affected by autoimmune disorders such as SLE, SS and rheumatoid arthritis indicates that the dysregulation of BAFF is linked to disease pathogenesis in humans. For this reason, a number of inhibitory

molecules have been developed and used to treated patients with autoimmune diseases, obtaining significant therapeutic benefits.

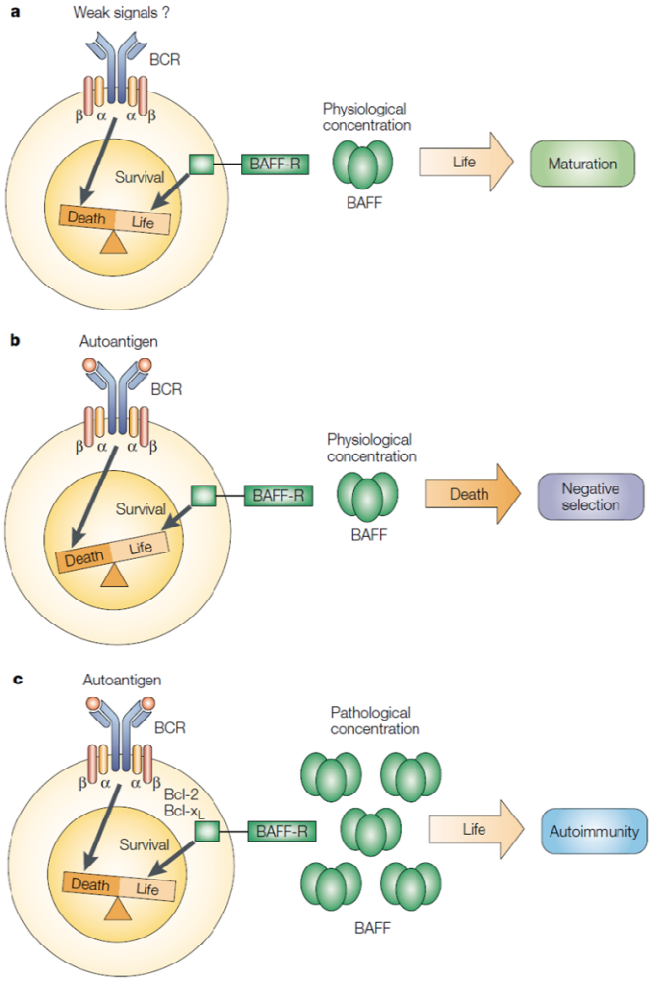

Figure 14. Role of BAFF in B-cell tolerance and autoimmunity. Normal concentration of BAFF allows the cells to survive and mature (a). Strongly autoreactive B cells in normal conditions are eliminated after binding to autoantigen (b). In pathological situation characterized by high concentrations of BAFF, self reactive B cells are positively selected and proliferate (c).

Given the importance of BAFF in B-cell homeostasis regulation, it is not surprising that a high soluble BAFF concentration has been detected in patients with chronic GvHD (cGvHD) after allo-HSCT. In these cases, the high amount of BAFF is linked to an increased number of CD27+ activated pre-germinal center (GC) B cells and post-GC "plasmablast-like" cells which can produce IgG without additional antigen stimulation. Consequently, these patients show significantly higher BAFF:B-cell ratio than patients without cGvHD. Patients with cGvHD also show a delay in reconstitution of naive B cells despite the large amount of BAFF available. The excess of BAFF after HSCT promotes survival of pathologically activated B-cell subsets in cGvHD patients. These data suggest a clear involvement of BAFF and B cells in cGvHD pathogenesis. The use of therapies targeting B cells or BAFF axis has been suggested to prevent cGvHD in the post-HSCT setting [194].

Nowadays, several studies reported the importance of BAFF and BAFF-R in the context of various B-cell malignancies. Rodig *et al.* described the over-expression of BAFF-R in a wide range of B-cell lymphoproliferative disorders such as mantle cell lymphomas, splenic marginal zone lymphomas, MALT lymphomas, follicular lymphomas, hairy cell leukemia and B-cell chronic lymphocytic leukemia (B-CLL) [195]. Subsequently, the aberrant expression of BAFF-R on pre-B-ALL has been described by Parameswaran and colleagues [196]. Interestingly, BAFF-R is not present on normal pre-B-cell precursors despite the detection of the mRNA transcript of BAFF-R. This observation suggests the presence of a post-transcriptional

regulation system of BAFF-R expression in early B-cell development which is lost due to malignant transformation [197].

Moreover, in B-ALL context, BAFF cytokine has been detected not only on malignant B cells themselves, as an autocrine loop of stimulation, but also within the tumor microenvironment in which it exerts a paracrine support facilitating tumor cell growth and protection from apoptosis [196,197]. In B-ALL it has been proved that, within the leukemic niche, BM endothelial cells are responsible for supporting leukemic cells by producing and secreting BAFF. This data provide evidence about the involvement of BAFF/BAFF-R axis in the survival of malignant B cells and in maintenance of the tumor within the BM niche [197].

The binding of BAFF to BAFF-R promotes the survival, proliferation and resistance of B-ALL blasts to chemotherapy, as demonstrated by Parameswaran and collaborators. Adding BAFF to culture medium, BAFF-R-expressing ALL blasts are protected from conventional chemotherapy. Afterwards, they further demonstrated that the presence of aberrant expression of BAFF-R on ALL blasts and the abundant production of BAFF confer a clear survival advantage to malignant cells [198].

Considering the specificity of expression of BAFF-R on B-ALL surface and the contemporary absence on healthy B-cell precursors, this antigen could used for a selective targeting of B-ALL blasts. Moreover, a variety of therapeutic strategies have been proposed in order to avoid the interaction between BAFF and BAFF-R, blocking in this way the autocrine/paracrine loop of stimulation. Other approaches using

BAFF-R as target antigen have already been tested in B-ALL setting, obtaining promising results. For example, the competitive inhibition of BAFF-R by means of a fusion protein composed of BAFF and recombinant gelonin toxin named rGel/Blys showes selective killing of B-ALL blasts in preclinical mouse models. Indeed, rGel/Blys binds BAFF-R-expressing blasts, inducing apoptosis upon internalization and release of gelonin toxin that inhibits protein synthesis. Besides, the authors demonstrated an increased efficacy of the fusion protein if combined with AMD3100 which mobilizes leukemic cells from the BM [199]. Another report from the same group proposes an antibody directed towards BAFF-R and optimized for ADCC that displays a reduction in the survival of B-ALL blasts, especially when combined with other drugs such as vincristine and nilotinib, and promotes selective killing of ALL blasts by NK cells [198].

Taken all together, the features of BAFF-R render this antigen an intriguing target for the selective eradication of relapsed/refractory B-ALL.

Scope of the thesis

The goal of the present PhD project was to generate a CAR mediated immunotherapeutic approach targeting BAFF-R as tumor-associated antigen over-expressed by B-ALL blasts. Moreover, will be characterized the impact of modifications into spacer moiety and single chain orientation on CAR expression and stability and on interaction with the antigen through in vitro evaluation of CAR T-cell early and later effector functions.

The first chapter provides a general introduction on B-ALL pathological features, as well as on current and promising therapeutic strategies, focusing in particular on recent advances in the field of CAR T-cell therapy and CAR design, supplying basic literature elements to better understand the present project.

The second chapter presents our first study, focused on the investigation of the potential role of BAFF-BAFF-R axis in B-ALL pediatric patients analyzing this pathway in BM and peripheral blood primary samples obtained at diagnosis, relapse and during the follow-up.

The third chapter presents our second study, focused on the characterization of BAFF-R as a possible immunotherapeutic target for the treatment of refractory/relapsed B-ALL patients, in particular for the CD19-negative ones. In order to identify the anti-BAFFR CAR

characterized by the best interaction with the antigen, the impact of CAR design on modified T cells effector functions has been evaluated. For this reason, CARs with spacer moiety of different lengths and with scFv in the VL-VH orientation or VH-VL have been compared. The development of anti-BAFFR CARs allows to evaluate the cytotoxic profile towards leukemic cell lines and primary samples derived from B-ALL patients. Finally, has been assessed whether the use of pooled T cells expressing anti-BAFFR.CAR and anti-CD19.CAR may be an efficacious dual targeting strategy, equipped with an *in vitro* anti-tumor efficacy higher than single CARs.

The fourth chapter reports our published work about the development of a novel clinical-grade protocol to obtain CAR-modified cytokine-induced killer cells using the Sleeping Beauty transposon system.

The fifth chapter provides general conclusions of the study, summarizing the main findings and describing the future perspectives.

References

1. Chiarini, F. *et al.* Advances in understanding the acute lymphoblastic leukemia bone marrow microenvironment: From biology to therapeutic targeting. *Biochim. Biophys. Acta* **1863,** 449–463 (2015).
2. Greaves, M. Leukemia 'firsts' in cancer research and treatment. *Nat. Rev. Cancer* **16,** 163–172 (2016).
3. Nowell, P. C. The clonal evolution of tumor cell populations. *Science* **194,** 23–8 (1976).
4. Anderson, K. *et al.* Genetic variegation of clonal architecture and propagating cells in leukaemia. *Nature* **469,** 356–61 (2011).
5. Greaves, M. & Maley, C. C. Clonal evolution in cancer. *Nature* **481,** 306–313 (2012).
6. Potter, N. E. *et al.* Single-Cell mutational profiling and clonal phylogeny in cancer. *Genome Res.* **23,** 2115–2125 (2013).
7. Navin, N. E. Cancer genomics: one cell at a time. *Genome Biol.* **15,** 452 (2014).
8. Mullighan, C. G. *et al.* Genomic analysis of the clonal origins of relapsed acute lymphoblastic leukemia. *Science (80-.).* **322,** 1377–1380 (2008).
9. Ma, Y. *et al.* Developmental timing of mutations revealed by whole-genome sequencing of twins with acute lymphoblastic leukemia. *Proc. Natl. Acad. Sci. U. S. A.* **110,** 7429–7433 (2013).
10. Cazzaniga, G. *et al.* Developmental origins and impact of BCR-

ABL1 fusion and IKZF1 deletions in monozygotic twins with Ph + acute lymphoblastic leukemia Developmental origins and impact of BCR-ABL1 fusion and IKZF1 deletions in monozygotic twins with Ph ƨ acute lymphoblastic . **118,** 5559–5564 (2014).

11. Jaiswal, S. *et al.* Age-related clonal hematopoiesis associated with adverse outcomes. *N. Engl. J. Med.* **371,** 2488–98 (2014).
12. Liran I. Shlush, Sasan Zandi, Amanda Mitchell, Weihsu Claire Chen, J. M. B. and V. G. Identification of pre-leukaemic haematopoietic stem cells in acute leukaemia. *Nature* **506,** 328 (2014).
13. Ford, A. M. *et al.* Protracted dormancy of pre-leukemic stem cells. *Leukemia* **29,** 2202–2207 (2015).
14. Huntly, B. J. P. & Gilliland, D. G. Leukaemia stem cells and the evolution of cancer-stem-cell research. *Nat. Rev. Cancer* **5,** 311–321 (2005).
15. Dean, M., Fojo, T. & Bates, S. Tumour stem cells and drug resistance. *Nat Rev Cancer* **5,** 275–284 (2005).
16. Bonnet, D. & Dick, J. E. Human acute myeloid leukemia is organized as a hierarchy that originates from a primitive hematopoietic cell. *Nat. Med.* **3,** 730–737 (1997).
17. Notta, F. *et al.* Evolution of human BCR-ABL1 lymphoblastic leukaemia-initiating cells. *Nature* **469,** 362–367 (2011).
18. Colmone, A. *et al.* Normal Hematopoietic Progenitor Cells. **322,** 1861–1865 (2008).
19. Raaijmakers, M. H. G. P. *et al.* Bone progenitor dysfunction induces myelodysplasia and secondary leukaemia. *Nature* **464,**

852–7 (2010).

20. Dührsen, U. & Hossfeld, D. K. Stromal abnormalities in neoplastic bone marrow diseases. *Ann. Hematol.* **73,** 53–70 (1996).
21. Huan, J. *et al.* RNA trafficking by acute myelogenous leukemia exosomes. *Cancer Res.* **73,** 918–929 (2013).
22. Preston, D. L. *et al.* Cancer incidence in atomic bomb survivors. Part III. Leukemia, lymphoma and multiple myeloma, 1950-1987. *Radiat. Res.* **137,** S68–S97 (1994).
23. Greaves, M. Infection, immune responses and the aetiology of childhood leukaemia. *Nat. Rev. Cancer* **6,** 193–203 (2006).
24. Kinlen, L. Evidence for an infective cause of childhood leukaemia: comparison of a scottish new town with nuclear reprocessing sites in britain. *Lancet* **332,** 1323–1327 (1988).
25. Lange, B. The management of neoplastic disorders of haematopoiesis in children with Down's syndrome. *Br. J. Haematol.* **110,** 512–524 (2000).
26. Korenberg, J. R. *et al.* Down syndrome phenotypes: the consequences of chromosomal imbalance. *Proc. Natl. Acad. Sci. U. S. A.* **91,** 4997–5001 (1994).
27. Little, J. *Epidemiology of Childhood Cancer*. **149,** (1999).
28. Henderson, E. S. & Lister, T. A. *Leukemia*. (1990).
29. Hoelzer. *Neoplastic disease of blood*. (1999).
30. Armstrong, S. A. & Look, A. T. Molecular genetics of acute lymphoblastic leukemia. *J. Clin. Oncol.* **23,** 6306–6315 (2005).
31. Greaves, M. F. & Wiemels, J. Origins of chromosome

translocations in childhood leukaemia. *Nat Rev Cancer* **3,** 639–649 (2003).

32. Romana, S. P. *et al.* The t(12;21) of acute lymphoblastic leukemia results in a tel-AML1 gene fusion. *Blood* **85,** 3662–3670 (1995).
33. Mori, H. *et al.* Chromosome translocations and covert leukemic clones are generated during normal fetal development. *Proc Natl Acad Sci U S A* **99,** 8242–8247 (2002).
34. Yeoh, E. J. *et al.* Classification, subtype discovery, and prediction of outcome in pediatric acute lymphoblastic leukemia by gene expression profiling. *Cancer Cell* **1,** 133–143 (2002).
35. Nourse, J. *et al.* Chromosomal translocation t(1;19) results in synthesis of a homeobox fusion mRNA that codes for a potential chimeric transcription factor. *Cell* **60,** 535–545 (1990).
36. Ribeiro, R. C. *et al.* Clinical and biologic hallmarks of the Philadelphia chromosome in childhood acute lymphoblastic leukemia. *Blood* **70,** 948–53 (1987).
37. Mullighan, C. G. *et al.* Deletion of IKZF1 and prognosis in acute lymphoblastic leukemia. *N. Engl. J. Med.* **360,** 470–480 (2009).
38. Meyer, C. *et al.* The MLL recombinome of acute leukemias in 2013. *Leukemia* **27,** 2165–76 (2013).
39. Pui, C.-H., Relling, M. V & Downing, J. R. Acute lymphoblastic leukemia. *N. Engl. J. Med.* **350,** 1535–1548 (2004).
40. Ye, Z. X. & Wang, S. J. Mixed phenotype acute leukemia. *Chinese Medical Journal* **127,** 2999–3003 (2014).

41. Stein, E. M. & Tallman, M. S. Mixed lineage rearranged leukaemia: pathogenesis and targeting DOT1L. *Curr. Opin. Hematol.* **22,** 92–6 (2015).

42. Russell, L. J. *et al.* Deregulated expression of cytokine receptor gene, CRLF2, is involved in lymphoid transformation in B-cell precursor acute lymphoblastic leukemia. *Blood* **114,** 2688–2698 (2009).

43. Mullighan, C. G. *et al.* Rearrangement of CRLF2 in B-progenitor- and Down syndrome-associated acute lymphoblastic leukemia. *Nat. Genet.* **41,** 1243–6 (2009).

44. Bennett, J. M. *et al.* Proposals for the Classification of the Acute Leukaemias French-American-British (FAB) Co-operative Group. *Br. J. Haematol.* **33,** 451–458 (1976).

45. Bassan, R., Gatta, G., Tondini, C. & Willemze, R. Adult acute lymphoblastic leukaemia. *Crit. Rev. Oncol. Hematol.* **50,** 223–261 (2004).

46. Bene, M. C. *et al.* Proposals for the immunological classification of acute leukemias. European Group for the Immunological Characterization of Leukemias (EGIL). *Leukemia* **9,** 1783–1786 (1995).

47. Ustwani, O. Al *et al.* Clinical updates in adult acute lymphoblastic leukemia. *Crit. Rev. Oncol. Hematol.* **99,** 189–199 (2016).

48. Vardiman JW, Thiele J, A. D. E. A. The 2008 revision of the WHO classification of myeloid neoplasms and acute leukemia: rationale and important changes. *Blood* **114,** 937–952 (2008).

49. Hiroto Inaba, MD, Prof.Mel Greaves, PhD, and Charles G.Mullighan, M. Acute Lymphoblastic Leukemia. *Lancet* **381,** 1–27 (2013).

50. Carroll. *The biology of acute lymphoblastic leukemia, childhood leukemia*. (2011).

51. Pui, C.-H. *et al.* Treating childhood acute lymphoblastic leukemia without cranial irradiation. *N. Engl. J. Med.* **360,** 2730–41 (2009).

52. Pui, C., Campana, D. & Evans, W. W. E. Childhood acute lymphoblastic leukaemia – current status and future perspectives. *Lancet Oncol.* **2,** 597–607 (2001).

53. Mastrangelo, R. *et al.* Report and recommendations of the Rome workshop concerning poor-prognosis acute lymphoblastic leukemia in children: biologic bases for staging, stratification, and treatment. *Med Pediatr Oncol* **14,** 191–194 (1986).

54. Pui, C.-H., Robison, L. L. & Look, A. T. Acute lymphoblastic leukaemia. *Lancet (London, England)* **371,** 1030–43 (2008).

55. Bont, J. M. d. *et al.* Significant difference in outcomes of adolescents with acute lymphoblastic leukemia treated on pediatric versus adult protocols. *Pediatr.Blood Cancer* **43,** 343 (2004).

56. Barry, E. *et al.* Favorable outcome for adolescents with acute lymphoblastic leukemia treated on Dana-Farber Cancer Institute Acute Lymphoblastic Leukemia Consortium protocols. *J. Clin. Oncol.* **25,** 813–819 (2007).

57. Landau, H. & Lamanna, N. Clinical manifestations and treatment of newly diagnosed acute lymphoblastic leukemia in adults. *Curr. Hematol. Malig. Rep.* **1,** 171–179 (2006).

58. Lowe, E. J. *et al.* Early complications in children with acute lymphoblastic leukemia presenting with hyperleukocytosis. *Pediatr. Blood Cancer* **45,** 10–5 (2005).

59. Kadan-Lottick, N. S., Ness, K. K., Bhatia, S. & Gurney, J. G. Survival variability by race and ethnicity in childhood acute lymphoblastic leukemia. *JAMA* **290,** 2008–2014 (2003).

60. Pui, C. & Evans, W. E. Treatment of Acute Lymphoblastic Leukemia. *N. Engl. J. Med.* **354,** 166–178 (2006).

61. Conter, V. *et al.* Molecular response to treatment redefines all prognostic factors in children and adolescents with B-cell precursor acute lymphoblastic leukemia: results in 3184 patients of the AIEOP-BFM ALL 2000 study. *Blood* **115,** 3206–3214 (2010).

62. Barnes DW, Corp MJ, Loutit JF, N. F. Treatment of murine leukaemia with X rays and homologous bone marrow; preliminary communication. *Br. Med. J.* **2,** 626–7 (1956).

63. Weiden, P. L. *et al.* Antileukemic effect of graft-versus-host disease in human recipients of allogeneic-marrow grafts. *N Engl J Med* **300,** 1068–1073 (1979).

64. Couriel, D., Caldera, H., Champlin, R. & Komanduri, K. Acute graft-versus-host disease: Pathophysiology, clinical manifestations, and management. *Cancer* **101,** 1936–1946 (2004).

65. Appelbaum, F. R. Haematopoietic cell transplantation as immunotherapy. *Nature* **411,** 385–389 (2001).

66. Nguyen, K. *et al.* Factors influencing survival after relapse from acute lymphoblastic leukemia: a Children's Oncology Group study. *Leukemia* **22,** 2142–50 (2008).

67. Tallen, G. *et al.* Long-term outcome in children with relapsed acute lymphoblastic leukemia after time-point and site-of-relapse stratification and intensified short-course multidrug chemotherapy: Results of trial ALL-REZ BFM 90. *J. Clin. Oncol.* **28,** 2339–2347 (2010).

68. Hunter, T. The Croonian Lecture 1997. The phosphorylation of proteins on tyrosine: its role in cell growth and disease. *Philos. Trans. R. Soc. Lond. B. Biol. Sci.* **353,** 583–605 (1998).

69. Arora, a & Scholar, E. M. Role of tyrosine kinase inhibitors in cancer therapy. *J Pharmacol Exp Ther* **315,** 971–979 (2005).

70. Schultz, K. R. *et al.* Improved early event-free survival with imatinib in Philadelphia chromosome-positive acute lymphoblastic leukemia: a children's oncology group study. *J. Clin. Oncol.* **27,** 5175–81 (2009).

71. Pui, C.-H. & Jeha, S. New therapeutic strategies for the treatment of acute lymphoblastic leukaemia. *Nat. Rev. Drug Discov.* **6,** 149–65 (2007).

72. Magnani, C. F. *et al.* Advanced targeted, cell and gene-therapy approaches for pediatric hematological malignancies: results and future perspectives. *Front. Oncol.* **3,** 106 (2013).

73. Brown, P. *et al.* FLT3 inhibition selectively kills childhood acute

lymphoblastic leukemia cells with high levels of FLT3 expression. *Blood* **105,** 812–820 (2005).

74. Jabbour, E., Brien, S. O., Ravandi, F. & Kantarjian, H. Monoclonal antibodies in acute lymphoblastic leukemia. *Blood* **125,** 4010–4017 (2015).

75. Hochberg, J., El-Mallawany, N. K. & Cairo, M. S. Humoral and cellular immunotherapy in ALL in children, adolescents, and young adults. *Clin. Lymphoma, Myeloma Leuk.* **14,** S6–S13 (2014).

76. Hoelzer, D. Targeted therapy with monoclonal antibodies in acute lymphoblastic leukemia. *Curr. Opin. Oncol.* **25,** 701–6 (2013).

77. Coiffier, B. *et al.* Long-term outcome of patients in the LNH-98 . 5 trial , the first randomized study comparing rituximab-CHOP to standard CHOP chemotherapy in DLBCL patients : a study by the Groupe d ' Etudes des Lymphomes de l ' Adulte. *Blood* **116,** 1–8 (2010).

78. Sousou, T. & Friedberg, J. Rituximab in indolent lymphomas. *Semin. Hematol.* **47,** 133–142 (2010).

79. Thomas, D. A. *et al.* Chemoimmunotherapy with hyper-CVAD plus rituximab for the treatment of adult Burkitt and Burkitt-type lymphoma or acute lymphoblastic leukemia. *Cancer* **106,** 1569–1580 (2006).

80. Thomas, D. A. *et al.* Chemoimmunotherapy with a modified hyper-CVAD and rituximab regimen improves outcome in de novo Philadelphia chromosome - Negative precursor B-lineage

acute lymphoblastic leukemia. *J. Clin. Oncol.* **28,** 3880–3889 (2010).

81. Wierda, W. G. *et al.* Ofatumumab as single-agent CD20 immunotherapy in fludarabine-refractory chronic lymphocytic leukemia. *J. Clin. Oncol.* **28,** 1749–1755 (2010).

82. Jabbour, E. *et al.* Phase II Study Of The Hyper-CVAD Regimen In Combination With Ofatumumab As Frontline Therapy For Adults With CD20 Positive Acute Lymphoblastic Leukemia (ALL). *ASH Abstr.* 2664 (2013).

83. Thomas, X. Inotuzumab ozogamicin in the treatment of B-cell acute lymphoblastic leukemia. *Expert Opin. Investig. Drugs* **21,** 871–8 (2012).

84. Kantarjian, H. *et al.* Inotuzumab ozogamicin, an anti-CD22-calecheamicin conjugate, for refractory and relapsed acute lymphocytic leukaemia: A phase 2 study. *Lancet Oncol.* **13,** 403–411 (2012).

85. Nagorsen, D., Kufer, P., Baeuerle, P. A. & Bargou, R. Blinatumomab: A historical perspective. *Pharmacol. Ther.* **136,** 334–342 (2012).

86. Löffler, A. *et al.* A recombinant bispecific single-chain antibody, CD19 x CD3, induces rapid and high lymphoma-directed cytotoxicity by unstimulated T lymphocytes. *Blood* **95,** 2098–103 (2000).

87. Topp, M. S. *et al.* Phase II trial of the anti-CD19 bispecific T cell-engager blinatumomab shows hematologic and molecular remissions in patients with relapsed or refractory B-precursor

acute lymphoblastic leukemia. *J. Clin. Oncol.* **32,** 4134–4140 (2014).

88. Bassan, R. Toward victory in adult ALL: Blinatumomab joins in. *Blood* **120,** 5094–5095 (2012).

89. June, C. H. C. Adoptive T cell therapy for cancer in the clinic. *J. Clin. Invest.* **117,** 1466–1476 (2007).

90. Kolb, H. J. *et al.* Donor leukocyte transfusions for treatment of recurrent chronic myelogenous leukemia in marrow transplant patients. *Blood* **76,** 2462–2465 (1990).

91. Deol, A. & Lum, L. G. Role of donor lymphocyte infusions in relapsed hematological malignancies after stem cell transplantation revisited. *Cancer Treatment Reviews* **36,** 528–538 (2010).

92. Marks, D. I. *et al.* The toxicity and efficacy of donor lymphocyte infusions given after reduced-intensity conditioning allogeneic stem cell transplantation. *Blood* **100,** 3108–3114 (2002).

93. Keil, F. *et al.* Donor leukocyte infusion for leukemic relapse after allogeneic marrow transplantation: lack of residual donor hematopoiesis predicts aplasia. *Blood* **89,** 3113–3117 (1997).

94. Rosenberg, S. A., Spiess, P. & Lafreniere, R. A new Approach To the Adoptive Immunotherapy of Cancer With Tumor-Infiltrating Lymphocytes. *Science (80-.).* **233,** 1318–1321 (1986).

95. Rosenberg, S. A. & Restifo, N. P. Adoptive cell transfer as personalized immunotherapy for human cancer. *Science (80-.).* **348,** 62–68 (2015).

96. Lu, P. H. & Negrin, R. S. A novel population of expanded human CD3+CD56+ cells derived from T cells with potent in vivo antitumor activity in mice with severe combined immunodeficiency. *J. Immunol.* **153,** 1687–1696 (1994).

97. Alvarnas, J. C., Linn, Y.-C., Hope, E. G. & Negrin, R. S. Expansion of cytotoxic CD3+ CD56+ cells from peripheral blood progenitor cells of patients undergoing autologous hematopoietic cell transplantation. *Biol. Blood Marrow Transplant.* **7,** 216–222 (2001).

98. Giroux, M. & Denis, F. CD1d-unrestricted human NKT cells release chemokines upon Fas engagement. *Blood* **105,** 703–710 (2005).

99. Linn, Y. C. *et al.* Characterization of the recognition and functional heterogeneity exhibited by cytokine-induced killer cell subsets against acute myeloid leukaemia target cell. *Immunology* **126,** 423–435 (2009).

100. Siegel, J. P. & Puri, R. K. Interleukin-2 toxicity. *J. Clin. Oncol.* **9,** 694–704 (1991).

101. Pievani, A. *et al.* Dual-functional capability of CD3 +CD56 + CIK cells, a T-cell subset that acquires NK function and retains TCR-mediated specific cytotoxicity. *Blood* **118,** 3301–3310 (2011).

102. Edinger, M. *et al.* Revealing lymphoma growth and the efficacy of immune cell therapies using in vivo bioluminescence imaging. *Blood* **101,** 640–648 (2003).

103. Nishimura, R. *et al.* In vivo trafficking and survival of cytokine-induced killer cells resulting in minimal GVHD with retention of

antitumor activity. *Blood* **112,** 2563–2574 (2008).

104. Mase, S. *et al.* Allogeneic Cytokine-Induced Killer Cells Eliminate Host Dendritic Cells Due To The Enhanced Killing Activity By IFN-Gamma , Leading To Less Graft-Versus-Host Disease. *ASH Abstr.* **122,** 4495 (2013).
105. Marin, V. *et al.* Characterization of in vitro migratory properties of anti-CD19 chimeric receptor-redirected CIK cells for their potential use in B-ALL immunotherapy. *Exp. Hematol.* **34,** 1218–1228 (2006).
106. Schmeel, L. C., Schmeel, F. C., Coch, C. & Schmidt-Wolf, I. G. H. Cytokine-induced killer (CIK) cells in cancer immunotherapy: report of the international registry on CIK cells (IRCC). *J. Cancer Res. Clin. Oncol.* **141,** 839–849 (2015).
107. Introna, M. *et al.* Repeated infusions of donor-derived cytokine-induced killer cells in patients relapsing after allogeneic stem cell transplantation: a phase I study. *Haematologica* **92,** 952–959 (2007).
108. Lussana, F. *et al.* Final Analysis of a Multicenter Pilot Phase 2 Study of Cytokine Induced Killer (CIK) Cells for Patients with Relapse after Allogeneic Transplantation. *ASH Abstr.* 1160 (2016).
109. Ramos, C. A. & Dotti, G. Chimeric antigen receptor (CAR)-engineered lymphocytes for cancer therapy. *Expert Opin. Biol. Ther.* **11,** 855–73 (2011).
110. Pule, M., Finney, H. & Lawson, A. Artificial T-cell receptors. *Cytotherapy* **5,** 211–226 (2003).

111. Bachmann, M. *et al.* Chimeric antigen receptor-engineered T cells for immunotherapy of cancer. *J. Biomed. Biotechnol.* **2010,** (2010).

112. Ma, Q., Gonzalo-Daganzo, R. M. & Junghans, R. P. Genetically engineered T cells as adoptive immunotherapy of cancer. *Cancer Chemother Biol Response Modif.* **20,** 315–341 (2002).

113. Biagi, E. *et al.* Chimeric T-cell receptors: New challenges for targeted immunotherapy in hematologic malignancies. *Haematologica* **92,** 381–388 (2007).

114. Kershaw, M. H., Teng, M. W. L., Smyth, M. J. & Darcy, P. K. Supernatural T cells: genetic modification of T cells for cancer therapy. *Nat. Rev. Immunol.* **5,** 928–940 (2005).

115. Rappl, G. *et al.* The CD3-zeta chimeric antigen receptor overcomes TCR hypo-responsiveness of human terminal late-stage t cells. *PLoS One* **7,** 1–10 (2012).

116. Kowolik, C. M. *et al.* CD28 costimulation provided through a CD19-specific chimeric antigen receptor enhances in vivo persistence and antitumor efficacy of adoptively transferred T cells. *Cancer Res.* **66,** 10995–11004 (2006).

117. Long, A. H. *et al.* 4-1BB costimulation ameliorates T cell exhaustion induced by tonic signaling of chimeric antigen receptors. *Nat. Med.* **21,** 581–90 (2015).

118. Milone, M. C. *et al.* Chimeric receptors containing CD137 signal transduction domains mediate enhanced survival of T cells and increased antileukemic efficacy in vivo. *Mol Ther* **17,** 1453–1464 (2009).

119. Tammana, S. *et al.* 4-1BB and CD28 signaling plays a synergistic role in redirecting umbilical cord blood T cells against B-cell malignancies. *Hum. Gene Ther.* **21,** 75–86 (2010).

120. Pule, M. A. *et al.* Virus-specific T cells engineered to coexpress tumor-specific receptors: persistence and antitumor activity in individuals with neuroblastoma. *Nat. Med.* **14,** 1264–70 (2008).

121. Park, T. S., Rosenberg, S. A. & Morgan, R. A. Treating cancer with genetically engineered T cells. *Trends Biotechnol.* **29,** 550–557 (2011).

122. Morgan, R. a *et al.* Case report of a serious adverse event following the administration of T cells transduced with a chimeric antigen receptor recognizing ERBB2. *Mol. Ther.* **18,** 843–851 (2010).

123. Ferrara, J., Abhyankar, S. & Gilland, D. cytokine storm of graft-versus-host-disease: a critical effector role for interleukin-1. *Transpl. Proc* **25,** 1216–1217 (1993).

124. Teachey, D. T. & Grupp, S. A. Cytokine Release Syndrome after Haploidentical Stem Cell Transplantation. *Biol. Blood Marrow Transplant.* **22,** 1736–1737 (2016).

125. Teachey, D. T. *et al.* Cytokine release syndrome after blinatumomab treatment related to abnormal macrophage activation and ameliorated with cytokine-directed therapy. *Blood* **121,** 5154–5157 (2013).

126. Xu, X. J. *et al.* Inflammatory cytokine measurement quickly discriminates gram-negative from gram-positive bacteremia in pediatric hematology/oncology patients with septic shock.

Intensive Care Med. **39,** 319–326 (2013).

127. de Jong, M. D. *et al.* Fatal outcome of human influenza A (H5N1) is associated with high viral load and hypercytokinemia. *Nat. Med.* **12,** 1203–1207 (2006).
128. Bugelski, P. J., Achuthanandam, R., Capocasale, R. J., Treacy, G. & Bouman-Thio, E. Monoclonal antibody-induced cytokine-release syndrome. *Expert Rev. Clin. Immunol.* **5,** 499–521 (2009).
129. Xu, X. J. & Tang, Y. M. Cytokine release syndrome in cancer immunotherapy with chimeric antigen receptor engineered T cells. *Cancer Lett.* **343,** 172–178 (2014).
130. Henter, J. I. *et al.* HLH-2004: Diagnostic and therapeutic guidelines for hemophagocytic lymphohistiocytosis. *Pediatric Blood and Cancer* **48,** 124–131 (2007).
131. Davila, M. L. *et al.* Efficacy and toxicity management of 19-28z CART cell therapy in B cell acute lymphoblastic leukemia. *Sci. Transl. Med.* **6,** 224ra25 (2014).
132. Brentjens, R. J. *et al.* Safety and persistence of adoptively transferred autologous CD19-targeted T cells in patients with relapsed or chemotherapy refractory B-cell leukemias. *Blood* **118,** 4817–4828 (2011).
133. Maus, M. V., Grupp, S. A., Porter, D. L. & June, C. H. Antibody-modified T cells: CARs take the front seat for hematologic malignancies. *Blood* **123,** 2625–2635 (2014).
134. Moritz, D. & Groner, B. A spacer region between the single chain antibody-and the CDS ζ-chain domain of chimeric T cell

receptor components is required for efficient ligand binding and signaling activity. *Gene Therapy* **2,** 539–546 (1995).

135. Guest, R. D. *et al.* The role of extracellular spacer regions in the optimal design of chimeric immune receptors: evaluation of four different scFvs and antigens. *J Immunother* **28,** 203–211 (2005).
136. Hudecek, M. *et al.* Receptor affinity and extracellular domain modifications affect tumor recognition by ROR1-specific chimeric antigen receptor T cells. *Clin. Cancer Res.* **19,** 3153–3164 (2013).
137. Hudecek, M. *et al.* The nonsignaling extracellular spacer domain of Chimeric Antigen Receptors is decisive for in vivo antitumor activity. *Cancer Immunol. Res.* **3,** 125–135 (2015).
138. Hombach, A., Hombach, A. & Abken, H. Adoptive immunotherapy with genetically engineered T cells: modification of the IgG1 Fc 'spacer' domain in the extracellular moiety of chimeric antigen receptors avoids 'off-target' activation and unintended initiation of an innate immune response. *Gene Ther.* **17,** 1206–121391 (2010).
139. Clemenceau, B. *et al.* In Vitro and In Vivo Comparison of Lymphocytes Transduced with a Human CD16 or with a Chimeric Antigen Receptor Reveals Potential Off-Target Interactions due to the IgG2 CH2-CH3 CAR-Spacer. *J. Immunol. Res.* **2015,** (2015).
140. Kay, M. A. *et al.* Viral vectors for gene therapy : the art of turning infectious. *Nat. Publ. Gr.* **7,** 33–40 (2001).

141. Scholler, J. *et al.* Decade-long safety and function of retroviral-modified chimeric antigen receptor T cells. *Sci. Transl. Med.* **4,** 132ra53 (2012).

142. Ginn, S. L., Alexander, I. E., Edelstein, M. L., Abedi, M. R. & Wixon, J. Gene therapy clinical trials worldwide to 2012 - an update. *Journal of Gene Medicine* **15,** 65–77 (2013).

143. Bessis, N., GarciaCozar, F. J. & Boissier, M.-C. Immune responses to gene therapy vectors: influence on vector function and effector mechanisms. *Gene Ther.* **11 Suppl 1,** S10–S17 (2004).

144. Muruve, D. a. The innate immune response to adenovirus vectors. *Hum. Gene Ther.* **15,** 1157–1166 (2004).

145. Thomas, C. E., Ehrhardt, A. & Kay, M. a. Progress and problems with the use of viral vectors for gene therapy. *Nat. Rev. Genet.* **4,** 346–358 (2003).

146. Cattoglio, C. *et al.* High-definition mapping of retroviral integration sites identifies active regulatory elements in human multipotent hematopoietic progenitors. *Blood* **116,** 5507–5517 (2010).

147. Hackett, P. B., Largaespada, D. A. & Cooper, L. J. A Transposon and Transposase System for Human Application. *Mol. Ther.* **18,** 674–683 (2010).

148. Izsvák, Z., Chuah, M. K. L., VandenDriessche, T. & Ivics, Z. Efficient stable gene transfer into human cells by the Sleeping Beauty transposon vectors. *Methods* **49,** 287–297 (2009).

149. Baus, J., Liu, L., Heggestad, A. D., Sanz, S. & Fletcher, B. S.

Hyperactive transposase mutants of the Sleeping Beauty transposon. *Mol. Ther.* **12,** 1148–1156 (2005).

150. Ivics, Z., Hackett, P. B., Plasterk, R. H. & Izsvák, Z. Molecular Reconstruction of Sleeping Beauty, a Tc1-like Transposon from Fish, and Its Transposition in Human Cells. *Cell* **91,** 501–510 (1997).
151. Geurts, A. M. *et al.* Gene transfer into genomes of human cells by the Sleeping Beauty transposon system. *Mol. Ther.* **8,** 108–117 (2003).
152. Izsvák, Z., Ivics, Z. & Plasterk, R. H. Sleeping Beauty, a wide host-range transposon vector for genetic transformation in vertebrates. *J. Mol. Biol.* **302,** 93–102 (2000).
153. Magnani, C. F. *et al.* Immunotherapy of acute leukemia by chimeric antigen receptor-modified lymphocytes using an improved Sleeping Beauty transposon platform. *Oncotarget* **5,** (2016).
154. Wang, K., Wei, G. & Liu, D. CD19: a biomarker for B cell development, lymphoma diagnosis and therapy. *Exp. Hematol. Oncol.* **1,** 36 (2012).
155. Davila, M. L., Kloss, C. C., Gunset, G. & Sadelain, M. CD19 CAR-Targeted T Cells Induce Long-Term Remission and B Cell Aplasia in an Immunocompetent Mouse Model of B Cell Acute Lymphoblastic Leukemia. *PLoS One* **8,** 1–14 (2013).
156. Kochenderfer, J. N. *et al.* Eradication of B-lineage cells and regression of lymphoma in a patient treated with autologous T cells genetically engineered to recognize Brief report

Eradication of B-lineage cells and regression of lymphoma in a patient treated with autologous T cells. **116,** 4099–4102 (2010).

157. Brentjens, R. *et al.* CD19-targeted T cells rapidly induce molecular remissions in adults with chemotherapy-refractory acute lymphoblastic leukemia. *Sci Transl Med* **5,** 177–38 (2013).
158. Maude, S. L. *et al.* Chimeric Antigen Receptor T Cells for Sustained Remissions in Leukemia. *N. Engl. J. Med.* **371,** 1507–1517 (2014).
159. Lee, D. W. *et al.* T cells expressing CD19 chimeric antigen receptors for acute lymphoblastic leukaemia in children and young adults: A phase 1 dose-escalation trial. *Lancet* **385,** 517–528 (2015).
160. Maude, S. L. Sustained remissions with CD19-specific chimeric antigen receptor (CAR)-modified T cells in children with relapsed/refractory ALL. *ASCO2016l* (2016).
161. Grupp, S. A. *et al.* Durable Remissions in Children with Relapsed/Refractory ALL Treated with T Cells Engineered with a CD19-Targeted Chimeric Antigen Receptor (CTL019). *Blood* **126,** 681 LP-681 (2015).
162. Ruella, M. *et al.* Dual CD19 and CD123 targeting prevents antigen-loss relapses after CD19-directed immunotherapies. *J. Clin. Invest.* **126,** 3814–3826 (2016).
163. Sotillo, E. *et al.* Convergence of acquired mutations and alternative splicing of CD19 enables resistance to CART-19 immunotherapy. *Cancer Discov.* **5,** 1282–1295 (2015).
164. Gardner, R. *et al.* Acquisition of a CD19-negative myeloid

phenotype allows immune escape of MLL-rearranged B-ALL from CD19 CAR-T-cell therapy. *Blood* **127,** 2406–2410 (2016).

165. Rayes, A., Mcmasters, R. L. & O'Brien, M. M. Lineage Switch in MLL-Rearranged Infant Leukemia Following CD19-Directed Therapy. *Pediatr. Blood Cancer* **63,** 1113–1115 (2016).
166. Jacoby, E. *et al.* CD19 CAR immune pressure induces B-precursor acute lymphoblastic leukaemia lineage switch exposing inherent leukaemic plasticity. *Nat. Commun.* **7,** 12320 (2016).
167. Braig, F. *et al.* Resistance to anti-CD19/CD3 BiTE in acute lymphoblastic leukemia may be mediated by disrupted CD19 membrane trafficking. *Blood* (2016). doi:10.1182/blood-2016-05-718395
168. Haso, W. *et al.* Anti-CD22-chimeric antigen receptors targeting B-cell precursor acute lymphoblastic leukemia. *Blood* **121,** 1165–1171 (2013).
169. Haso, W., Qin, H., Zhang, L., Orentas, R. J. & Fry, T. J. CD22-Targeted Chimeric Antigen Receptor (CAR) T Cells Containing The 4-1BB Costimulatory Domain Demonstrate Enhanced Persistence and Superior Efficacy Against B-Cell Precursor Acute Lymphoblastic Leukemia (ALL). *Blood* **122,** 1431 (2013).
170. Fry, T. J. *et al.* Clinical Activity and Persistence of Anti-CD22 Chimeric Antigen Receptor in Children and Young Adults with Relapsed/Refractory Acute Lymphoblastic Leukemia (ALL). *Blood* **126,** 1324 (2015).
171. Anurathapan, U. *et al.* Kinetics of tumor destruction by

chimeric antigen receptor-modified T cells. *Mol Ther* **22,** 623–633 (2014).

172. Hegde, M. *et al.* Combinational targeting offsets antigen escape and enhances effector functions of adoptively transferred T cells in glioblastoma. *Mol. Ther.* **21,** 2087–101 (2013).

173. Hegde, M. *et al.* Tandem CAR T cells targeting HER2 and IL13Ralpha2 mitigate tumor antigen escape. *J. Clin. Invest.* **126,** 3036–3052 (2016).

174. Mackay, F. & Browning, J. L. BAFF: a fundamental survival factor for B cells. *Nat. Rev. Immunol.* **2,** 465–475 (2002).

175. Mackay, F. & Schneider, P. Cracking the BAFF code. *Nat. Rev. Immunol.* **9,** 491–502 (2009).

176. Schneider, P. *et al.* BAFF, a novel ligand of the tumor necrosis factor family, stimulates B cell growth. *J. Exp. Med.* **189,** 1747–56 (1999).

177. Naradikian, M. S., Perate, A. R. & Cancro, M. P. BAFF receptors and ligands create independent homeostatic niches for B cell subsets. *Curr. Opin. Immunol.* **34,** 126–129 (2015).

178. Vincent, F. B., Saulep-Easton, D., Figgett, W. A., Fairfax, K. A. & Mackay, F. The BAFF/APRIL system: Emerging functions beyond B cell biology and autoimmunity. *Cytokine Growth Factor Rev.* **24,** 203–215 (2013).

179. Avery, D. T. *et al.* BAFF selectively enhances the survival of plasmablasts generated from human memory B cells. *J. Clin. Invest.* **112,** 286–297 (2003).

180. O'Connor, B. P. *et al.* BCMA is essential for the survival of long-lived bone marrow plasma cells. *J. Exp. Med.* **199,** 91–8 (2004).
181. Xu, S. & Lam, K.-P. B-cell maturation protein, which binds the tumor necrosis factor family members BAFF and APRIL, is dispensable for humoral immune responses. *Mol. Cell. Biol.* **21,** 4067–74 (2001).
182. Yan, M. *et al.* Identification of a receptor for BLyS demonstrates a crucial role in humoral immunity. *Nat. Immunol.* **1,** 37–41 (2000).
183. Von Bülow, G. U., Van Deursen, J. M. & Bram, R. J. Regulation of the T-independent humoral response by TACI. *Immunity* **14,** 573–582 (2001).
184. Day, E. S. *et al.* Selectivity of BAFF/BLyS and APRIL for binding to the TNF family receptors BAFFR/BR3 and BCMA. *Biochemistry* **44,** 1919–1931 (2005).
185. Mihalcik, S. a, Huddleston, P. M., Wu, X. & Jelinek, D. F. The structure of the TNFRSF13C promoter enables differential expression of BAFF-R during B cell ontogeny and terminal differentiation. *J. Immunol.* **185,** 1045–54 (2010).
186. Tussiwand, R., Rauch, M., Flück, L. A. & Rolink, A. G. BAFF-R expression correlates with positive selection of immature B cells. *Eur. J. Immunol.* **42,** 206–216 (2012).
187. Warnatz, K. *et al.* B-cell activating factor receptor deficiency is associated with an adult-onset antibody deficiency syndrome in humans. *Proc. Natl. Acad. Sci. U. S. A.* **106,** 13945–50 (2009).
188. Gross, J. A. *et al.* TACI-Ig neutralizes molecules critical for B cell

development and autoimmune disease: Impaired B cell maturation in mice lacking BLyS. *Immunity* **15,** 289–302 (2001).

189. Thompson, J. S. *et al.* BAFF-R, a newly identified TNF receptor that specifically interacts with BAFF. *Science (80-.).* **293,** 2108–2111 (2001).
190. Grumont, R. J., Strasser, A. & Gerondakis, S. B Cell growth is controlled by phosphatidylinosotol 3-kinase-dependent induction of Rel/NF-κB regulated c-myc transcription. *Mol. Cell* **10,** 1283–1294 (2002).
191. Bannish, G., Fuentes-Pananá, E. M., Cambier, J. C., Pear, W. S. & Monroe, J. G. Ligand-independent Signaling Functions for the B Lymphocyte Antigen Receptor and Their Role in Positive Selection during B Lymphopoiesis. *J. Exp. Med* **121400,** 1583–1596 (2001).
192. Stadanlick, J. E. & Cancro, M. P. BAFF and the plasticity of peripheral B cell tolerance. *Curr. Opin. Immunol.* **20,** 158–161 (2008).
193. Thien, M. *et al.* Excess BAFF rescues self-reactive B cells from peripheral deletion and allows them to enter forbidden follicular and marginal zone niches. *Immunity* **20,** 785–798 (2004).
194. Sarantopoulos, S. *et al.* Altered B-cell homeostasis and excess BAFF in human chronic graft-versus-host disease. *Blood* **113,** 3865–3874 (2009).
195. Rodig, S. J., Shahsafaei, A., Li, B., Mackay, C. R. & Dorfman, D. M. BAFF-R, the major B cell-activating factor receptor, is

expressed on most mature B cells and B-cell lymphoproliferative disorders. *Hum. Pathol.* **36,** 1113–1119 (2005).

196. Parameswaran, R., Muschen, M., Kim, Y. M., Groffen, J. & Heisterkamp, N. A functional receptor for B-cell-activating factor is expressed on human acute lymphoblastic leukemias. *Cancer Res.* **70,** 4346–4356 (2010).
197. Maia, S. *et al.* Aberrant expression of functional baff-system receptors by malignant b-cell precursors impacts leukemia cell survival. *PLoS One* **6,** (2011).
198. Parameswaran, R. *et al.* Effector-Mediated Eradication of Precursor B Acute Lymphoblastic Leukemia with a Novel Fc-Engineered Monoclonal Antibody Targeting the BAFF-R. *Mol. Cancer Ther.* **13,** 1567–77 (2014).
199. Parameswaran, R. *et al.* Treatment of acute lymphoblastic leukemia with an rGel/BLyS fusion toxin. *Leukemia* **26,** 1786–96 (2012).

Chapter 2

BAFF-Receptor is expressed both at diagnosis and relapse in childhood B-Cell Precursor Acute Lymphoblastic Leukemia

Fazio G.[1], **Turazzi N.[1]**, Cazzaniga V.[1], Kreuzaler M.[2], Maglia O.[1], Magnani CF.[1], Biagi E.[1], Rolink A.[2], Biondi A.[1] and Cazzaniga G.[1]

[1]Centro Ricerca Tettamanti, Clinica Pediatrica, Università di Milano-Bicocca, Osp.San Gerardo/Fondazione MBBM, Monza, Italy

[2]Department of Biomedicine, University of Basel, Switzerland

Manuscript submitted

B cell-activating factor (BAFF) and proliferation-inducing ligand (APRIL) belong to the tumor necrosis factor (TNF) family.[1,2] Physiologically, BAFF mediates the behavior of most B cells through interactions with its family receptors.[3] However, only the BAFF receptor (BAFF-R) interacts specifically with BAFF, being the main responsible for primary B cell survival, selection and differentiation, in physiological and disease conditions.[4,5,6] A role for BAFF/BAFFR has been proposed in autoimmune diseases; indeed, the BAFF/BAFF-R system plays a key role in the development of autoimmunity,[7] especially in systemic lupus erythematosus (SLE).[8] Moreover, a role for BAFF/BAFF-R was revealed in patients who developed Graft-versus Host Disease, with delayed reconstitution of naïve B cells despite persistent BAFF elevation.[9] This feature delineated specific abnormalities of B cell homeostasis in patients with cGVHD and suggested that BAFF/BAFF-R targeting agents may be useful in this disease.[9] However, few data are available on a direct role of BAFF/BAFF-R axis in B-cell disorders, such as in hematological malignancies.[10,11] Interestingly, a physiological role for BAFF-R has been shown not only in mature B cells but also during the development of precursor B cells.[12]

Herein, we aimed to investigate the potential role of BAFF/BAFF-R axis in B-Cell Precursor Acute Lymphoblastic Leukemia (BCP-ALL). With this purpose, we analyzed the pathway in primary BM and PB samples from children affected by BCP-ALL, both at diagnosis, follow-up and relapse, as well as in hematological tumor cell lines. RT-PCR and RQ-PCR assays were implemented to determine *BAFF* and *BAFF-*

R expression in BCP-ALL patient samples and in leukemic cell lines (see detail in Supplementary file), while BAFF-R protein on blast cells in BM and PB at diagnosis and in follow-up samples was assessed by Flow cytometry analysis. ELISA analysis has been used to evaluate BAFF concentration in plasma samples.

Firstly, we investigated *BAFF-R* gene expression in leukemic cell lines, in normal hematopoietic tissues and BCP-ALL blast cells, demonstrating that BAFF-R is expressed in patient samples at diagnosis as well as in B-lymphoid leukemic cell lines, such as MUTZ5, REH, TOM1 and NALM-6 (Supplemental Figure S1). Its expression is also detectable, although at lower levels, in mixed lymphoid/myeloid phenotype cell lines (such as THP1 and RS4;11), in myeloid K562 cells as well as in U937 histiocytic lymphoma cell lines (Supplemental Figure S1). By RQ-PCR analysis, we showed that BAFF-R was highly expressed in BCP-ALL cell lines (MUTZ-5 and CALL-4), in healthy donors BM and PBMCs (RNA commercial library, Human Total Master Panel II, Clontech, Takara, Takara Bio Europe, Saint-Germain-en-Laye, France), and in BCP-ALL samples, although with a wide range of expression (Figure 1). Data are expressed as fold change, calculated with the ΔΔCt method,[13] using as a reference the stomach organ.

Supported by these data, we further investigated BAFF-Receptor protein expression in diagnostic and short-term follow up BCP-ALL samples. We collected BM and/or PB of 26 consecutive diagnostic samples of pediatric BCP-ALL, enrolled in the AIEOP-BFM ALL2009 protocol in Monza. For each patient, in addition to the diagnostic sample, we analyzed at least one follow up sample (i.e. PB at day +8

or both PB/BM at day +15, if available). We analyzed BAFF-R expression by flow cytometry, using a biotinilated anti-BAFF-R antibody revealed by PE-conjugated streptavidin antibody. In the same sample, we used the hCD19 (FITC), hCD10 (APC) and hCD45 (PerCP) direct staining to recognize leukemic blast cells (CD45dim expression on CD10+/CD19+ cells) among the residual normal cells (CD45-high expression on CD10-/CD19+ cells). Interestingly, at diagnosis we detected high levels of BAFF-R on CD19+/CD10+/CD45dim leukemic cells (mean of 18.96% $\pm$22.68 and 32.20%$\pm$25.31, in n=25 BM and n=26 PB, respectively). Overall data are reported in Figure 2A, while Supplementary Table S1 reports detailed results of FACS analyses, and a representative phenotype of each time point is shown in Supplementary Figure S2.

Importantly, BAFF-R protein persisted during the follow up treatment. At day +8, the residual tumor burden was very low due to pharmacological treatment by Prednisone or Dexamethasone, according to the randomization in the current AIEOP-BFM ALL2009 treatment protocol. At day+8, we detected a statistically significant increase of BAFF-R, up to 63.18% ($\pm$21.66) as compared to diagnosis PB samples (T test, $p=2.86x10^{-5}$, n=22) (Figure 2A). A statistically significant increase of BAFF-R in PB leukemic cells is still shown at day+15 (66.37$\pm$21.18) (T test versus diagnostic levels, $p=1.58x10^{-4}$, n=12). In BM at day+15, we detected an increase up to 58.01% ($\pm$21.77) compared to diagnostic BM samples (T test, $p=1.82x10^{-4}$, n=10) (Figure 2A). The statistical analyses have been performed by ANOVA with Bonferroni's Multiple Comparison Test, confirming the

significance of T test in all comparisons (PB DX vs. PB day+8 and PB day+15, BM DX vs. BM day+15, with p values <0.001).

In PB leukemic samples at BCP-ALL diagnosis, we detected high plasmatic BAFF concentrations (4.57±5.58 ng/ml, n=16) (Figure 2B, left panel), significantly higher than in BM (T test, p=0.038, n=7) and PB day +8 (p=0.018, n=17), also compared to healthy donors reported in a previous study[14]. Detailed results are reported in Supplementary Table S2 and in Figure 2B. More interestingly, by expressing the ratio of BAFF level (ng/ml) over the number CD19+ blast cells (n°/mmc), we could demonstrate that the BAFF cytokine is consumed by blast cells at diagnosis, and its level reaches physiological threshold after leukemic cell clearance, in early follow up samples (Figure 2B, right panel).

In the 6 patients who experienced ALL relapse, we had the opportunity to assess BAFF-R expression in matched samples of diagnosis vs. intermediate remission vs. relapse (Supplementary Table S3). To avoid any confounding effect due to experimental time delay, we performed contemporarily the staining of matched samples of diagnosis/remission/relapse, using frozen available samples for all time points (Anti-human CD268/ BAFF-R PE-conjugated antibody, Ancell Corporation, Bayport, MN, USA). In all patients, BAFF-R expression showed a trend towards a reduction in the remission phase and subsequent increase in relapse, similar to the diagnostic level. Indeed, mean BAFF-R expression on total CD19+ cells was 48.50% (±11.46, range 38.4-67.2) at diagnosis, 31.87% (±6.58, 21.6-41.2) at remission and 56.40% (±17.52, 38.4-88.7) at

relapse, while the BAFF-R expression in normal BM was 20.80% (±11.34, 11.2-34.20) (Figure 2C and Supplementary Table S3). Although the number of available relapsed samples was rather low, both the decrease from diagnosis to remission (36% less) and the successive increase to relapse (77% high) reached a statistical significance (T test, p=0.02 in both comparison), whereas the difference between diagnostic and relapse value was not significant (16% increase, T test p=0.38).

Altogether, in the present study we assessed the expression of BAFF-R on leukemic blast cells of BCP-ALL patients. Of note, during the early drug treatment, its expression is maintained or even increased on residual tumor cells, suggesting a positive selection and survival of BAFF-R positive blast cells. Moreover, leukemic cells can have a role in BAFF cytokine consuming in presence of a bulk disease (e.g. at the onset of disease). Data in relapsed cases further suggest the potential importance of BAFF/BAFF-R pathway, demonstrating the persistence of tumor cells bearing the receptor at levels higher than on normal B-cells of the same patient and respect to healthy donors. Although additional studies are required to comprehend its role in the pathogenesis of leukemia, the present data revealed that BAFF/BAFF-R axis could have a role in BCP-ALL, thus suggesting the potential targeting of these molecules in future advanced treatment approaches.

Supplementary Methods

RNA Isolation

Total RNA was extracted following the standard guanidinium thiocyanate-phenol-chloroform extraction method,[1] both in patients' and cell line samples.

RT-PCR

One μg of total RNA was reversely transcribed to cDNA with Superscript II reverse transcriptase (Thermo Fisher Scientific, Invitrogen Corporation, MA USA). RT-PCR was performed on cell lines cDNA, using following BAFF-REC or BAFF specific primers to amplify both genes: hBAFF-left 5'-CCTCACGGTGGTGTCTTTCT-3' and hBAFF-right 5'-GTCCCATGGCGTAGGTCTTA-3' (product length 449 bp); hBAFFR-left 5'-TCATTCTGTCTCCGGGAATC-3' and hBAFFR-right 5'-AAGGGCTGTCAAAGATGGTG (product length 382 bp). All the RT-PCR reactions were performed in the following conditions: one activation step (2' at 94°C), thirty-five cycles of amplification (30 s at 94°C, 30 s at 60°C, 30 s at 72°C), using Platinum® Taq DNA Polymerase (Thermo Fisher Scientific).

RQ-PCR

Quantitative RT-PCR experiments on cells were performed using Light Cycler 480II with Universal Probe Master system (Roche Diagnostics, Basel, Switzerland).

BAFF-Receptor primers were selected according to the Software Probe Finder (Roche Diagnostics) and are reported here: hBAFFRupl-left 5'-CTGGTCCTGGTGGGTCTG-3', hBAFFRupl-right 5'-ACCTTGTCCA-GGGGCTCT-3'. UPL probe number 78 was used in combination.

Data were expressed using the comparative ΔΔCt method, [2] using two housekeeping genes as reference: ABL1 (QIAGEN *Ipsogen* ABL Control Gene Standards kit, QIAGEN GmbH, Hilden, Germany) and HPRT1 (Human HPRT1 (HGPRT) Endogenous Control VIC⁄MGB Probe, Thermo Fisher Scientific, Applied Biosystems Corporation, MA USA). Three independent replicates were performed.

Supplementary References

1 Chomczynski, P. & Sacchi, N. Single-step method of RNA isolation by acid guanidinium thiocyanate-phenol-chloroform extraction. *Anal Biochem* **162**, 156-159, doi:10.1006/abio.1987.9999-0003-2697(87)90021-2 (1987).

2 Livak, K. & Schmittgen, T. D. Analysis of relative gene expression data using real-time quantitative PCR and the 2(-Delta Delta C(T)) Method. *Methods* **25**, 402-408 (2001).

Figures

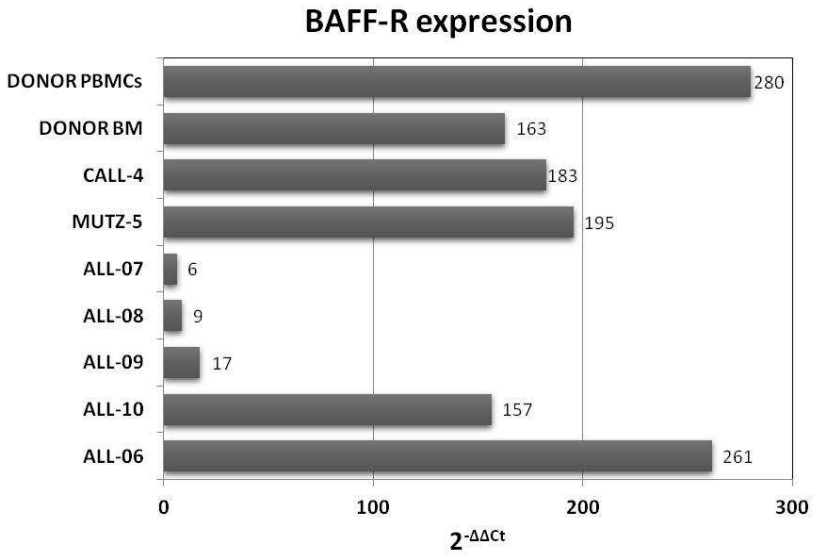

Figure 1. RQ-PCR BAFF-R in normal tissues, leukemic cell lines and BCP-ALL patients. On X axis, its expression is showed as fold change, calculated as $2^{-\Delta\Delta Ct}$ using as reference in stomach organ used as calibrator ($2^{-\Delta\Delta Ct}$ =1), which is included in a RNA library of normal tissues, together with healthy BM and PBMCs (RNA commercial library, Human Total Master Panel II, Clontech). RNA library samples are extracted from different human organs and the subjects are both male and female.

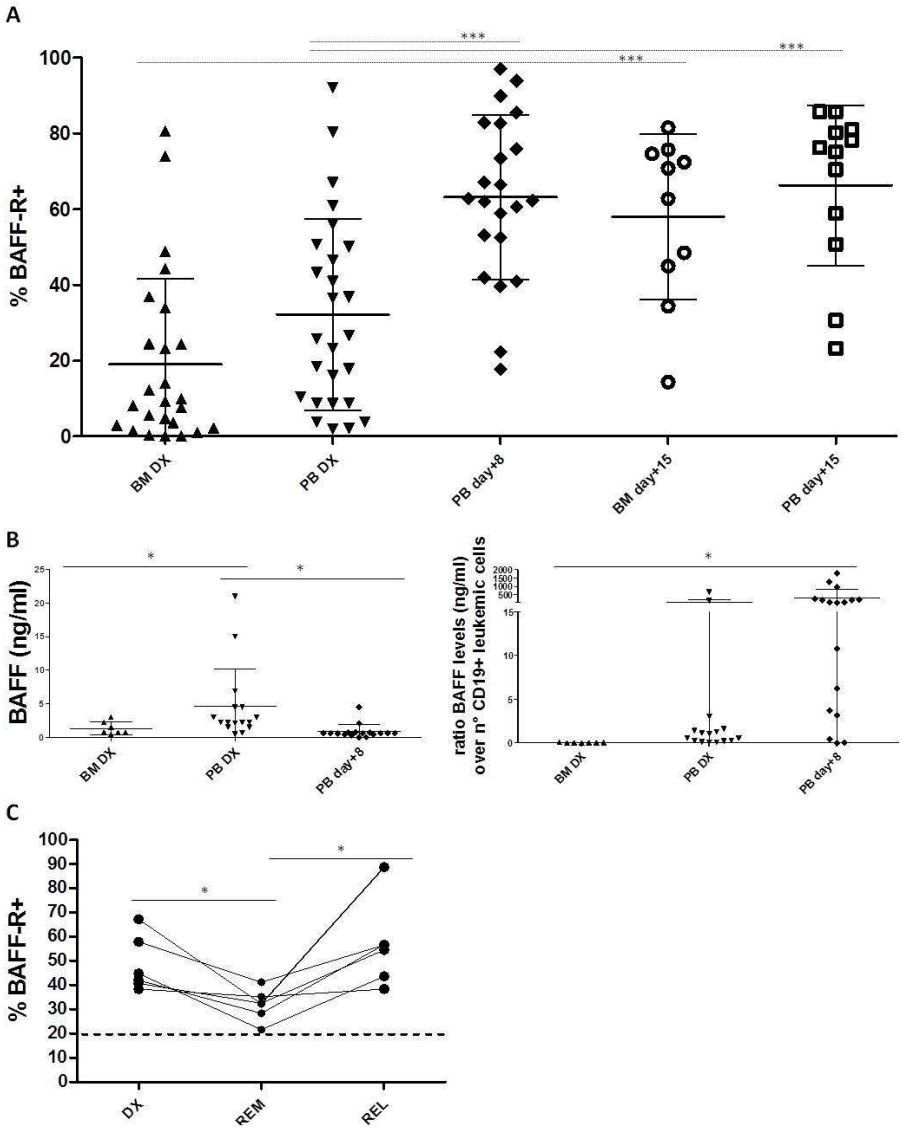
A
***
***
***
100
80
60
40
20
0
% BAFF-R+
BM DX
PB DX
PB day+8
BM day+15
PB day+15
B
*
*
BAFF (ng/ml)
25
20
15
10
5
0
BM DX
PB DX
PB day+8
*
ratio BAFF levels (ng/ml) over n° CD19+ leukemic cells
2000
1500
1000
500
15
10
5
0
BM DX
PB DX
PB day+8
C
*
*
% BAFF-R+
100
90
80
70
60
50
40
30
20
10
0
DX
REM
REL

Figure 2. (A) BAFF-R protein persists on diagnostic and follow up samples at day+8 and +15 (FACS ANALYSIS gated on CD19+CD10+CD45dim leukemic cells). The T test statistical analyses revealed the significance in all comparisons, PB DX vs. PB day+8 and PB day+15, BM DX vs. BM day+15, with p values <0.001 (indicated by ***), in addition to BM DX vs. PB day+15 (***), BM DX vs. PB day+8 (***) and PB DX vs. BM day+15 (*) (not indicated graphically). (B) BAFF is detected in plasmatic samples of B-ALL, by ELISA as shown in left panel. More importantly, BAFF is consumed by leukemic cells, as shown by calculating ratio between cytokine level and number of CD19 positive leukemic cells (right panel). (C) BAFF-Receptor is expressed on leukemic cells at diagnosis, at lower levels on normal B cells at remission, increasing on leukemic cells at an eventual relapse. In all Figures, T test statistical analysis is indicated by * ($p<0.05$), ** ($p<0.01$), *** ($p<0.001$).

A

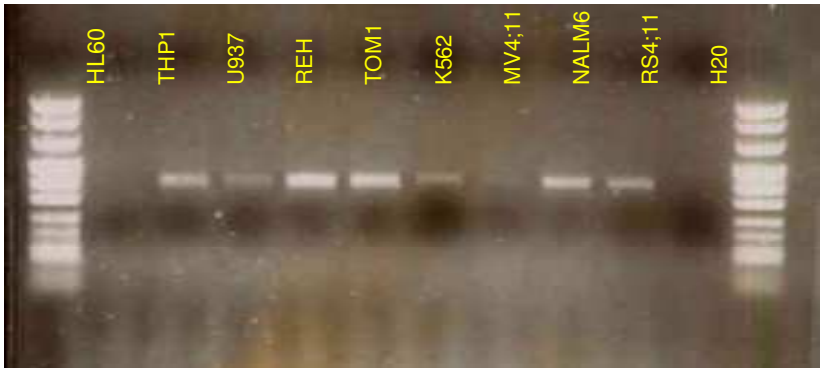

B

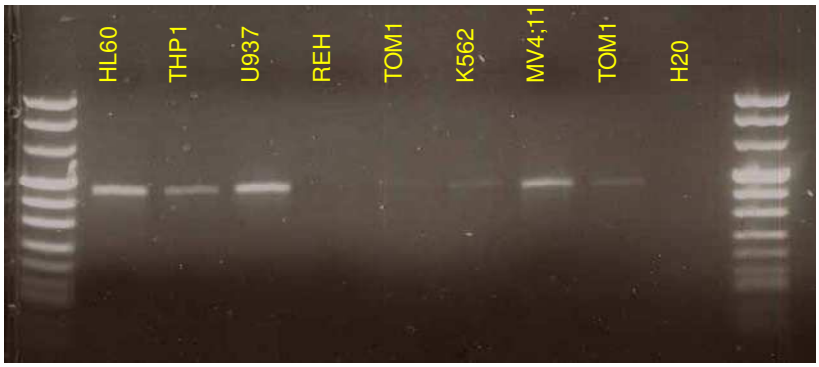

Supplementary Figure S1. (A) RT-PCR BAFF-REC in leukemic cell lines demonstrated its expression in pre-B but not in HL-60 cells. (B) RT-PCR BAFF in leukemic cell lines.

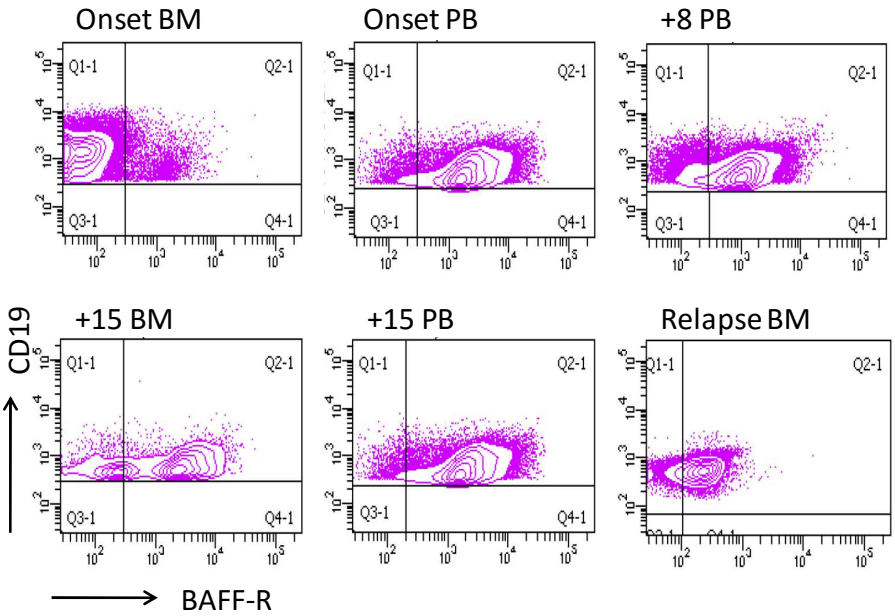

Supplementary Figure S2 Representative phenotype of a BCP-ALL patient.

REFERENCES

1 Bossen, C. & Schneider, P. BAFF, APRIL and their receptors: Structure, function and signaling. *Seminars in immunology* **18**, 263-275, doi:10.1016/j.smim.2006.04.006 (2006).

2 Daridon, C., Youinou, P. & Pers, J.-O. BAFF, APRIL, TWE-PRIL: Who's who? *Autoimmunity Reviews* **7**, 267-271, doi:10.1016/j.autrev.2007.05.002 (2008).

3 Mackay, F. & Browning, J. L. BAFF: A fundamental survival factor for B cells. *Nature Reviews Immunology* **2**, 465-475, doi:10.1038/nri844 (2002).

4 Rolink, A. G. & Melchers, F. BAFF led B cells survive and thrive: roles of BAFF in B-cell development. *Curr Opin Immunol* **14**, 266-275, doi:S0952791502003321 [pii] (2002).

5 Cancro, M. P. Living in Context with the Survival Factor BAFF. *Immunity* **28**, doi:10.1016/j.immuni.2008.02.010 (2008).

6 Gardam, S., Sierro, F., Basten, A., Mackay, F. & Brink, R. TRAF2 and TRAF3 Signal Adapters Act Cooperatively to Control the Maturation and Survival Signals Delivered to B Cells by the BAFF Receptor. *Immunity* **28**, 391-401, doi:10.1016/j.immuni.2008.01.009 (2008).

7 Gommerman, J. L. & Browning, J. L. Lymphotoxin/LIGHT, lymphoid microenvironments and autoimmune disease. *Nature Reviews Immunology* **3**, doi:10.1038/nri1151 (2003).

8 Vincent, F. B., Saulep-Easton, D., Figgett, W. A., Fairfax, K. A. & Mackay, F. The BAFF/APRIL system: Emerging functions

beyond B cell biology and autoimmunity. *Cytokine & Growth Factor Reviews* **24**, 203-215, doi:10.1016/j.cytogfr.2013.04.003 (2013).

9 Sarantopoulos, S. *et al.* Altered B-cell homeostasis and excess BAFF in human chronic graft-versus-host disease. *Blood* **113**, 3865-3874, doi:10.1182/blood-2008-09-177840 (2009).

10 Hildebrand, J. M. *et al.* A BAFF-R mutation associated with non-Hodgkin lymphoma alters TRAF recruitment and reveals new insights into BAFF-R signaling. *The Journal of Experimental Medicine* **207**, 2569-2579, doi:10.1084/jem.20100857 (2010).

11 Tangye, S. G., Bryant, V. L., Cuss, A. K. & Good, K. L. BAFF, APRIL and human B cell disorders. *Seminars in immunology* **18**, 305-317, doi:10.1016/j.smim.2006.04.004 (2006).

12 Tussiwand, R., Rauch, M., Flück, L. A. & Rolink, A. G. BAFF-R expression correlates with positive selection of immature B cells. *European Journal of Immunology* **42**, 206-216, doi:10.1002/eji.201141957 (2012).

13 Livak, K. & Schmittgen, T. D. Analysis of relative gene expression data using real-time quantitative PCR and the 2(-Delta Delta C(T)) Method. *Methods* **25**, 402-408 (2001).

14 Kreuzaler, M. *et al.* Soluble BAFF Levels Inversely Correlate with Peripheral B Cell Numbers and the Expression of BAFF Receptors. *The Journal of Immunology* **188**, 497-503, doi:10.4049/jimmunol.1102321 (2011).

Chapter 3

BAFF Receptor (BAFF-R)-redirected T cells efficiently target B-Cell Acute Lymphoblastic Leukemia (B-ALL)

Turazzi, N.[1], Fazio, G.[1], Rossi, V.[1], Rolink, A.[2], Cazzaniga, G.[1], Biondi, A.[1], Magnani, C.F.[1], Biagi, E.[1]

[1]Centro Ricerca Tettamanti, Clinica Pediatrica, Università di Milano-Bicocca, Osp.San Gerardo/Fondazione MBBM, Monza, Italy

[2]Department of Biomedicine, University of Basel, Switzerland

Manuscript submitted

ABSTRACT

B-cell Acute Lymphoblastic Leukemia (B-ALL) is most common in children (80%), but it has also a peak of incidence in adult age. Recently, immunotherapeutic approaches targeting the CD19 molecule have demonstrated remarkable success in the treatment of relapsed and refractory B-ALL, which remains a major clinical need. Important downsides of these strategies are the emergence of CD19-negative relapses and B-cell aplasia as a result of anti-CD19 CAR T-cell persistence. In this context, we hypothesized that the receptor for B-cell activating factor (BAFF-R), a transmembrane protein fundamental in B-cell maturation and survival, could be an interesting molecule to be targeted, taking the advantage that this receptor is undetectable on bone marrow B-cell precursors.

Here we showed that BAFF-R is highly expressed in B-ALL primary samples at the onset and relapse. In order to develop a chimeric antigen receptor (CAR) approach targeting BAFF-R molecule, six anti-BAFFR CAR genes that differ for the inversion of the VH and VL and the length of the spacer domain have been generated. Cytokine-induced Killer (CIK) cells, engineered using an improved *Sleeping Beauty* (SB) transposon system, stably expressed anti-BAFFR.CARs, and maintained their characteristic phenotype. Among the newly constructed CARs, the shortest VHVL CAR exerted the highest anti-leukemic activity towards target cells, such as NALM-6, with an *in vitro* killing activity of 60%. We also evaluated later effector functions in terms of cytokine release by intracellular staining (8,9±2% of IFN-γ

and 16,4±5,5% of IL-2 producing cells). Importantly, we also detected a specific cytotoxic activity towards primary B-ALL blasts (average 65,6±4,5%, n=9). Simultaneous incubation of INVsh.CAR and CD19.CAR CIK positive cells together with ALL targets resulted in superior antitumor activity compared to the single CAR population.

Furthermore, by using a sample collected from a patient relapsed with CD19 negative disease, we demonstrated the ability of the INVsh.CAR to lysate CD19-negative blasts.

Taken together, these findings make this receptor a safe and attractive target for a second line B-ALL immunotherapy in case of relapse after CD19-targeting therapies or for a double targeted approach. Being restricted to mature B cells, but absent in precursors and plasmablasts, our strategy could have an inferior toxicity concerning the emergence of B-cell aplasia observed in patients treated with anti-CD19 CAR-modified T cells.

INTRODUCTION

Patients with refractory/relapsed (R/R) B-ALL are still difficult to cure with standard chemotherapies, being an unmet clinical need in children and, particularly, in adults who demonstrated the poorest prognosis with an overall survival of 30-40% [1]. The possibility to redirect T cell activity towards malignant cells has dramatically modified the therapy concept in different tumor subtypes [2–4]. Among these, the outcome of R/R B-ALL has definitely changed with the advent of CD19-targeted immunotherapies such as anti-CD19 CAR T cells and anti-CD3/CD19 BiTE (Blinatumomab), generating outstanding complete response rates [5]. Blinatumomab is able to recruit patient's own cytotoxic T cells and induce a transient synapse between T cells and tumor cells, necessary for the lysis of malignant cells. Hence, a continuous infusion is essential to ensure drug activity [6]. On the other hand, T cells genetically modified *ex vivo* to express an anti-CD19 chimeric receptors (CARs) are able to recognize and kill tumor cells, proliferating and being persistent up to several years [7]. Despite an initial optimism with an observed response rate of 90% evaluated at 1 month and an EFS of around 70% at 6 months, selective pressure and tumor plasticity led to the appearance of CD19-negative relapses in around 45% of patients with a median follow-up of around 12 months [8]. This side effect rises doubts about a real significant role done by CD19 antigen in leukemia fitness until now attributed to intracellular kinases recruitment. In this regard, very recently, Weiland and colleagues demonstrated that B-ALL

leukemic blasts that lose the expression of CD19 continue to be able to survive, proliferate and engraft NSG mice [9]. Moreover, these data support previous reported observations about the ability of $CD34^{+}/CD19^{-}$ primary blasts to maintain leukemia in immunodeficient mice [10].

BAFF-R is one of the main receptors recognized by BAFF cytokine. During B-cell development, BAFF-R is expressed starting from immature B cells, upon acquiring a functional B cell receptor (BCR), and it is responsible for maturation and survival of B cells [11–14]. BAFF-R is over-expressed in a wide range of B-cell lymphoproliferative disorders such as mantle cell lymphomas, splenic marginal zone lymphomas, MALT lymphomas, follicular lymphomas, hairy cell leukemia and B-cell chronic lymphocytic leukemia (B-CLL) and B-ALL [15,16]. Moreover, in B-ALL context, BAFF has been detected not only on malignant B cells themselves, but also within the leukemic niche where endothelial cells produce and secrete this cytokine. In the niche, BAFF exerts a paracrine support promoting the survival, proliferation and resistance of B-ALL blasts to chemotherapy [15,17,18]. Considering this characteristics, multiple therapeutic strategies have been tested in B-ALL setting in order to avoid the interaction between BAFF and BAFF-R, by blocking, in this way, the autocrine/paracrine loop of stimulation, which showed selective killing of B-ALL blasts in preclinical mouse models. For example, the competitive inhibition of BAFF-R by means of a fusion protein composed of BAFF and recombinant gelonin toxin named rGel/Blys shows selective killing of B-ALL blasts in preclinical mouse models

inducing apoptosis upon internalization and release of gelonin toxin that inhibits protein synthesis [19]. Another report from the same group proposes an antibody directed towards BAFF-R and optimized for antibody-dependent cellular cytotoxicity (ADCC) that displays a reduction in the survival of B-ALL blasts, especially when combined with other drugs such as vincristine and nilotinib, and promotes selective killing of ALL blasts by NK cells [15,18,19].

Here we proposed an additional modality to target BAFF-R exploiting the CAR-based approach. Therefore, we generated and tested an anti-BAFFR CARs panel, comprising six constructs that differ for the inversion of the VH and VL and the length of the spacer domain, with the purpose to select the one which retains the best distance for optimal interaction with the antigen. With the aim of preventing tumor escape, we simultaneously targeted both CD19 and BAFF-R molecules demonstrating a superior antitumor activity of the combination *in vitro*. We also found that BAFF-R expression is maintained by samples from a CD19-negative relapsed patient and that $CD45^{+}CD19^{-}$ blasts can be lysed by selected anti-BAFFR.CAR *in vitro* in combination with CD19.CAR.

Materials and Methods

Cell lines and primary cells

NALM-6 and REH cell lines have been obtained from the American Type Culture Collection (ATCC, Manassas, Virginia, USA). Cell lines were maintained in culture with Advanced RPMI medium (Invitrogen, San Giuliano Milanese, Italy) supplemented with 10% heat-inactivated Fetal Bovine Serum (FBS), 2 mM L-glutamine, 25 IU/ml of penicillin and 25 mg/ml of streptomycin (Lonza, Bergamo, Italy).

Bone marrow and peripheral blood cells from children with B-ALL were collected and frozen at diagnosis, and relapse. The Institutional Review Board of the Ethical Committee of San Gerardo Hospital approved this study and informed consent was obtained from patients or their guardians according to institutional guidelines and to the Helsinki Declaration.

Plasmids production

The high-affinity human scFv for the CD19 antigen was generated starting from the DNA encoding mAb clone FMC63 kindly provided by Martin Pule, University College of London, UK. The scFv was cloned in frame with CH2CH3-CD28-OX40-ζ from SFG-anti-CD33-CD28-OX40-ζ as a transposon into a SB expression plasmid, pT-MNDU3-eGFP replacing the eGFP sequence to obtain anti-CD19/pTMNDU3.

The codon-optimized plasmid for SB transposase, pCMV-SB11, was obtained from University of Minnesota, USA.

Anti-BAFFR.CARs were generated starting from the DNA encoding mAb clone HuBR9.1, kindly provided by Antonius Rolink, University of Basel, Switzerland. The DNA sequence of anti-BAFFR scFv with canonical (VL-VH) or inverted (VH-VL) orientation were cloned in place of the anti-CD19 scFv to obtain anti-BAFFR/pTMNDU3 and anti-INV.BAFFR/pTMNDU3 plasmids. Intermediate and short anti-BAFFR and anti-INV.BAFFR variants were generated using overlapping PCR or the *In-Fusion* cloning system (*In-Fusion* HD Cloning Kit, Clontech, Takara Bio USA, Inc., Mountain View, USA). Two sets of primers were designed for overlapping PCR: for amplification of fragment 1, FW1 (5' GGGTTCGACTTTTCCAGGTACTGGATGTCTTGGGTGCGC 3') and RV1 (5' AACCACCACCAGCACCCAAAAGGCGCTCAC-GGTGACCAGTGTG 3'); and for amplification of fragment 2, FW2 (5' CACACTGGTCACCGTGAGC-GCCTTTTGGGTGCTGGTGGTGGTT 3') and RV2 (5' ATAGGGCTGGTAA-TGCTTGCGGGTGGGCCC 3'). The used PCR program has been reported below:

98°C	2min	
98°C	42sec	} 30 cycles
68°C	30sec	
72°C	30sec	
72°C	10min	
16°C	∞	

PCR products were separated by gel electrophoresis and purified using QIAquick Gel Extraction Kit (Qiagen, Hilden, Germania) according to the manufacturer's protocol. Subsequently the amplified fragment and anti-BAFFR/pTMNDU3 plasmid were digested

with Van91I and ApaI restriction enzymes and ligated using Rapid DNA Dephos & Ligation kit (Roche, Basel, Switzerland).

Primer sets for In-Fusion cloning system were designed using SnapGene program and listed below: FW-Frag-VLVH - 5' GGATCT-ACTGGCGATGATGTGCTGATG 3'; FW-Frag-VHVL - 5' GGATCTACT-GGCGATGAGGTCAAGCTG 3'; RV-Frag-short - 5' ACCCATACATGCCCCC-CTTGTCCTTTTTGGGTGCTGGTG 3'; RV-Frag-Int - 5' CCATACATGCCCC-CCTTGTCCTGGGCAGCCCCGAGAA; FW-Vect-short - 5' TTTTGGGTGCT-GGTGGTGGT 3'; FW-Vect-Int - 5' GGGCAGCCCCGAGAAC 3'; RV-Vect - 5' GCCCGGATCTACTGGCGAT 3'. Primers pairs shared 15 homologous bases at each end. The PCR amplification reactions were performed using CloneAmp HiFi PCR Premix (Clontech, Takara Bio USA, Inc.) in a total volume of 20µL containing 12.5µL of 5x Premix, 1 µL (7.5 µM) of each primer, 1ng of each plasmid DNA and H_2O. The PCR reaction was made using the following cycling conditions:

98°C	10sec	} 30 cycles
55°C	15sec	
72°C	5sec/kb	

PCR amplification products of the expected sizes were purified with NucleoSpin Gel and PCR Clean-up kit (Macherey-Nagel, Düren, Germany). To generate final products, was performed the In-Fusion cloning reaction in a total volume of 20µL containing 4µL of 5x In-Fusion HD Enzyme Premix, 10ng of Insert fragment, 50ng of Vector fragment and H_2O. The reaction mix was incubated 15min at 50°C. Subsequently each reaction was used for competent cells

transformation (Stellar Competent Cells, Clontech, Takara Bio USA, Inc.).

Cytotoxic Induced Killer (CIK)-cell generation and modification with CAR plasmids

CIK cells were generated starting from human PBMCs from healthy donors, obtained after centrifugation of fresh blood on a density gradient using Ficoll-Hypaque (Pharmacia LKB, Uppsala, Sweden). Then, PBMCs were resuspended in Amaxa Nucleofector solution, provided with the P3 Primary Cell 4D-Nuceofector X kit (Lonza, Bergamo, Italy), together with 5 µg of pCMV-SB11 plasmid encoding for SB11X transposase and 15 µg of DNA plasmids encoding for one of the anti-BAFFR.CAR variants and transfected using the 4D-Amaxa Nucleofector™ device (Lonza). As positive control of modification efficiency, the Amaxa GFP episomal plasmid was used. As positive control of expression and efficacy or as alternative target antigen CD19.CAR and CD123.CAR were used. After nucleofection, PBMCs were transferred into a 6-well plate containing 4 ml of pre-warmed medium (Advanced RPMI supplemented with 20% of heat-inactivated FBS and 1% of L-glutamine) and 1000 U/ml of IFN-γ (Dompè Biotec S.p.A, Milano, Italy) were added into each well. Moreover, according to our established optimized platform (patent EP3018200A1)[20] PBMCs from the same source, irradiated with 60Gy of 137Cs γ-rays, were added to previously electroporated samples. Twenty-four hours later, IL-2 (Chiron B.V, Emeryville, USA) and OKT-3 (Janssen-Cilag S.p.A., Cologno Monzese, Italy) were added at 300 U/ml and at 50

ng/ml, respectively. Fresh medium and IL-2 were added twice a week and cell concentration was maintained around $0.75x10^6$ cells/ml. Cells were then cultured for 21 days.

Flow cytometry

Immunostaining and flow cytometric analysis were performed with the following antibodies: Allophycocianin (APC)-anti-CD123 (Becton Dickinson, BD, San Jose, USA), Phycoerythrin (PE)-anti-CD123 (BD), Peridinin-chlorophyll-protein complex (PerCP)-anti-CD45 (BD), PerCP-anti-CD3, PE-anti-CD56 (BD), Fluorescein isothiocyanate (FITC)-anti-CD8 (BD), PE anti-CD4 (BD), PE-anti-CD62L (BD), FITC-anti-CD45RO (BD), Alexa Fluor 647- F(ab')2-anti-IgG (H+L) (anti-Fc), PE-anti-IL-2, FITC-anti-IFN-γ, FITC-anti-CD19 (BD), PE-anti-CD19 (BD), APC-anti-CD10 (eBioscience, San Diego, USA), FITC-anti-CD107a (BD), PE-anti-BAFFR (Vinci-Biochem, Florence, Italy).

To detect CARs deprived of spacer region a BAFFR-Fc fusion protein specific to human anti-BAFFR CARs was used before proceeding with anti-Fc staining (R&D Systems, Minneapolis, MN). Engineered T cells were incubated 15 minutes at room temperature with 100µL of BAFFR-Fc chimera (1µg/mL). Cells were washed with 200 µL of wash buffer and then were stained at room temperature for 15 minutes with Alexa Fluor 647 labeled anti-Fc.

Cell death and apoptosis were detected using the GFP-Certified™ Apoptosis/Necrosis detection kit (Enzo Life Sciences, Inc., Farmingdale, NY, USA), according to the manufacturer's instructions. Cell membrane labeling was also performed using 5(6)-

Carboxyfluorescein diacetate N-succinimidyl ester (CFSE) (eBioscience).

To quantify the number of CD19 and BAFF-R molecules on the surface of the target cell lines and primary ALL samples, we used the QuantiBRITE PE^{TM} fluorescence quantitation kit (BD), which allows the conversion of cell fluorescence intensity values into absolute numbers of receptors per cell, through the creation of a calibration curve.

Flow cytometry was performed on FACSCanto II flow cytometer (BD), and data were analyzed using BD FACS DIVA software version 6.1.3.

Quantitative Real-time PCR analysis for detection of BAFF-R mRNA

Total RNA was extracted from samples collected from B-ALL patients and cell lines using RNeasy Mini kit (Qiagen, Hilden, Germany). For examining the expression of BAFF-R gene in human normal tissues, Human Total RNA Master Panel II was purchased from Clontech (Takara Bio USA, Inc., Mountain View, CA, USA). The cDNA was synthesized with SuperScript II Reverse Transcriptase in the presence of RNaseOUT Ribonuclease Inhibitor (Life Technologies, Carlsbad, CA), according to manufacturer's instructions. cDNA samples (25ng RNA equivalent) were run in triplicate, and levels of BAFF-R transcript were determined as relative expression by normalizing with ABL and HPRT (Applied Biosystems, Foster City, CA), housekeeping genes.

Cytotoxic assays

To evaluate the killing ability of both unmodified and CAR-redirected CIK cells, cytotoxic assays were performed. In this assays CIK cells were co-cultured for 4 hours or overnight with CD19/BAFF-R positive targets (NALM-6, REH and primary ALL blasts), previously labeled with CFSE, at an Effector:Target (E:T) *ratio* of 5:1. At the end of the incubation, target cell killing was measured through the apoptosis detection by flow cytometry gating on the $CFSE^+$ target cells. The percentage of dead cells was calculated according to the following formula:

$$\frac{(\%\ of\ Annexin\ V^+target\ cells + \%\ of\ Annexin\ V^+7AAD^+target\ cells)\ after\ co-culture\ with\ CIK\ cells}{(\%\ of\ Annexin\ V^+target\ cells + \%\ of\ Annexin\ V^+7AAD^+target\ cells)\ alone}$$

Alternatively, flow cytometry-based quantitative analysis was employed by using counting beads (Flow-Count™ Fluorospheres, Backman Coulter, Milan, Italy).

Gating on ($hCD45^+HLA\text{-}DR^+CD3^-$) target cells, the percentage of viable target cells recovered from culture was determined using the following formula:

$$\%\ of\ viable\ cells = \frac{(n°\ of\ target\ cells)\ after\ co-culture\ with\ CIK\ cells}{(n°\ of\ target\ cells)\ alone}\ x\ 100$$

$$\%\ of\ dead\ cells = 100\% - \%\ of\ viable\ cells$$

Degranulation Assay

T-cell degranulation was evaluated by using a CD107a flow cytometric assay. The day before we prepare BAFFR-coated wells by diluting BAFF-R protein in Tris-HCl 0,1M, ph 9,5, to a final concentration of 10μg/mL. The next day CIK cells were plated with target cells, at an E:T *ratio* of 1:1, in the presence anti-CD107a FITC mAb (4 μL/well). After 2 hours and 30 minutes, monensin A (Sigma-Aldrich, St Louis, MO) was added (30 μg/mL). After additional 2 hours and 30 minutes of incubation, cells were washed and stained with anti-CD3 and anti-Fc.

Cytokine detection with intracellular staining (ICS) assay

Cytokines producing ability of CAR-modified CIK cells was evaluated following a 5-hour co-culture with CD19/BAFF-R positive targets at an E:T *ratio* of 1:3. After 2 hours and 30 minutes, BD GolgiStop™ was added. The co-culture was then maintained for additional 2 hours and 30 minutes, after which cells were collected and stained for the anti-CD3 and anti-Fc. Finally, an intracellular cytokine staining for IL-2 and IFN-γ, was performed using the BD Cytofix/Cytoperm kit, according to manufacturer's protocol. Specimens were then acquired by flow cytometry.

Proliferation assay

The proliferation ability of CAR-modified CIK cells was evaluated after co-culture with target cells γ-irradiated at 60 Gy at an E:T *ratio* of 1:2. CIK cells were pre-labeled with CFSE. After a 5 days co-culture, cells

were collected, stained for CD3 and anti-Fc and then analyzed by flow cytometry, by performing the detection of $CFSE^{+}$ cells.

Statistical analysis

Data were analyzed using GraphPad Prism 5 software (GraphPad Software Inc). Paired t test, One Way ANOVA and Two Way ANOVA statistical tests were performed according to the type of data set analyzed. Values of the statistical analyses are reported as Mean ± SEM. All P values are provided in the figure legends.

Results

Leukemic B-ALL blasts express BAFF-R at diagnosis and at relapse

In order to evaluate the specificity of BAFF-R distribution we assessed the mRNA expression in normal tissues and pathological samples. As expected, BAFF-R mRNA is absent in analysed normal tissues except for B cell-containing organs such as BM, spleen and peripheral blood. Conversely, BAFF-R mRNA is strongly represented in B-ALL cell lines and primary samples (Figure 1A). BAFF-R is expressed on the surface of most B-ALL blast samples obtained from the same patients at onset and at relapse. We detected a statistically significant increase in percentage of BAFF-R expressing cells in relapses (54,9±4,6%) if compared to diagnostic samples (44,3±5,1%, n=20) (Figure 1B and C). Because of its favourable expression pattern, BAFF-R could be then considered as target antigen for the development of a CAR-mediated immunotherapeutic approach.

Spacer domain modification affects CAR expression but its elimination augments tumor recognition

After obtaining the sequences of the variable regions from a BAFF-R specific monoclonal antibody, we generated two anti-BAFF-R CAR expressing plasmids with different VL and VH orientation, hereinafter named as BAFFR.CAR the one with canonical VLVH orientation and INV.CAR the one with inverted VHVL orientation. Since we did not have the possibility to know where the recognized epitope was located, we generated and compared a panel of anti-BAFFR CARs that

were different for the length of the spacer domain (hereinafter named as intermediate and short according to the presence of CH3 domain only or complete absence of CH2CH3 moiety)(Figure 2A). Using a previously optimized Sleeping Beauty transposon platform, CIK effector cells where genetically modified with anti-BAFFR variants expressing plasmids. The characteristic CIK cell phenotype was minimally affected and comparable to NO DNA control, except for CD4/CD8 proportion in INV.CAR and short INV.CAR (INVsh.CAR) conditions (*Supplementary Figure S1A and S1B*). CIK cells modified with anti-BAFFR CARs showed an exponential growth, which is typical of this effector population, comparable to NO DNA, CD19.CAR and CD123.CAR controls (*Supplementary Figure S1C*).

In order to verify the impact of spacer modification, transfection efficiency was evaluated at the end of the culture (day 21). Short BAFFR.CAR (BAFFRsh.CAR, 15,7±4%) and both intermediate (18,3±5,2% for BAFFRint.CAR and 14,7±5,8% for INVint.CAR) conditions showed a reduced transfection efficiency in terms of percentage of CAR positive cells. Conversely, effector cells were efficiently modified with BAFFR.CAR (42,1±10,8%), INV.CAR (66,3±8,8%) and INVsh.CAR (52±8%) (Figure 2B and D). Furthermore, in comparison to INV.CAR (4392±1052) we observed a decreased CAR expression in terms of mean fluorescence intensity of INVsh.CAR (1612±334) (Figure 2C).

Analysis of the *in vitro* cytotoxic activity of anti-BAFFR CARs demonstrated that only short variants showed a specific anti-leukemic killing activity towards NALM-6 cell line that accounts for

59±3,2% for BAFFRsh.CAR and 61,7±3,5% for INVsh.CAR (Figure 3A and B). However, only INVsh.CAR exerted superior later effector functions (8,9±2% of IFN-γ and 16,4±5,5% of IL-2 producing cells) upon stimulation with NALM-6 compared to other variants (Figure 3C). In order to further screen newly constructed anti-BAFFR CARs for their ability to specifically interact with the antigen, we evaluated the degranulation ability upon stimulation with coated BAFF-R antigen which is independent from the distance of the recognized epitope from the cell membrane. This assay showed that only inverted variants were able to optimally degranulate after antigen recognition (Figure 3D).

These results underline that an inverted VHVL orientation and the removal of CH2CH3 domain allowed a better interaction with the target antigen, suggesting that the used scFv binds to an epitope positioned in the membrane-distal region of BAFF-R protein [21].

INVsh.CAR variant retains superior anti-tumor activity towards B-ALL targets than INV.CAR variant

After the initial characterization, we selected the anti-BAFFR CAR which retained the best features in terms of CAR expression, cytolytic activity and cytokine production. For this reason, in future experiments we focused our attention on INVsh.CAR. The phenotype of effector cells and CAR expression at the end of differentiation was comparable to previously obtained results *(Supplementary Figure 2)*. We showed in a 4-hour cytotoxic assay at an effector target ratio of 5:1, that CIK cells modified with INVsh.CAR specifically killed NALM-6

(66,7±5%), REH (37,76±3,9%) and primary B-ALL blasts (28,1±5,9%), with different efficiencies if compared to INV.CAR control (43,2±5,2%, 21,9±2,6%, 14,5±2,7%, respectively) (Figure 4A). The degranulation ability of INVsh.CAR CIK cells was consistent with the apoptosis/necrosis cytotoxic activity (Figure 4D). In an overnight cytotoxic assay, we observed an overall increase of tumor lysis where INVsh.CAR reached 65,6±8,6% towards REH cell line and 65,6±4,5% against primary blasts (Figure 4B). The different efficiency of lysis noted for INVsh.CAR between NALM-6 and REH and primary ALL correlated with the difference in the antigen density, evaluated as number of antigen molecules per cell, on target cells that accounted for 3848,6±598,2, for NALM-6, 1461,3±299,2, for REH and 911,5±44,5 and 3584,5±1011,9 for primary blasts (Figure 4C). Analysis of cytokine production and proliferation revealed that INVsh.CAR is able to specifically proliferate and secrete IFN-γ and IL-2, particularly when stimulated by NALM-6 cell line. By contrast, upon stimulation with REH and primary ALL, the anti-BAFFR control variant did not respond by cytokines secretion (Figure 4E and F).

The combination of CD19.CAR and INVsh.CAR produces superior antitumor activity

To determine whether a double-targeting CAR approach may results more effective than targeting a single antigen, we set up *in vitro* assays co-culturing effector cells modified with CD19.CAR or INVsh.CAR with $CD19^{+}BAFF\text{-}R^{+}$ target cells. 4-hour cytotoxicity assay at the 5:1 effector target ratio, showed that the combination of

CD19.CAR and INVsh.CAR produced a higher lysis (78,1±7% vs. NALM-6; 72,2±2,8% vs. primary B-ALL) compared to NO DNA+CD19.CAR (69,4±6,7% vs. NALM-6; 55,8±2,9% vs. primary B-ALL) and NO DNA+INVsh.CAR (54,8±5,9% vs. NALM-6; 34,3±6,4% vs. primary B-ALL) control conditions (Figure 5A and B). With degranulation assay, the superior antitumor activity of CD19.CAR and INVsh.CAR combination (33,7±2,4% vs. NALM-6; 35,1±2,7% vs. primary B-ALL) compared to NO DNA+CD19.CAR (23,7±2,4% vs. NALM-6; 24,2±1,5% vs. primary B-ALL) and NO DNA+INVsh.CAR (15,4±1,3% vs. NALM-6; 15±2% vs. primary B-ALL) resulted even more evident (Figure 5C). Combination of the two constructs was able to produce a greater amount of cytokines in response to stimulation by double positive targets (Figure 5E-F). Finally, effector cells were labelled with CFSE to measured dye dilution by proliferating cells after 5 days of co-culture with target cells. Proliferation assay demonstrated that combination of CD19.CAR and INVsh.CAR proliferated mostly in response to ALL targets (Figure 5D).

The INVsh.CAR in combination with CD19.CAR is active towards CD19-negative blasts

Having previously confirmed the higher efficacy of a double targeting approach against NALM-6 cell line as well as primary B-ALL samples, we next wanted to evaluate the activity of the same conditions towards B-ALL blasts derived from a patient relapsed with a CD19-negative leukemia after Blinatumomab treatment. Notably, despite B-ALL cells from this patient have lost CD19 expression, they retained

the expression of BAFF-R on the cell surface (Figure 6A). As expected, the INVsh.CAR alone maintained specific cytotoxic activity (41,9±9,5%). Furthermore, combination of CD19.CAR and INVsh.CAR effectors showed a statistically significant killing ability compared to NO DNA+CD19.CAR condition (52,74±8,75%)(Figure 6B). The same trend of efficacy was observable also in degranulation and cytokine release assays (Figure 6C and D).

Discussion

In last ten years, great progresses have been made in the context of cancer immunotherapy. For B-ALL, approaches targeting CD19 antigen now produced deep and durable responses giving new hope to patients with unfavorable prognosis. However, about 60% of patients treated with CART19 and 30% treated with Blinatumomab, relapses because of antigen loss or mutations that make B-ALL blasts invisible to these CD19-specific therapies [8,22–24].

First evidences about mechanisms involved in CD19 loss as tumor escape system have been documented in the pioneering work of Sotillo and collegues. They found alternative exon splicing forms of CD19 gene where exon 2 was frequently spliced out leading to the removal of epitope recognized by CART. Moreover, this isoform is predominantly cytoplasmatic and for this reason is un-targetable by CART [22]. Subsequently, Gardner and collaborators reported the case of two patients with MLL rearrangement who relapsed with a myeloid phenotype and loss of B lymphoid antigens after CART19 treatment. Both were clonally related to the initial disease, but two different mechanisms were observed: (1) the reprogramming/de-differentiation of a committed B lymphoid progenitor and (2) the myeloid differentiation of a non-committed precursor or selection by means of CART treatment of a pre-existing myeloid clone [24]. A similar event was observed in a case of infant B-ALL with MLL-AFF1 rearrangement treated with blinatumomab and relapsed with an AML phenotype [25]. Since this event occurs more frequently in

subtypes of B-ALL having a genetic background characterized by innate plasticity, such as mixed phenotype leukemias, it is conceivable that the selective pressure exerted by CD19-targeted therapies may have led to modifications in the differentiation program [26]. More recently, a report on a newly identified resistance mechanism has been published by Braig *et al*. Despite the wild-type sequence of CD19 gene and the detection of CD19 mRNA, the analyzed patient's sample showed a complete antigen-loss on cell membrane, suggesting an evasive mechanism based on post-translational altered regulation. This patient also displayed negative surface expression for CD21 and CD81. In particular, absence of CD81 seriously affects CD19 trafficking to membrane [23]. Altogether these findings confirmed that CD19 may not be fundamental for B-ALL survival as already demonstrated by Weiland *et al*. [9].

In this scenario new antigens to be targeted can be proposed, such as TSLPR, CD20, CD22 and CD123 [8,27–29]. Here, we described, for the first time at our knowledge, the development of a CAR specific for BAFF-R for the treatment of B-ALL. BAFF-R represents an interesting antigen to be targeted by a CAR-mediated strategy. Nowadays, several studies have reported the expression of this receptor in various B-cell malignancies, including B-ALL, but not on the normal B-cell precursors [15,16]. Interestingly, very recently our group reported the preservation of BAFF-R expression during early drug treatment. Furthermore, the BAFF cytokine was initially consumed by leukemic bulk but, following chemotherapy, the physiological threshold of

BAFF over blast cells number was restored (Fazio G. *et al.*, *manuscript submitted*).

Being BAFF-BAFF-R axis crucial for maturation and survival of B-cells and for survival of B-ALL blasts within the leukemic niche, we hypothesized that the event of downregulation of the antigen, as reported for CD19, might be infrequent. In our study, we confirmed a B-cell restricted distribution of BAFF-R, being the mRNA transcript present in primary B-ALL samples and in B-cells containing organs, and absent in other healthy tissues. This native distribution makes BAFF-R a safer target antigen than CD19 as far as concerns the phenomenon of B-cell aplasia. Furthermore, the comparison of BAFF-R surface expression between relapsed and onset samples indicated that not only the expression of this receptor has been preserved during chemotherapy, but it significantly increased at time of relapse. The development and the initial screening of anti-BAFFR CAR variants allowed us to demonstrate the feasibility of targeting BAFF-R antigen and to evaluate the effect of spacer modification on CAR expression and functionality. Currently, Guest and collaborators demonstrated the existence of an optimal distance between T cell and target cell, which is strictly dependent on the location of the recognized epitope. Consequently, the modification of spacer length affects tumor recognition and T-cell response [21]. Exploiting this variable in the CAR design, we were able to identify the optimal configuration for our anti-BAFFR CAR which resulted in best performances. In our hands, spacer truncation heavily impaired CAR expression, mostly in terms of percentage of CAR expressing cells but also in terms of MFI.

Additionally, we evaluated also different single chain orientations, since it is known that changing the orientation of the variable domains can affect the expression and activity of a scFv [30]. More efficient effector functions were observed in absence of the CH2CH3 moiety and with the single chain in the inverted orientation, suggesting that this configuration could promote the best interaction with the antigen.

In our model, a greater number of $CD4^+$ T cells in INV.CAR and INVsh.CAR conditions was observed. It has been reported that BAFF is able to stimulate a subset of BAFF-R expressing $CD4^+$ T cells [31]. Thus, we hypothesized that the presence of BAFF producing cells, including monocytes, neutrophilis and dendritic cells, within the γ-irradiated PBMC feeder used after elettroporation, may have determined initially a preferential stimulation of $CD4^+$ T cells. The presence of a greater rate of $CD4^+$ T cells did not affected their functionality and could represent an advantage. Indeed, it has been demonstrated that this subpopulation combined with the $CD8^+$ T-cell counterpart could provide a synergistic antitumor effect [32].

We then further investigated the capability of the selected INVsh.CAR variant to eliminate target cells. INVsh.CAR was able to specifically produce strong lytic activity against NALM-6 target, which has the highest BAFF-R antigen density, and to recognize, although with slightly lower activity, REH cell lines and primary B-ALL blasts, despite both of them retain inferior antigen density. Higher degree of tumor lysis of these targets was obtained prolonging the co-incubation period. As recently reported by our group, the antigen density

represent an extremely important aspect to consider for the priming, in particular, of later effector functions (Arcangeli S. *et al*., *manuscript under revision*). In our case, we observed that the different target antigen density showed by NALM-6, REH and primary cells impact on later functions such as cytokine secretion.

To address the drawback of CD19-negative relapse, we proposed to target multiple antigens. Anurathapan and collaborators demonstrated that combining CAR T cells specific for MUC1 and PSCA antigens, frequently co-expressed by pancreatic cancer cells, an additive anti-tumor effect could be achieved [33]. Ruella and colleagues showed that using a combinatorial preemptive approach mediated by CART123 and CART19 cells CD19-negative relapses could be prevented in B-ALL. In our case, we combined CD19, which is strongly expressed by blast cells, and BAFF-R, which has been shown to be important for B-ALL survival and chemoresistance. We found that a simultaneous treatment with both CD19.CAR and INVsh.CAR T cells led to a superior cytotoxic effect compared to single effector population *per se*. The combination of CD19.CAR and INVsh.CAR T cells was able to exert antitumor activity also towards a case of CD19-negative B-ALL blasts from a blinatumomab-treated patient. Despite CD19 resulted undetectable by flow cytometry, a significantly increased in cytotoxic activity was observed compared to a residual lytic activity exerted by CD19.CAR, which reflects basal anti-tumor activity of unmodified CIK cells.

In conclusion, here we confirmed the feasibility to target BAFF-R antigen by using a CAR platform. In our setting the inversion of the

variable regions within the scFv and the removal of the spacer moiety resulted in superior effector functions, suggesting an improved antigen recognition. A further investigation in terms of screening higher numbers of mAbs could be interesting with the purpose to find the best clone able to show optimal antitumor activity towards target cells with low target antigen density. Altogether, these data demonstrated that targeting BAFF-R is an effective and safer therapeutic strategy, compared to other targeted antigens, for a second line treatment in case of CD19-negative relapses or in combination with them to avoid antigen escape.

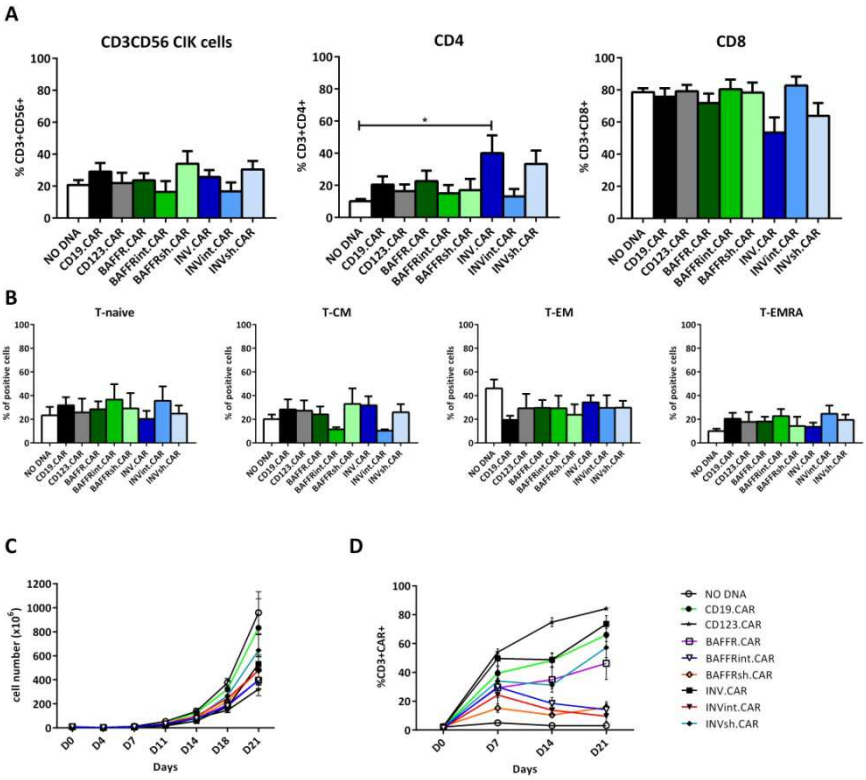

Figure S1. NO DNA control and redirected CIK cells phenotype, proliferation and CAR expression at the end of differentiation protocol (Day 21). (A) NK-like, T-CD4^{+} and T-CD8^{+} phenotype. (B) Memory phenotype: naive, central memory (CM), effector memory (EM), effector memory RA (EMRA). (C) Nucleofected CIK-cell expansion monitored during differentiation protocol. (D) CAR expression monitored during differentiation until day 21. Data represented are the result of mean ± SEM, n=8 for NO DNA, CD19.CAR, BAFFR.CAR, INV.CAR and INVsh.CAR conditions and n=4 for CD123.CAR, BAFFRint.CAR, BAFFRsh.CAR and INVint.CAR conditions (*p<0,05, One way ANOVA, Bonferroni test).

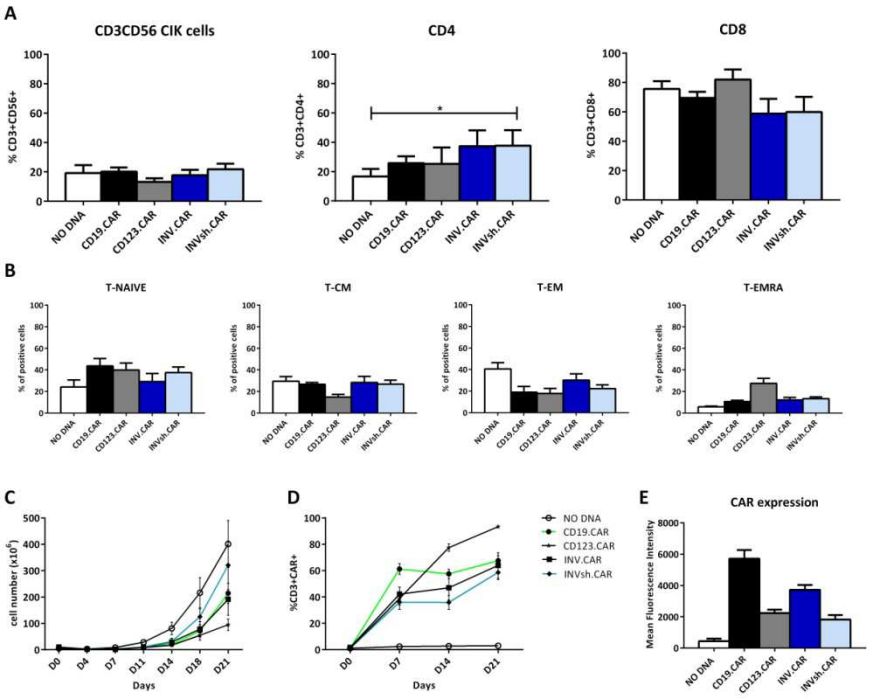

Figure S2. CIK-cell phenotype, proliferation and CAR expression at the end of differentiation protocol (day 21). (A) NK-like, T-CD4^{+} and T-CD8^{+} phenotype. (B) Memory phenotype: naive, central memory (CM), effector memory (EM), effector memory RA (EMRA). (C) Nucleofected CIK cells expansion monitored during differentiation protocol. (D) CAR expression monitored during differentiation until day 21. Data represented are the result of mean ± SEM, n=8 for NO DNA, CD19.CAR, CD123.CAR and INVsh.CAR conditions and n=5 for INV.CAR condition (*p<0,05, One way ANOVA, Bonferroni test).

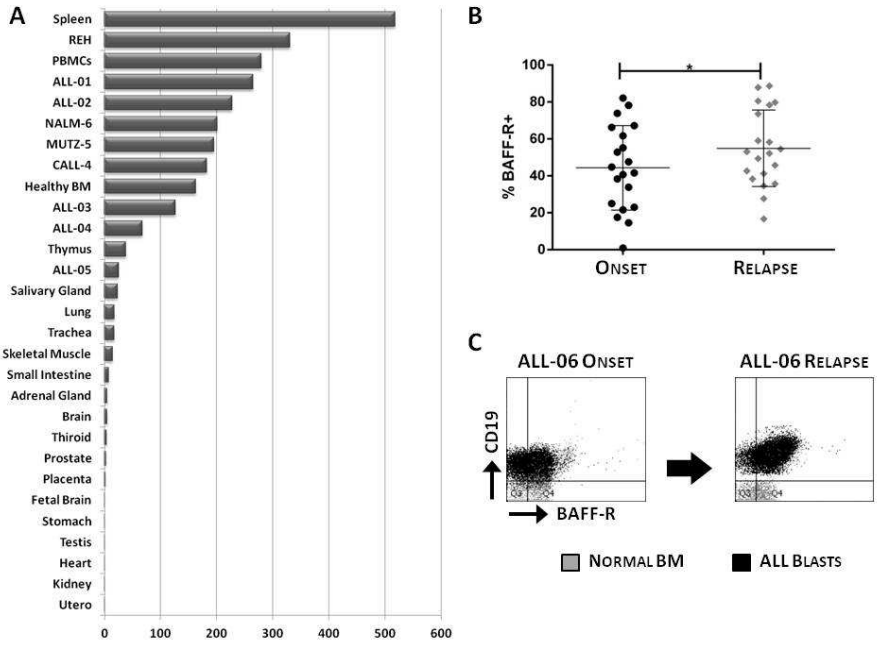

Figure 1. BAFF-R expression by B-ALL cell lines and primary cells. (A) mRNA quantification evaluated by Real-Time PCR and reported as $2^{-\Delta\Delta Ct}$. Detected values were normalized on Abelson and HPRT housekeeping genes and by using a BAFF-R negative sample as reference gene. (B) Surface expression of BAFF-R on matched diagnosis and relapse samples. Data represented are the result of mean ± SEM, n=20 (*p<0,05, paired t test) (C) Example panel of BAFF-R surface expression in B-ALL blasts obtained from the same patient at onset and at relapse.

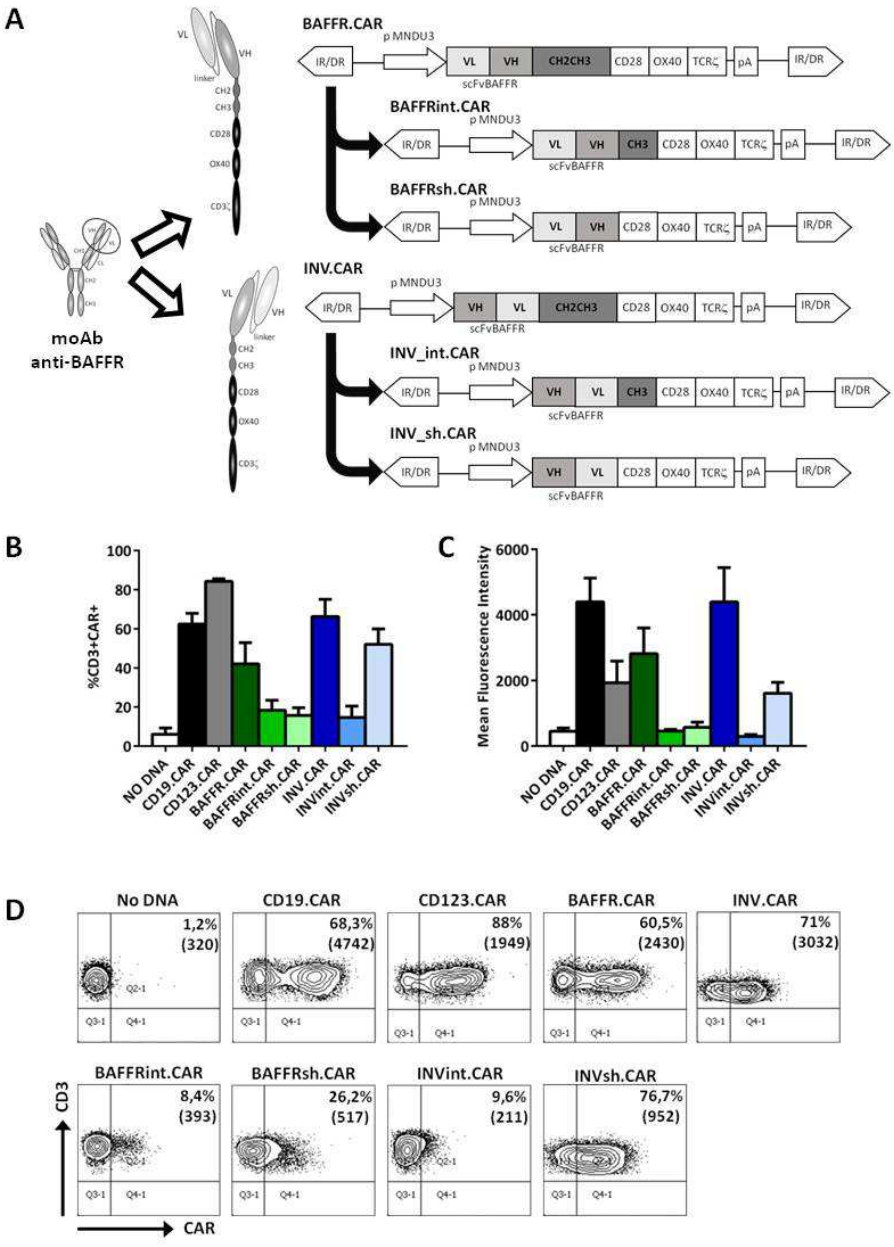
A
BAFFR.CAR
p MNDU3
IR/DR
VL
VH
CH2CH3
CD28
OX40
TCRζ
pA
IR/DR
scFvBAFFR
BAFFRint.CAR
CH3
BAFFRsh.CAR
INV.CAR
INV_int.CAR
INV_sh.CAR
moAb
anti-BAFFR
linker
CH2
CH3
B
%CD3+CAR+
C
Mean Fluorescence Intensity
NO DNA
CD19.CAR
CD123.CAR
BAFFR.CAR
BAFFRint.CAR
BAFFRsh.CAR
INV.CAR
INVint.CAR
INVsh.CAR
D
No DNA
1,2%
(320)
CD19.CAR
68,3%
(4742)
CD123.CAR
88%
(1949)
BAFFR.CAR
60,5%
(2430)
INV.CAR
71%
(3032)
BAFFRint.CAR
8,4%
(393)
BAFFRsh.CAR
26,2%
(517)
INVint.CAR
9,6%
(211)
INVsh.CAR
76,7%
(952)
CD3
CAR

Figure 2. anti-BAFFR CAR CIK cells expressing long, intermediate and short variants. (A) Representation of third generation anti-BAFFR CARs inserted in SB transposon; IR/DR, SB inverted/direct repeats; MNDU3/p, constitutive promoter from the U3 region of the MND retrovirus; pA, polyadenlation signal. Transfection efficiency profile evaluated at the end of culture in terms of percentage of positive cells (B) and CAR expression evaluated in terms of MFI (in brackets) (C). (D) Representative panel of CAR expressing CIK cells. Percentage of modification and MFI (in brackets) is reported in the top-right quadrant. Data represented are the result of mean ± SEM, n=8 for NO DNA, CD19.CAR, BAFFR.CAR, INV.CAR and INVsh.CAR conditions and n=4 for CD123.CAR, BAFFRint.CAR, BAFFRsh.CAR and INVint.CAR conditions.

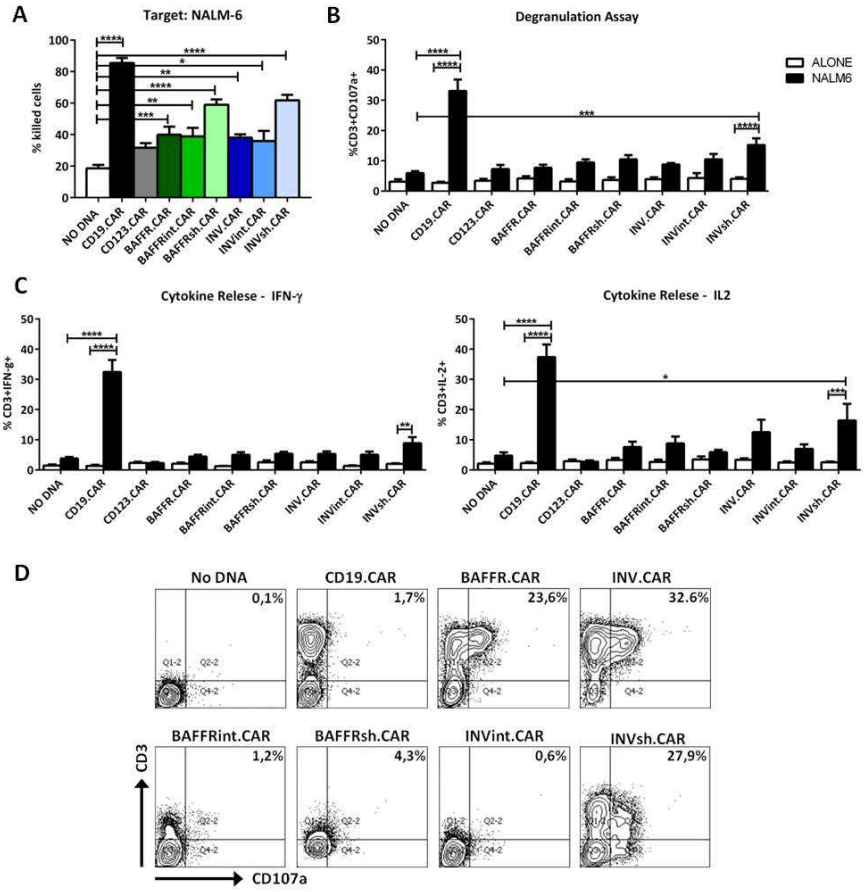
A
Target: NALM-6
% killed cells
NO DNA
CD19.CAR
CD123.CAR
BAFFR.CAR
BAFFRint.CAR
BAFFRsh.CAR
INV.CAR
INVint.CAR
INVsh.CAR
B
Degranulation Assay
%CD3+CD107a+
ALONE
NALM6
C
Cytokine Relese - IFN-γ
% CD3+IFN-g+
Cytokine Relese - IL2
% CD3+IL-2+
D
No DNA
0,1%
CD19.CAR
1,7%
BAFFR.CAR
23,6%
INV.CAR
32.6%
BAFFRint.CAR
1,2%
BAFFRsh.CAR
4,3%
INVint.CAR
0,6%
INVsh.CAR
27,9%
CD3
CD107a

Figure 3. Functional characterization of anti-BAFFR CAR variants. (A) Apoptosis/Necrosis assay to evaluate lytic activity. (B) Degranulation assay. (C) Cytokine release of anti-BAFFR CAR variants towards NALM-6 target. Data represented are the result of mean ± SEM, n=8 for NO DNA, CD19.CAR, BAFFR.CAR, INV.CAR and INVsh.CAR conditions and n=4 for CD123.CAR, BAFFRint.CAR, BAFFRsh.CAR and INVint.CAR conditions (*p<0,05, **p<0,01, ***p<0,001, ****p<0,0001, One way or Two way ANOVA, Bonferroni test) (D) Example panel of CD107a degranulation upon stimulation with coated BAFF-R antigen. The panel is representative of n=6 for NO DNA, CD19.CAR, BAFFR.CAR, INV.CAR and INVsh.CAR conditions, n=4 for BAFFRsh.CAR and n=2 for BAFFRint.CAR, and INVint.CAR conditions.

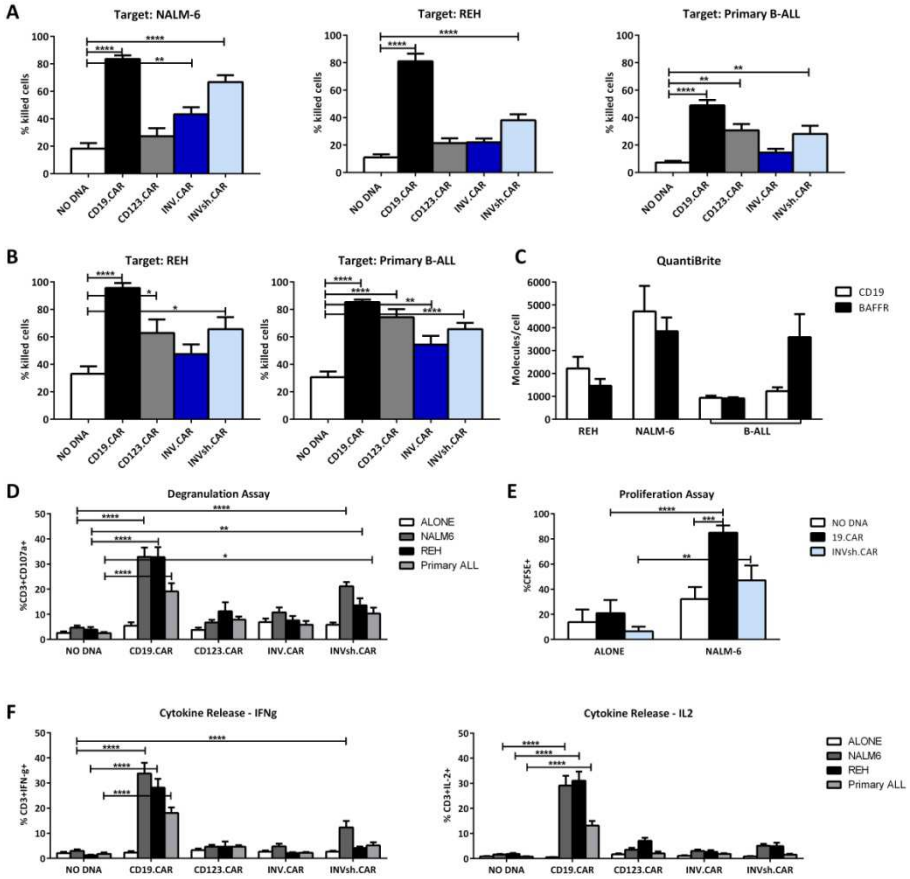
A
Target: NALM-6
Target: REH
Target: Primary B-ALL
% killed cells
NO DNA
CD19.CAR
CD123.CAR
INV.CAR
INVsh.CAR
B
Target: REH
Target: Primary B-ALL
C
QuantiBrite
Molecules/cell
CD19
BAFFR
REH
NALM-6
B-ALL
D
Degranulation Assay
%CD3+CD107a+
ALONE
NALM6
REH
Primary ALL
E
Proliferation Assay
%CFSE+
NO DNA
19.CAR
INVsh.CAR
ALONE
NALM-6
F
Cytokine Release - IFNg
% CD3+IFN-g+
Cytokine Release - IL2
% CD3+IL-2+

Figure 4. Antitumor activity of INVsh.CAR redirected CIK cells towards CD19^{+}BAFF-R^{+} targets. (A) 4-hour Apoptosis/Necrosis assay to evaluate lytic activity. (B) Overnight Apoptosis/Necrosis assay. REH: n=6; Primary B-ALL: n=10 for NO DNA and INVsh.CAR, n=9 for CD19.CAR, n=7 for CD123.CAR and INV.CAR. (C) Quantification by QuantiBrite assay of CD19 and BAFF-R molecules per cell in REH, NALM-6 and primary blasts. (D) Degranulation assay towards NALM-6, REH and primary B-ALL samples. (E-F) Cytokine release and proliferation by modified CIK cells. NALM-6: n=11 for NO DNA, and INVsh.CAR, n=8 for INV.CAR and CD123.CAR, n=10 for CD19.CAR; REH: n=11 for NO DNA, CD19.CAR, INV.CAR and INVsh.CAR, n=5 for CD123.CAR; Data represented are the result of mean ± SEM (*p<0,05, **p<0,01, ***p<0,001, ****p<0,0001, One way or Two way ANOVA, Bonferroni test).

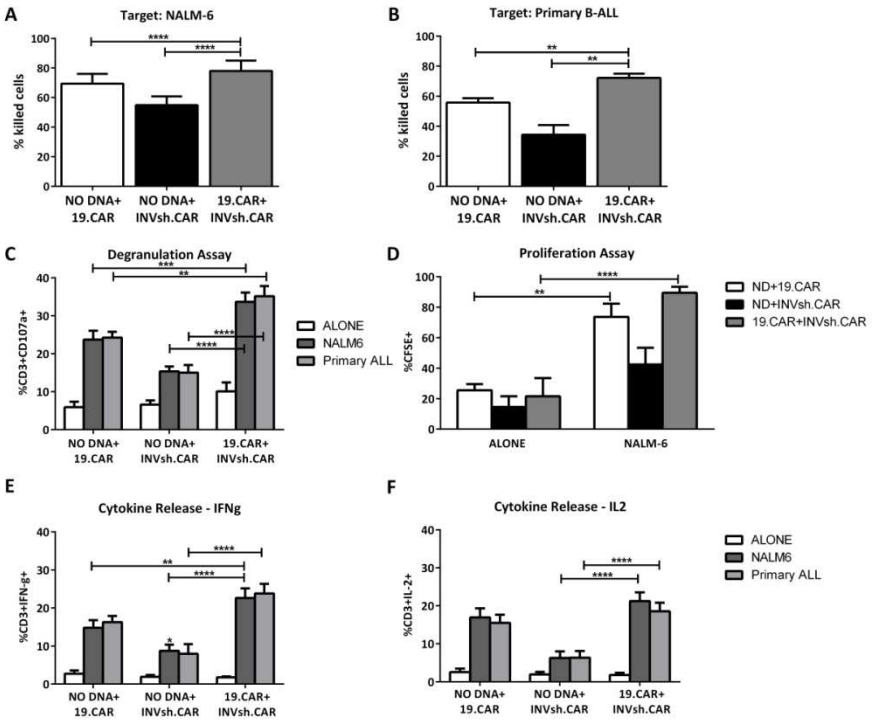

Figure 5. Combination of effector cells redirected towards CD19 and BAFF-R antigens. (A) Short term Apoptosis/Necrosis assay towards NALM-6 and primary B-ALL blasts. (B) CD107a degranulation assay towards NALM-6 and primary blasts. (C) Cytokine release assay upon stimulation with NALM-6 and B-ALL blasts. n=10 for NALM-6; n=5 for Primary B-ALL. (D) Proliferation assay after incubation with NALM-6 (n=5). Data represented are the result of mean ± SEM (*p<0,05, **p<0,01, ***p<0,001, ****p<0,0001, Paired t test or Two way ANOVA, Bonferroni test).

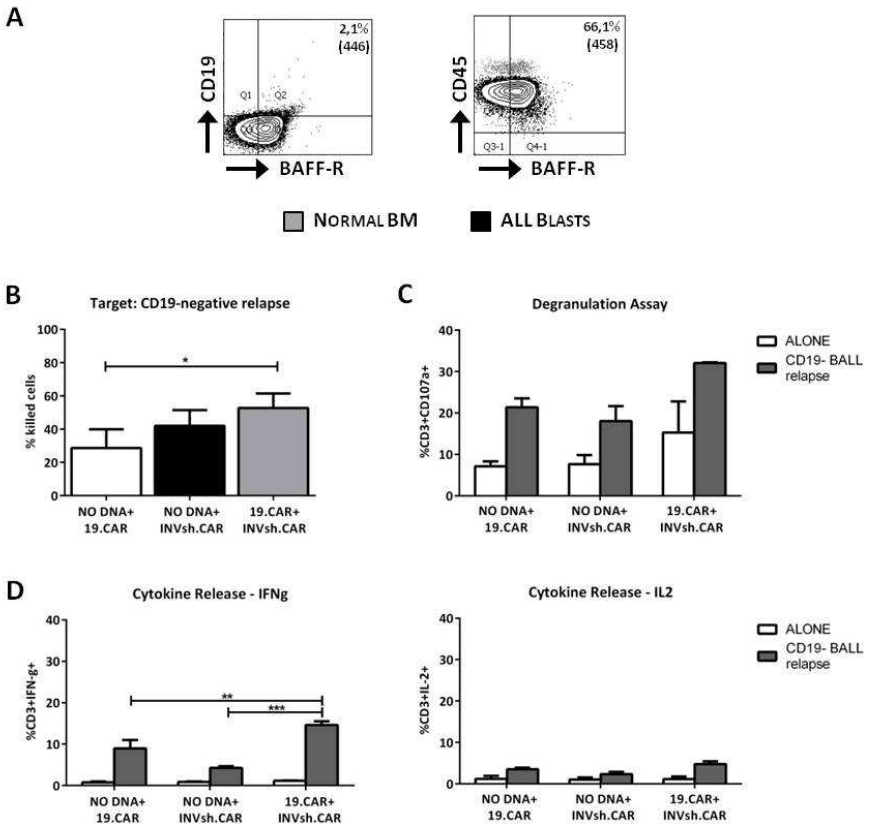

Figure 6. Antitumor activity of the combination of CD19.CAR and anti-BAFFR INVsh.CAR towards CD19-negative blasts. (A) FACS analysis of CD19- relapsed sample. (B) Short term Apoptosis/Necrosis assay. (C) CD107a degranulation assay. (D) Cytokine release assay. n=3. Data represented are the result of mean ± SEM (*p<0,05, **p<0,01, ***p<0,001, Paired t test or Two way ANOVA, Bonferroni test).

References

1. Paul, S., Kantarjian, H. & Jabbour, E. J. Adult Acute Lymphoblastic Leukemia. *Mayo Clin Proc* **91,** 1645–1666 (2016).
2. Luo, Y. *et al.* First-in-Man CD123-Specific Chimeric Antigen Receptor-Modified T Cells for the Treatment of Refractory Acute Myeloid Leukemia. *Blood* **126,** 3778 (2015).
3. Ali, S. A. *et al.* T cells expressing an anti-B-cell maturation antigen chimeric antigen receptor cause remissions of multiple myeloma. *Blood* **128,** 1688–1700 (2016).
4. Louis, C. U. *et al.* Antitumor activity and long-term fate of chimeric antigen receptor – positive T cells in patients with neuroblastoma. *Mol. Ther. J. Am. Soc. Gene Ther.* **14,** 1324–1334 (2011).
5. Ruella, M. & Gill, S. How to train your T cell: genetically engineered chimeric antigen receptor T cells versus bispecific T-cell engagers to target CD19 in B acute lymphoblastic leukemia. *Expert Opin. Biol. Ther.* **15,** 761–766 (2015).
6. Bassan, R. Toward victory in adult ALL: Blinatumomab joins in. *Blood* **120,** 5094–5095 (2012).
7. Maude, S. L. *et al.* Chimeric Antigen Receptor T Cells for Sustained Remissions in Leukemia. *N. Engl. J. Med.* **371,** 1507–1517 (2014).
8. Ruella, M. *et al.* Dual CD19 and CD123 targeting prevents antigen-loss relapses after CD19-directed immunotherapies. *J.*

Clin. Invest. **126,** 3814–3826 (2016).

9. Weiland, J. *et al.* BCP-ALL blasts are not dependent on CD19 expression for leukaemic maintenance. *Leukemia* **30,** 1920–1923 (2016).
10. le Viseur, C. *et al.* In Childhood Acute Lymphoblastic Leukemia, Blasts at Different Stages of Immunophenotypic Maturation Have Stem Cell Properties. *Cancer Cell* **14,** 47–58 (2008).
11. Day, E. S. *et al.* Selectivity of BAFF/BLyS and APRIL for binding to the TNF family receptors BAFFR/BR3 and BCMA. *Biochemistry* **44,** 1919–1931 (2005).
12. Mihalcik, S. a, Huddleston, P. M., Wu, X. & Jelinek, D. F. The structure of the TNFRSF13C promoter enables differential expression of BAFF-R during B cell ontogeny and terminal differentiation. *J. Immunol.* **185,** 1045–54 (2010).
13. Gross, J. A. *et al.* TACI-Ig neutralizes molecules critical for B cell development and autoimmune disease: Impaired B cell maturation in mice lacking BLyS. *Immunity* **15,** 289–302 (2001).
14. Thompson, J. S. *et al.* BAFF-R, a newly identified TNF receptor that specifically interacts with BAFF. *Science (80-.).* **293,** 2108–2111 (2001).
15. Parameswaran, R., Muschen, M., Kim, Y. M., Groffen, J. & Heisterkamp, N. A functional receptor for B-cell-activating factor is expressed on human acute lymphoblastic leukemias. *Cancer Res.* **70,** 4346–4356 (2010).
16. Rodig, S. J., Shahsafaei, A., Li, B., Mackay, C. R. & Dorfman, D. M. BAFF-R, the major B cell-activating factor receptor, is

expressed on most mature B cells and B-cell lymphoproliferative disorders. *Hum. Pathol.* **36,** 1113–1119 (2005).

17. Maia, S. *et al.* Aberrant expression of functional baff-system receptors by malignant b-cell precursors impacts leukemia cell survival. *PLoS One* **6,** (2011).
18. Parameswaran, R. *et al.* Effector-Mediated Eradication of Precursor B Acute Lymphoblastic Leukemia with a Novel Fc-Engineered Monoclonal Antibody Targeting the BAFF-R. *Mol. Cancer Ther.* **13,** 1567–77 (2014).
19. Parameswaran, R. *et al.* Treatment of acute lymphoblastic leukemia with an rGel/BLyS fusion toxin. *Leukemia* **26,** 1786–96 (2012).
20. Magnani, C. F. *et al.* Immunotherapy of acute leukemia by chimeric antigen receptor-modified lymphocytes using an improved Sleeping Beauty transposon platform. *Oncotarget* **5,** (2016).
21. Guest, R. D. *et al.* The role of extracellular spacer regions in the optimal design of chimeric immune receptors: evaluation of four different scFvs and antigens. *J Immunother* **28,** 203–211 (2005).
22. Sotillo, E. *et al.* Convergence of acquired mutations and alternative splicing of CD19 enables resistance to CART-19 immunotherapy. *Cancer Discov.* **5,** 1282–1295 (2015).
23. Braig, F. *et al.* Resistance to anti-CD19/CD3 BiTE in acute lymphoblastic leukemia may be mediated by disrupted CD19

membrane trafficking. *Blood* (2016). doi:10.1182/blood-2016-05-718395

24. Gardner, R. *et al.* Acquisition of a CD19-negative myeloid phenotype allows immune escape of MLL-rearranged B-ALL from CD19 CAR-T-cell therapy. *Blood* **127,** 2406–2410 (2016).
25. Rayes, A., Mcmasters, R. L. & O'Brien, M. M. Lineage Switch in MLL-Rearranged Infant Leukemia Following CD19-Directed Therapy. *Pediatr. Blood Cancer* **63,** 1113–1115 (2016).
26. Jacoby, E. *et al.* CD19 CAR immune pressure induces B-precursor acute lymphoblastic leukaemia lineage switch exposing inherent leukaemic plasticity. *Nat. Commun.* **7,** 12320 (2016).
27. Qin, H. *et al.* Eradication of B-ALL using chimeric antigen receptor-expressing T cells targeting the TSLPR oncoprotein. *Blood* **126,** 629–639 (2015).
28. Zhang, W. *et al.* Treatment of CD20-directed Chimeric Antigen Receptor-modified T cells in patients with relapsed or refractory B-cell non-Hodgkin lymphoma: an early phase IIa trial report. *Signal Transduct. Target. Ther.* **1,** 1–9 (2016).
29. Haso, W. *et al.* Anti-CD22-chimeric antigen receptors targeting B-cell precursor acute lymphoblastic leukemia. *Blood* **121,** 1165–1171 (2013).
30. Bühler, P. *et al.* Influence of structural variations on biological activity of anti-PSMA scFv and immunotoxins targeting prostate cancer. *Anticancer Res.* **30,** 3373–3379 (2010).
31. Ye, Q. *et al.* BAFF binding to T cell-expressed BAFF-R

costimulates T cell proliferation and alloresponses. *Eur. J. Immunol.* **34,** 2750–2759 (2004).

32. Sommermeyer, D. *et al.* Chimeric antigen receptor-modified T cells derived from defined CD8+ and CD4+ subsets confer superior antitumor reactivity in vivo. *Leukemia* **30,** 492–500 (2016).
33. Anurathapan, U. *et al.* Kinetics of tumor destruction by chimeric antigen receptor-modified T cells. *Mol Ther* **22,** 623–633 (2014).
34. Chiarini, F. *et al.* Advances in understanding the acute lymphoblastic leukemia bone marrow microenvironment: From biology to therapeutic targeting. *Biochim. Biophys. Acta* **1863,** 449–463 (2015).
35. Pule, M., Finney, H. & Lawson, A. Artificial T-cell receptors. *Cytotherapy* **5,** 211–226 (2003).
36. Couzin-Frankel, J. Breakthrough of the year 2013. Cancer immunotherapy. *Science* **342,** 1432–3 (2013).
37. Morgan, R. a *et al.* Case report of a serious adverse event following the administration of T cells transduced with a chimeric antigen receptor recognizing ERBB2. *Mol. Ther.* **18,** 843–851 (2010).
38. Brentjens, R. J. *et al.* Safety and persistence of adoptively transferred autologous CD19-targeted T cells in patients with relapsed or chemotherapy refractory B-cell leukemias. *Blood* **118,** 4817–4828 (2011).
39. Davila, M. L., Kloss, C. C., Gunset, G. & Sadelain, M. CD19 CAR-

Targeted T Cells Induce Long-Term Remission and B Cell Aplasia in an Immunocompetent Mouse Model of B Cell Acute Lymphoblastic Leukemia. *PLoS One* **8,** 1–14 (2013).

40. Tussiwand, R., Rauch, M., Flück, L. A. & Rolink, A. G. BAFF-R expression correlates with positive selection of immature B cells. *Eur. J. Immunol.* **42,** 206–216 (2012).

41. Grada, Z. *et al.* TanCAR: A Novel Bispecific Chimeric Antigen Receptor for Cancer Immunotherapy. *Mol. Ther. Nucleic Acids* **2,** e105 (2013).

Chapter 4

Immunotherapy of acute leukemia by chimeric antigen receptor modified lymphocytes using an improved *Sleeping Beauty* transposon platform

Chiara F. Magnani[1], **Nice Turazzi[1]**, Fabrizio Benedicenti[2], Andrea Calabria[2], Erika Tenderini[2], Sarah Tettamanti[1], Greta M.P. Giordano Attianese[1,3], Laurence J.N. Cooper[3], Alessandro Aiuti[2], Eugenio Montini[2], Andrea Biondi[1], Ettore Biagi[1]

[1]Tettamanti Research Center, Department of Pediatrics, University of Milano-Bicocca, San Gerardo Hospital/Fondazione MBBM, Monza, Italy

[2]San Raffaele Telethon Institute for Gene Therapy (HSR-TIGET), Milan, Italy

[3]University of Texas, MD Anderson Cancer Center, Houston, Texas, USA

Oncotarget, 2016

Abstract

Chimeric antigen receptor (CAR)-modified T-cell adoptive immunotherapy is a remarkable therapeutic option proven effective in the treatment of hematological malignancies. In order to optimize cell manufacturing, we sought to develop a novel clinical-grade protocol to obtain CAR-modified cytokine-induced killer cells (CIKs) using the Sleeping Beauty (SB) transposon system. Administration of irradiated PBMCs overcame cell death of stimulating cells induced by non-viral transfection, enabling robust gene transfer together with efficient T-cell expansion. Upon single stimulation, we reached an average of 60% expression of CD123- and CD19- specific 3rd generation CARs (CD28/OX40/TCRzeta). Furthermore, modified cells displayed persistence of cell subsets with memory phenotype, specific and effective lytic activity against leukemic cell lines and primary blasts, cytokine secretion, and proliferation. Adoptive transfer of CD123.CAR or CD19.CAR lymphocytes led to a significant antitumor response against acute myelogenous leukemia (AML) and acute lymphoblastic leukemia (ALL) disseminated diseases in NSG mice. Notably, we found no evidence of integration enrichment near cancer genes and transposase expression at the end of the differentiation. Taken all together, our findings describe a novel donor-derived non-viral CAR approach that may widen the repertoire of available methods for T cell-based immunotherapy.

Introduction

Adoptive transfer of chimeric antigen receptor (CAR)-modified T lymphocytes has recently been proposed as advanced treatment for relapsed and refractory chronic lymphocytic leukemia, acute lymphoblastic leukemia (ALL), CD19-positive lymphomas and multiple myeloma.[1-8] Developed to improve the graft-versus-leukemia effect, CAR molecules are designed by fusing the antigen-binding domain of a monoclonal antibody in the form of a single-chain fragment variable (scFv) with a signal transduction domain, usually the ζ chain of the TCR and costimulatory molecules, in a unique artificial receptor.[9] In this regard, CD19-directed CAR treatment of patients resulted in persistence of immunological memory, trafficking to the tumor sites, and non-HLA-restricted anti-tumor activity, which led to tumor regression and, in most of the patients, complete remission.[1-4, 6]

Concerning the aspect of *ex vivo* T-cell modification, in the past two decades, viral vectors have constituted a valuable tool for successful gene therapy thanks to their efficacy in mediating stable gene transfer into primary cells with standardized good manufacturing practice (GMP)-grade processes[10, 11] and overall safety in modifying differentiated immune cells.[12] In parallel, non-viral gene transfer methods have recently been developed with the goal of overcoming high manufacturing costs, regulatory hurdles and scale-up complexities, which have limited so far the range of application of CAR-based immunotherapy with respect to other easier approaches

such as monoclonal antibodies (mAbs).[13] However, commonly available non-viral methods are based on transient transfection by mRNA electroporation[14, 15] or stable, integrative methods that have limited transfection efficiency. In this context, the *Sleeping Beauty* (SB) transposon plasmid system[16] is quite inexpensive and easy to produce and purify. Furthermore, SB appears to be less immunogenic than viral vectors and, because it integrates randomly into the host genome,[17, 18] it retains a safer pattern compared to gamma retroviral vectors, which have the tendency to target gene promoters, thereby having an increased probability to induce aberrant gene expression.[19, 20] Thus, SB has been used in combination with electroporation for gene transfer in human primary T cells with the limitation of relatively low transfection efficiency.[21] Using the SB method, Singh *et al.* have successfully generated CD19-redirected CAR-modified T cells for Phase I and II clinical trials.[22] In order to obtain a consistent amount of CAR^+ T cells, the authors expanded and, simultaneously, selected effector cells by repetitive stimulation with $CD19^+$ artificial APC.[23]

With regard to the development of CAR therapies using cytokine-induced killer (CIK) -cell cultures,[24] effector lymphocytes with acquired NK-like cytotoxicity are usually generated by culturing PBMCs in the presence of IFN-γ, IL-2, and anti-CD3 mAbs. This cell population expresses T-cell markers (> 97% are $CD3^+$) and it is enriched in highly cytotoxic CD3+CD56+ cells. In the context of leukemia immunotherapy, we have previously shown that anti-CD19 and anti-CD123 CARs redirected the activity of CIK cells against

primary ALL and AML blasts, respectively.[25-27] The advantage of choosing donor-derived CIK-cell cultures stems from the fact that these cells display a non-HLA-restricted cytotoxicity[24] along with minimal alloreactivity.[28] Furthermore, it has been shown that an easy protocol could promote their rapid expansion *ex vivo* under validated pharmaceutical GMP conditions.[29] However, to our knowledge, none of the currently published non-viral methods has reached significant efficiency to be applied to easy-to-translate T-cell protocols.[23, 30-32] Here, we describe the development of a unique non-viral clinical-grade immunotherapy approach for acute leukemias. We were able to achieve stable and efficient CAR expression and, concomitantly, boost cell expansion while minimizing cell manipulation and preserving phenotype, viability, and effector functions of the redirected cells. In addition, we performed molecular analysis of SB-engineered CIK cells by high-throughput genomic integration site retrieval, bioinformatics, and transposase expression analysis.

Results

Transfection of primary T-cell precursors and CIK-cell differentiation by SB

First, we developed an optimized clinical-grade protocol to generate CIK-cell cultures expressing two distinct 3rd generation CARs (Figure 1). Nucleofection of PBMCs in the presence of SB plasmids caused consistent loss of the CD11c^{+} myeloid dendritic cells (DCs) and CD14^{+} monocytes and cell mortality. After nucleofection, the addition of γ-irradiated autologous PBMCs, as source of antigen-presenting cells (APC), partially restored the above mentioned loss of DCs and monocytes. This strategy, together with the concomitant stimulation by OKT3, rescued the impaired T-cell expansion observed using various nucleofection programs while preserving high CAR expression (Supplementary Figure 1A-1C). Cell survival rates at 24 hours reached a value of 52.6% (±6.2, n=13) for CD123.CAR and 45.0% (±8.4, n=7) for CD19.CAR (Supplementary Figure 1D-1E). Both CD123.CAR and CD19.CAR CIK cells showed efficient expansion without requiring any additional stimulation reaching, after 3 weeks, a 93.8±26.3 and 114.7±63.8 fold increase, with an average of 121 and 161 fold expansion of CD3^{+} T cells (Figure 2A).

At the end of the differentiation, cell viability was well-preserved with an average of 75.6% in CD123.CAR and 80% in CD19.CAR (Supplementary Figure 2A-2B). Our protocol minimally altered the phenotype of the CIK-cell product, leading to a slightly higher, albeit significant, proportion of CD3^{+}CD56^{+} (43.4%±3.5 in CD123.CAR *vs.*

26.4±2.3 in control cells (No DNA); 43.9%±4.3 in CD19.CAR *vs.* 30.0±2.6 in No DNA) (Figure 2B). Nucleofection average efficiency, as assessed by GFP expression levels at 24 hours, was 50.7% (±6.5, n=11) in CD123.CAR and 42.0% (±4.0, n=4) in CD19.CAR. The expression levels of CD123.CAR and CD19.CAR were stable in CIK cells and after 21 days reached values of 58.1%±2.7 (n=13) and 59.7%±5.1 (n=8), respectively (Figure 2C-2D), which were slightly higher than the transposon encoding GFP (SB GFP, Supplementary Figure 2C). GFP alone and SB GFP differed in the kinetic of the expression pattern. CAR molecules were stably expressed by each cell subset (i.e. $CD3^+CD56^+$, $CD3^+CD8^+$, and $CD3^+CD4^+$ cells) and found to be present in cells at all stages of differentiation and memory (Supplementary Figure 2D). Taken together, these data demonstrate that replacing impaired nucleofected stimulating cells with precursor PBMCs results in optimal expansion of CAR^+ CIK cells.

Redirected activities of CD123. and CD19. CAR CIK cells against AML and ALL blasts

An efficient lysis of AML THP-1 cell line (85.0%±4.9) and primary blasts (60.0%±3.6) by SB-modified CD123.CAR CIK cells was observed at the 4-hour time point at an effector target ratio of 5:1. Similar redirected cell killing was observed for CD19.CAR CIK cells incubated with ALL REH cell line (80.0%±6.0) and primary blasts (56.8%±7.7). In contrast to that, we did not observe significant cell killing by control CIK cells (No DNA) (Figure 3A). Both CD123 and CD19 antigen expression on target cells were assessed by flow cytometry (Table 1).

We obtained similar results when we measured cell killing using a quantitative cytotoxic assay (Figure 3B). In addition, when CD123.CAR CIK cells and CD19.CAR CIK cells were cocultured with leukemic blasts, they showed specific cytotoxic degranulation according to CD107a expression. Notably, cytotoxic degranulation was associated with CAR expression, further indicating specific target recognition by CAR and subsequent cell killing (Figure 3C).

In addition to that, we evaluated specific pro-inflammatory cytokine secretion of SB-modified CIK cells. Both CD123.CAR and CD19.CAR CIK cells exposed to THP-1 and AML primary cells or REH and ALL primary cells, respectively, released a significant higher amount of IFN-γ and TNF-α compared to No DNA CIK cells (Figure 4A-4B). CD123.CAR CIK cells produced both IFN-γ (28.5%±4.5 with THP-1, 13.4%±1.3 with primary AML, n=9) and IL-2 (10.1%±2.0 with THP-1; 5.8%±1.1 with primary AML, n=9), assessed by intracytoplasmic staining (Figure 4C and Supplementary Figure 3). Likewise, CD19.CAR CIK cells produced both IFN-γ (27.2%±5.8 with REH; 24.2%±3.5 with primary ALL) and IL-2 (10.1%± 1.2 with REH; 10.6%±1.6 with primary ALL). The response was restricted to CAR^+ CIK cells, indicating that cytokine secretion is stimulated upon specific CAR-triggering by the antigen expressed on leukemic cells.

We next directly compared our platform with the already established methods of conventional T-cell modification by SB.[31, 32] Our data showed expansion of CIK cells at higher rate compared to OKT3- and beads- activated T cells with a fold increase of 35.6±7.1 versus

13.4±4.3 and 7.2±3.9, respectively. Addition of γ-irradiated autologous PBMCs increased both OKT3- and beads- activated T-cell expansion (Supplementary Figure 4A-4B). CAR expression was similar in all conditions with the exception of the lower expressing beads-activated T cells (Supplementary Figure 4C-4D). CIK cells were slightly superior in cytotoxicity (Supplementary Figure 4E-4F) and cytokine secretion ability (Supplementary Figure 4G-4H). The observed difference of CAR expression in beads-activated T cells and of cytotoxicity in OKT3-activated T cells compared with CIK cells was restored by addition of γ-irradiated PBMCs.

SB-engineered CIK cells proliferate upon CAR-specific stimulation

We then evaluated whether CD123.CAR and CD19.CAR constructs containing a 3rd generation signaling domain could lead to specific proliferation. For this purpose, CD123.CAR and CD19.CAR CIK cells were cocultured with THP-1 and REH cell lines, respectively in the absence of rhIL-2. CD123.CAR and CD19.CAR CIK cells proliferated in the presence of AML and ALL cells, respectively, as determined by MTT assay. We observed a limited non specific proliferation of No DNA CIK cells after incubation with THP-1, but not with REH (Figure 5A). In order to better evaluate specific proliferation, CIK cells were co-stained with CFSE[33] and CAR-specific mAb. Antigen-triggered CAR activation led to specific proliferation of both CD123.CAR (54.5%±12.6 *vs.* 22.8%± 3.7 of No DNA; p=0.0471, n=5) and CD19.CAR CIK cells (79.3%±5.3 *vs.* 30.8%± 7.0; p=0.0076, n=5). In particular, the proliferating CFSE^{low} fraction cells were mainly CAR^{+}, suggesting

specific activation and selection of modified CIK cells upon encounter with cancer cells (Figure 5B).

SB-engineered CIK cells exert anti-tumor responses *in vivo*

We next evaluated the *in vivo* efficacy of CD123.CAR and CD19.CAR CIK cells against AML and ALL, respectively. For this purpose, we injected AML KG-1 or ALL Nalm-6 cells into the tail vein of immunodeficient NOD-SCID-γchain-/- (NSG) mice. Mice were grafted with KG-1 cells and, after 14 days, received an intravenous infusion of $1x10^7$ CD123.CAR or No DNA CIK cells from the same donor every 10 days, as previously reported[27] (Figure 6A). KG-1 cells engrafted either as disseminated leukemia or extramedullary tumor in animals treated with No DNA CIK cells. Conversely, treatment with CD123.CAR CIK cells eradicated KG-1 cells in the BM and significantly inhibited tumor growth as compared to No DNA CIK-treated mice (Figure 6B-6C). No extramedullary tumor was found in mice treated with CD123.CAR CIK cells.

In the ALL model, NSG mice were grafted with Nalm-6 cells and, subsequently, infused with $1X10^7$ CD19.CAR or No DNA CIK cells from the same donor at day +2 and +9 (Figure 6D). BM and spleen organs were collected and a significant reduction of tumor growth by CD19.CAR CIK cells was observed compared to No DNA CIK-treated mice (Figure 6E-6G). Collectively, these results indicate a potential therapeutic effect of multiple injections of SB-engineered CAR CIK cells in the absence of simultaneous administration of rhIL-2.

Safety and efficacy assessment in SB marked CIK cells

Next, we assessed the genomic distribution of SB integration sites (IS) by linear amplification-mediated (LAM)-PCR from the genomic DNA of CD123.CAR CIK cells. Spreadex gel electrophoresis of the LAM-PCR products showed a smeared pattern (Supplementary Figure 5), suggesting a polyclonal repertoire consistent with the TCR-Vβ analysis (Supplementary Figure 6A-6B). PCR products were subject to Illumina MiSeq next-generation sequencing, and the IS were mapped on the human genome using a previously described bioinformatics pipeline.[34, 35] This approach allowed us to retrieve 1,239,800 sequencing reads with valid vector/cellular genome junctions, corresponding to 978 of unique IS (473, 212 and 293 in healthy donor (HD) 1, 2, 3, respectively) (Supplementary Table 1). Considering that each IS has a unique genetic mark which allows the identification and tracking of a cell clone and its progeny among vector-marked cells, the high number of IS retrieved further supports the presence of a polyclonal repertoire. In accordance with De Jong J. et *al*.,[36] and Gogol-Doring et *al*.,[37] the SB IS were randomly distributed along the genome without preferences for gene dense regions and characterized by a low tendency to target gene promoters (Figure 7A-7B). Moreover, we were able to identify the canonical AT-rich conserved consensus at the genomic TA dinucleotides flanking the IS [T A T A/G T, Figure 7C].[18] The clonal abundance was estimated as the relative percentage of sequence counts representing each IS with respect to the total of sequences retrieved in the analysis. No signs of dominance of individual clones emerged from this analysis (Figure 7D

and Supplementary Table 2). Finally, we sought to determine whether SB integrations in specific gene classes or genomic locations (i.e. common insertion sites, CIS) were significantly enriched, which would have indicated a selective advantage conferred by this type of integrations. Gene ontology-based overrepresentation analysis using GREAT online software (http://bejerano.stanford.edu/great/public/html/)[38] showed a significant enrichment of genes expressed in T cells (Figure 7E), in agreement with the known moderate preference of SB transposons to integrate within expressed genes.[36, 37] CIS significance analysis was performed using Montecarlo simulations considering only CIS constituted by at least 4 IS contained in a window of 100Kb. We could not identify any CIS using this method (Supplementary Table 3).

It is established that the SB11X transposase-expressing plasmid, although at low frequency, can integrate randomly into the host genome and express the transposase, which could potentially lead to remobilization of the transposon in other genomic compartments. To evaluate the kinetics of SB11X transposase expression during CIK-cell culture, which could jeopardize the stability of the genomic content of the final cell product, we developed a quantitative RT-PCR assay. The slope of the standard curves was between 3.1 and 3.4 with a correlation coefficient >0.99 (Figure 8A). The quantities of transposase were detected at day 1, 4, 7, 14, and 21 in CIK cells and normalized to 10^5 GUS molecules (Figure 8B). The expression of transposase enzyme after nucleofection, which was of about 10^7 normalized molecules, was gradually lost overtime as the plasmids

were progressively degraded and diluted by cell proliferation and fell below the limit of detection in the final cellular products (Figure 8A-8B).

Discussion

In this study, we provide evidence of an innovative GMP-grade SB transposon platform which can efficiently modify and expand CAR^+ lymphocytes. Both CD123.CAR and CD19.CAR CIK cells exhibited a fully competent T-cell response characterized by specific killing, cytokine secretion and proliferation. Furthermore, SB-engineered CIK cells showed anti-tumor activity *in vivo*. Overall, gene transfer by SB displayed a safe pattern of integrations into the host genome and did not lead to transposase expression in the final T-cell product.

Transposon gene transfer has been previously carried out in primary human T cells. However, the significant cell damage induced by electroporation due to the strong magnetic field and high quantities of DNA severely impaired the survival of modified T cells. To overcome this limitation, several groups reported that the combined use of repetitive stimulations and specific selection using microbeads,[39] cell sorting,[21, 31, 32] or artificial APC[23] could generate higher numbers of modified T cells. In our hands, electroporation of PBMCs with SB plasmids led to complete depletion of DC and monocytes resulting in poor expansion of modified cells upon stimulation with anti-CD3 mAb. In order to re-establish a physiological T cell-APC contact, which then would enhance cell

survival and stimulation rates, we added irradiated PBMCs, derived from the same source, after nucleofection. To our knowledge, this is the first approach demonstrating that high efficiency could be achieved by non-viral modification of primary human T cells with limited manipulation and stimulation requirements.

The kinetics of CAR expression in modified CIK cells raises the question whether CAR^+ cells are selected during the differentiation or impaired in transgene expression after nucleofection. The polyclonal pattern observed in the TCR-Vβ and integration analysis indicates that modified CIK cells do not undergo a selection process of specific clones. Furthermore, the delayed expansion, with respect to No DNA CIK cells, suggests that the toxicity associated with nucleofection does indeed inhibit the cellular machinery. However, the lower transgene expression in the SB-GFP condition raises the possibility that specific signaling by $CD123^+$ and $CD19^+$ PBMC subsets could stimulate CAR-transduced cells, thus explaining the CAR expression kinetic.

The rationale for using CIK over standard CAR T cells comes from our clinical experience clearly demonstrating that repeated infusions of CIK cells in patients are safe and well-tolerated.[29] The possibility of using safe donor-derived cells is of particular relevance in patients who are lymphodepleted.[40] Up to now, nearly 3,000 patients, enrolled in 45 clinical trials investigating 22 different tumors in 25 years, have been treated with CIK cells.[41] Here, we provide evidence that CIK cells obtained through our customized non-viral method are characterized by high viability and phenotypic identity.

Furthermore, the final cell product shows high CAR expression levels in the $CD3^+CD56^+$, $CD3^+CD8^+$, and $CD3^+CD4^+$ cell subsets.

Emerging clinical evidence strongly supports the notion that the therapeutic efficacy of infused cells depends on the cell type, levels of CAR expression, dose of infused cells, and design of signaling moieties. In our cell type, the persistence of subsets with naive, effector, and stem cell memory[42, 43] (data not shown) phenotypes is indicative of a potential early and sustained response *in vivo*. Concerning CAR expression, cell numbers and effector activities, we demonstrated improved efficacy of our method when directly compared to available existing SB platforms applied to conventional T cells requiring repeated stimulations.[31, 32] An additional *in vivo* validation of our cell product in respect to already clinically proved CAR T-cell approaches may be of crucial interest before moving to human studies. With regard to signaling, in order to further increase specific proliferation, we performed combined CD28-OX40 costimulation, which has been previously shown to strengthen and sustain the activation signal and to reduce IL-10 secretion.[44, 45] Even though combined CD28-OX40 costimulation has been reported to stimulate CIK cells excessively,[46] we found that in immunodeficient mice CAR-redirected CIK cells were able to significantly decrease disease burden in previously established AML and ALL models.[27, 47]

Finally, contrary to viral vectors, we found a close-to-random distributions of SB integrations without preferences for gene dense regions and low tendency to integrate near gene promoters, as

previously reported.[17, 19, 36] Most importantly, SB modified CIK cells did not show dominance of individual clones and selection of common insertion sites, which have been associated with potential leukemogenic insertional events in preclinical and clinical gene therapy.[10] Interestingly, we found a significant enrichment of genes expressed in T-cells, probably caused by the temporal proximity of the modification and CD3-specific activation, since gene expression levels are known to influence SB intragenic integrations.[36] Furthermore, the loss of transposase expression during the third week of culture suggests that the remobilization of the transposon into deleterious loci should not occur.

In conclusion, here we provide evidence of a novel model of allogeneic non-viral gene transfer which represents a valid alternative to the use of viral vectors and patient-derived CAR T cells, currently restricted to only few specialized centers and a limited number of patients. Overall, the application of our method has the potential to address key clinical and manufacturing challenges in adoptive cell therapy in relapsed leukemic patients.

Materials and Methods

Ethics Statement. Investigation has been conducted in accordance with the ethical standards. The Institutional Review Board of the Ethical Committee of San Gerardo approved this study and informed consent has been obtained from patients or their guardians according to institutional guidelines and to the Helsinki Declaration.

Cell lines and primary cells. All cell lines were maintained in culture with Advanced RPMI medium (Invitrogen, Carlsbad, CA) supplemented with 10% heat-inactivated FBS, 2mM L-glutamine, 25 IU/ml of penicillin and 25 mg/ml of streptomycin (Lonza, Basel, Switzerland). The THP-1 cell line was kindly provided by Dr. K. Fleischhauer, whereas REH, KG-1 and Nalm-6 cell lines were purchased directly from ATCC, where short tandem repeat analysis and cytogenetic studies are used to authenticate human cell lines. Primary cells from patients affected by AML and ALL were obtained from bone marrow (BM) and PB cells collected and frozen at diagnosis in San Gerardo Hospital (Table 1).

Plasmids. The high-affinity human scFv for the CD123 antigen, generated starting from the DNA encoding mAb 7G3[26, 48], was cloned in frame with CH_2CH_3-CD28-OX40-ζ from SFG-anti-CD33-CD28-OX40-ζ[49] as a transposon into a SB expression plasmid, pT-MNDU3-eGFP[23] replacing the eGFP sequence to obtain anti-CD123/pTMNDU3. The anti-CD19/pTMNDU3 was generated by

replacing the scFvCD123 with the scFv from the SFG.aCD19 (clone FMC63[50] kindly provided by Martin Pule, University College of London. The codon-optimized plasmids for SB transposase, pCMV-SB11, are described elsewhere.[47]

CIK Cell differentiation and modification. Human PBMCs, obtained from HDs upon informed consent, were isolated over Ficoll-Hypaque gradients (Pharmacia LKB, Uppsala, Sweden) and electroporated by 4D-Nucleofector™ (Lonza) with 15 μg supercoiled DNA transposon plasmid coding for CARs or GFP (SB GFP, pT-MNDU3-eGFP) and 5 μg supercoiled DNA pCMV-SB11 plasmid coding for SB11 transposase using Amaxa™ 4D-Nucleofector™ EO-115 protocol (program 1) or EF-115 (program 2) and amaxa P3 Primary Cell 4D-Nucleofector kit (Lonza). As positive control of modification, the Amaxa GFP plasmid was employed according to the manufacturer's instruction. PBMCs, from the same source, irradiated with 60Gy of 137Cs γ-rays, were added to the samples previously electroporated in the presence of DNA. CIK-cell lines were differentiated by addition of IFN-γ (1000 U/ml; Dompè Biotec, Milano, Italy) at day 0 and of IL-2 (300 U/ml; Chiron B.V) and OKT-3 (50 ng/ml; Janssen-Cilag, Emeryville, CA) at day 1 as previously described.[25] Cells were then cultured for 21 days and fresh medium and IL-2 were added weekly. Subsequent analyses were performed on bulk CIK-cell lines.

Flow cytometric analysis. T cells were tested for the expression of CD3 (clone SK7), CD8 (clone RPA-T8), CD4 (clone SK3), CD56 (clone

B159), CD62L (clone DREG-56) and CD45RO (clone UCHL1) using specific antibodies (BD Bioscience, San Jose, CA), whereas leukemic blasts were assessed for CD45 (clone 2D1), CD33 (clone HIM3-4), CD123 (clone 7G3), CD19 (clone HIB19) expression (BD Bioscience) and CD10 (eBioCB-CALLA, eBioscience, San Diego, CA). For intracytoplasmic staining, T cells were stained with anti-CD3 mAb before fixation, permeabilization (Fixation/Permeabilization Solution Kit, BD Bioscience) and incubation with anti-human IFN-γ (B27) and IL-2 mAbs (MQ1-17H12, BD Pharmingen, San Diego, CA). CAR expression was detected using an anti-Human IgG (H+L) specific antibody (Jackson ImmunoResearch, Suffolk, UK), as previously described.[49] Samples were acquired using a BD FACS Canto flow cytometer (BD Biosciences), and data were analyzed with FlowJo 7.5.5 (Tree Star, Inc., Ashland, OR) and BD FACSDIVA™ (BD Biosciences). Quadrant markers were set accordingly to unstained controls.

Cytotoxic assay. Cytotoxicity was evaluated in a 4-h co-culture assay at an effector:target (E:T) ratio of 5:1 by apoptosis detection with GFP-Certified™ Apoptosis/Necrosis detection kit (Enzo Life Sciences, Farmingdale, NY) and gating on target cells previously labeled with 5-(and 6)- Carboxyfluorescein diacetate succinimidyl ester, CFDA SE (CFSE, 1 μM, eBioscience). Briefly, killed cells was determined as percentage of Annexin V^+Necrosis Detection Reagent (similar to 7-AAD)$^-$ plus Annexin V^+Necrosis Detection Reagent$^+$ in $CFSE^+$ target cells in co-culture with the effectors compared to target cells alone.

Alternatively, flow cytometry-based quantitative analysis was employed to determine the percentage of viable target cells recovered from culture, stained with PE-anti-CD33/CFSE for AML target or PE-anti-CD19 for ALL cells.[26]

CD107a/GZB mobilization assay. T-cell degranulation was evaluated in a CD107a flow cytometric assay. Briefly, 10^5 CIKs were plated with anti-CD107a FITC mAb (4 μL/well; BD Pharmingen) in the presence or absence of 10^5 target cells. After 3h, monensin A (Sigma-Aldrich, St Louis, MO) was added (30 μg/mL). After additional 3h of incubation, cells were washed and stained with anti-CD3, and anti-Human IgG (H+L) mAb.

Cytokine detection. 10^6 T cells/ml were stimulated with leukemic blasts irradiated with 40Gy of 137Cs γ-rays at ratio of 1:1. After 48 h, culture supernatants were harvested and levels of cytokines were determined by ELISA according to the manufacturer's instruction (R&D Systems, Minneapolis, MN). The limit of detection was 15.6 pg/ml.

Proliferation. 10^6 T cells/ml were stimulated with THP-1 and REH irradiated with 100 or 40Gy of 137Cs γ-rays, respectively, at 1:1 ratio. The ability of viable cells to cleave 3-(4,5-dimethylthiazol-2-yl)-2,5-diphenyltetrazolium bromide (MTT, Sigma-Aldrich) was measured according to the manufacturer's instruction. Alternatively, CIK-cell proliferation was determined by staining with 1 μM CFSE, as

described elsewhere,[33] and CFSE dilution was analyzed by flow cytometry together with CAR expression and calculated by gating on $CD3^+$ cells.

Mice. Female 7-9 week NOD-SCID-γchain-/- (NSG) mice (The Jackson laboratory, Bar Harbor, ME) were transplanted with $5X10^6$ KG-1 or $1X10^6$ Nalm-6 cells using intravenous injection. Mice were then treated with $1X10^7$ CIK cells infused intravenously. All experiments were performed according to protocols approved by the Institutional Committees of Ministero della Salute and Milano-Bicocca University (N. 102/2013-B). All efforts were made to minimize the number of animals used and their suffering. For each experiment, we used groups of $n \geq 3$ mice.

Integration site retrieval and analysis. LAM-PCR was performed starting from 100ng of genomic DNA to collect integration sites, as previously described,[51] by using three restriction enzymes (HpyCH4IV, AciI and BfaI) and sequencing on an Illumina MiSeq sequencer, detailed in Supplementary Material.

Quantitative Real-time PCR analysis for absolute detection of transposase enzyme. Total RNA was extracted with RNeasy Mini kit (Qiagen, Hilden, Germany), and cDNA was synthesized with SuperScript II Reverse Transcriptase in the presence of RNaseOUT Ribonuclease Inhibitor (Life Technologies, Carlsbad, CA) according to manufacturer's instructions. cDNA samples (25ng RNA equivalent)

were run in duplicate or triplicate, and levels of transposase transcript were determined as relative expression by normalizing to GUS Control Gene Standards (Quiagen), detailed in Supplementary Material.

Statistical analysis. Mean values were reported as Mean±SEM. Paired t test were used to determine the statistical significance of the data, with the exception of the *in vivo* experiments analyzed by the Mann-Whitney test. Two-tailed paired analysis was performed, unless otherwise specified in the text. Statistic calculations were performed with GraphPad Prism 5.0.

Acknowledgments

The authors thank Vincenzo Rossi and Simona Songia for PCR design, Michela Bardini for helping in animal experiments, and Virna Marin for initial contribution. A deep gratitude goes to Riccardo and Donatella Ruschi and the "Amici di Duccio" association, which generously supports C.F.M. fellowship, to "Quelli che… con Luca" association, which support S.T. fellowship and to the parents' committees "Comitato Maria Letizia Verga" and "Stefano Verri" for their constant support.

Conflicts of interest

The authors declare no conflict of interest.

Grant Support

This work was supported by grants from the AIRC Foundation (AIRC Molecular Clinical Oncology 5 per mille, 9962, AIRC 2014, 15992, and AIRC 2015, 17248), the Ministero della Salute (Progetto Integrato Oncologia 2006) and the Fondazione Just Italia. C.F.M., S.T., A.B., and E.B. own a patent on the method described in this report.

Table 1. patients' characteristics[a]

	Age	Diagnosis	Subtype[b]	%CD33+	%CD123+	Karyotype and Gene Mutations	Prognosis
UPN1	8 y[c]	AML	M4	50.0	43.7	46, XX, inv(16)(p13q22)[16]/46,XX[4]; normal FLT3-ITD[e], normal NPM1a	SR[f]
UPN2	13y	AML	M2	86.0	71.3	46,XX,t(8;21)(q22;q22)[20]; normal FLT3-ITD	SR
UPN3	4y	AML	M5a	86.0	95.5	47-48,XX,del(2)(p12),del(5)(p12), ?t(6;7)(q21;q32),t(9;?)(q34;?),-11,del(12)(p11),+19,+4markers[cp9]/46,XX[3]; normal FLT3-ITD, normal NPM1a t(10;11) positive by RT-PCR	HR[g]
UPN4	16y	AML	M2	85.0	56.6	45,XY,t(8;21)(q22;q22)[6]/46,XY[6]	SR
UPN5	9y	AML	M0	95.0	99.0	46,XX[9] normal FLT3-ITD, normal NPM1a	HR
UPN6	12y	AML	M1	48.0	93.5	46,XY[25] NPM1+; FLT3 D835+	SR
	Age	**Diagnosis**	**Subtype**	**%CD10+**	**%CD19+**	**Karyotype and Gene Mutations**	**Prognosis**
UPN7	8y	ALL	BALL-IV	90.6	91.0	46,XY,t(8;14)(q24;q32)[20]	HR
UPN8	4y	ALL	BALL-III	96.4	22.3	47,XX,+21c[14] (Down)	HR
UPN9	8m[d]	ALL	BALL-I	5.6	70.2	46,XY[14]	SR

[a]Karyotype defined as International Standing Committee on Human Cytogenetic Nomenclature (ISCN) 2013; [b]ALL subtype from classification EGIL[52]; [c]y= years; [d]m= month; [e]ITD= internal tandem duplication; [f]SR= standard risk; [g]HR= high risk; [ ], number of metaphases analyzed.

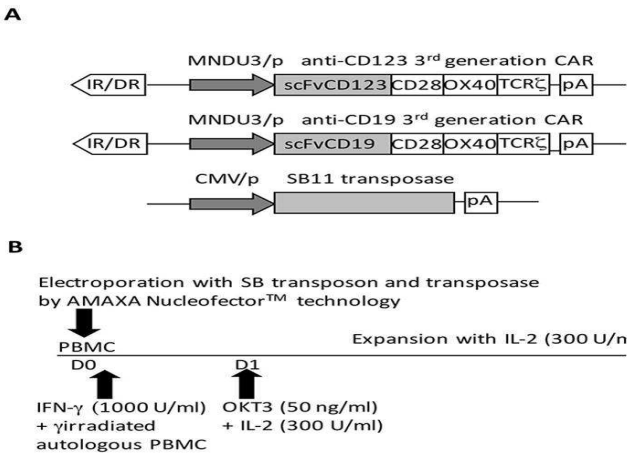

Figure 1. **Modification and expansion of mononuclear precursors by the SB system. A.** The diagram of the SB transposon and transposase constructs used in this study, encoding for CD123.CAR (upper panel), CD19.CAR (middle panel), and transposase (lower panel), is shown - IR/DR, SB inverted repeats/directed repeats; MNDU3/p, the constitutive promoter from the U3 region of the MND retrovirus; scFv, single chain fragment variable; pA, poyadenylation signal from bovine growth hormone; CMV/p, CMV promoter. **B.** The expansion and modification protocol used in this study is shown. PBMC from HDs were nucleofected at D0 with the transposon and transposase constructs using Amaxa Nucleofector™ technology. According to standard differentiation protocol, IFN-γ was added after nucleofection, whereas simultaneous addition of γ-irradiated autologous PBMCs was performed to re-establish the myeloid fraction of PBMCs impaired by the modification procedure. At day 1, the expansion protocol was started with OKT3 and IL-2 and the cells were cultured in the presence of IL-2 until day 21.

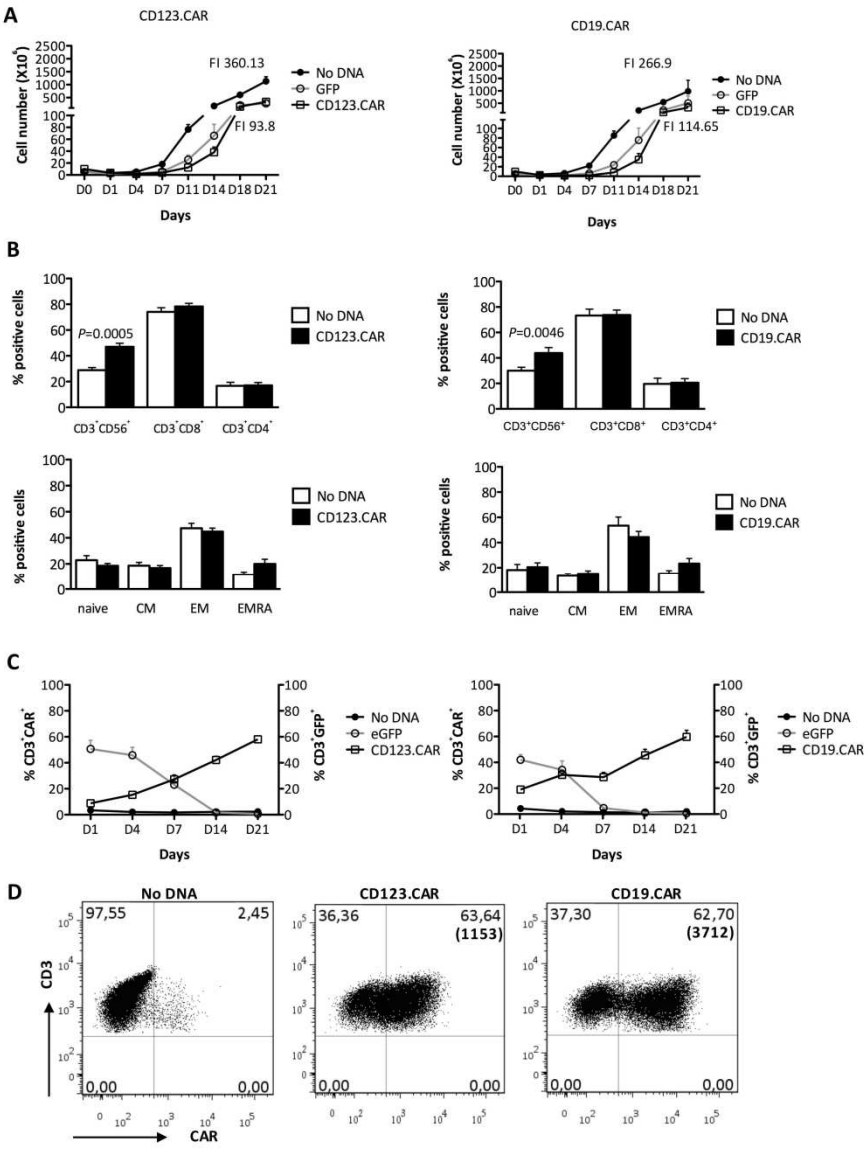
A
CD123.CAR
CD19.CAR
Cell number (X10⁴)
FI 360.13
FI 93.8
FI 266.9
FI 114.65
No DNA
GFP
CD123.CAR
CD19.CAR
D0 D1 D4 D7 D11 D14 D18 D21
Days
B
% positive cells
P=0.0005
P=0.0046
CD3⁺CD56⁺
CD3⁺CD8⁺
CD3⁺CD4⁺
naive
CM
EM
EMRA
C
% CD3⁺CAR⁺
% CD3⁺GFP⁺
eGFP
D1 D4 D7 D14 D21
D
No DNA
CD123.CAR
CD19.CAR
97,55
2,45
36,36
63,64
(1153)
37,30
62,70
(3712)
0,00
CD3
CAR

Figure 2. **Expansion, phenotype, and transgene expression of SB-modified CIK cells. A.** Proliferation of cells nucleofected in the absence of DNA, with GFP, and with SB encoding CD123.CAR (left panel) or CD19.CAR (right panel) were followed overtime by cell count. Fold increase (FI, total cell number at day 21 / cell count at day 1) is indicated. **B.** CD56/CD8/CD4, Central memory (CM)/Effector memory (EM)/Effector memory RA (EMRA) phenotype at D21. **C.** Modification was determined overtime by flow-cytometry. **A-C.** Mean±SEM were as follows: No DNA, CD123.CAR (n=13) and GFP (n=8); No DNA, CD19.CAR (n=8) and GFP (n=4). **D.** CAR expression was determined at day 21 of differentiation in one representative donor. Numbers represent the percentages of positive cells and MFI in bracket. P-values of the Paired t test are indicated.

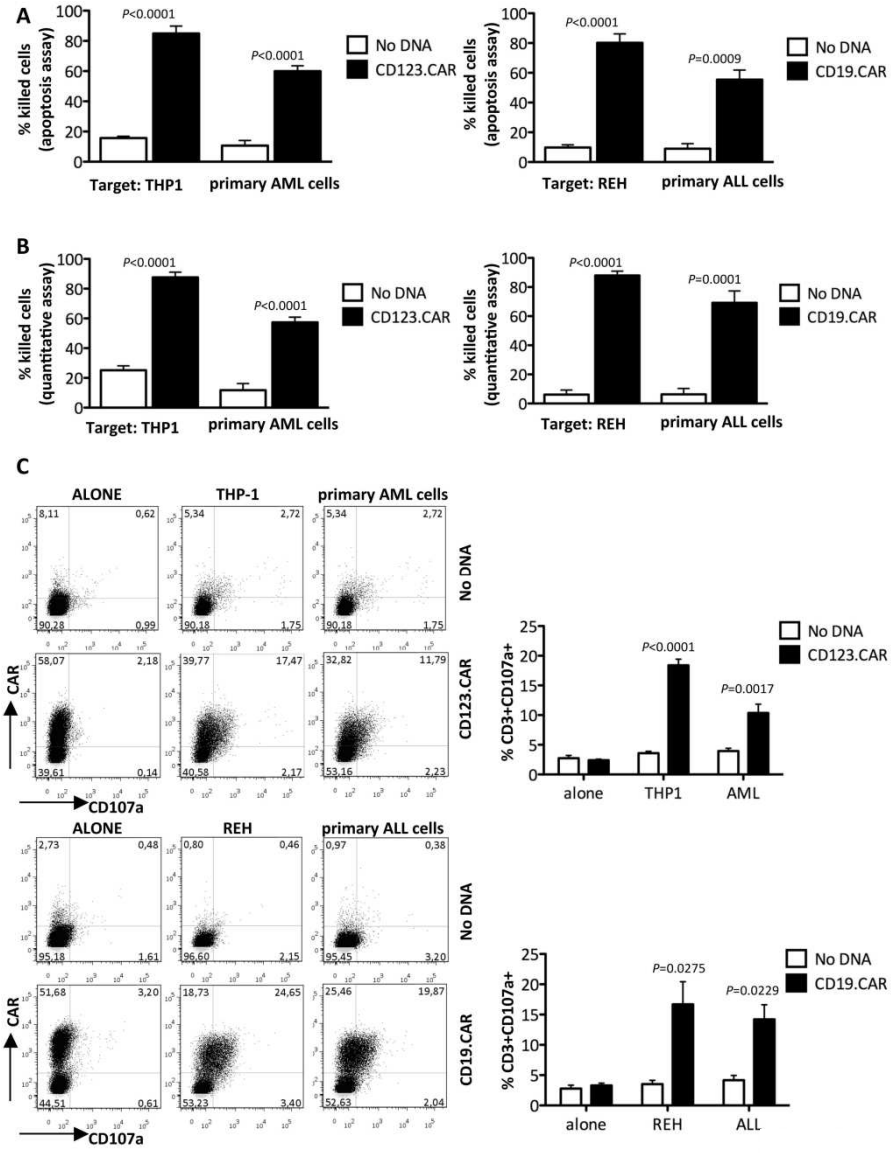
A
% killed cells (apoptosis assay)
P<0.0001
P<0.0001
No DNA
CD123.CAR
Target: THP1
primary AML cells
P<0.0001
P=0.0009
No DNA
CD19.CAR
Target: REH
primary ALL cells
B
% killed cells (quantitative assay)
P<0.0001
P<0.0001
No DNA
CD123.CAR
Target: THP1
primary AML cells
P<0.0001
P=0.0001
No DNA
CD19.CAR
Target: REH
primary ALL cells
C
ALONE
THP-1
primary AML cells
No DNA
CD123.CAR
CAR
CD107a
% CD3+CD107a+
P<0.0001
P=0.0017
No DNA
CD123.CAR
alone
THP1
AML
ALONE
REH
primary ALL cells
No DNA
CD19.CAR
CAR
CD107a
% CD3+CD107a+
P=0.0275
P=0.0229
No DNA
CD19.CAR
alone
REH
ALL

Figure 3. CD123.CAR and CD19.CAR redirect CIK-cell activity against CD123+ and CD19+ cells. A. Cytotoxic activity of modified CIK cells against target cells was determined by apoptosis detection assay. The E:T ratio was 5:1. Mean±SEM of THP-1 (n=6), REH (n=8), primary AML (n=10), and ALL cells (n=6) are indicated. **B.** Cytotoxic activity by quantitative detection was determined at an E:T ratio of 5:1. Mean±SEM of THP-1 and REH (n=7) and of primary AML (n=8) and ALL (n=7) cells are shown. **C.** CD107a expression was measured in CD123.CAR- or CD19.CAR- modified CIK cells co-cultured with target cells at an E:T ratio of 1:1. Representative results from one out of 9 donors for THP-1, 7 primary AML and 5 REH and ALL cells. Numbers represent the percentages of CD107a+ cells. Mean±SEM values are plotted alongside. P-values of the Paired t test are shown.

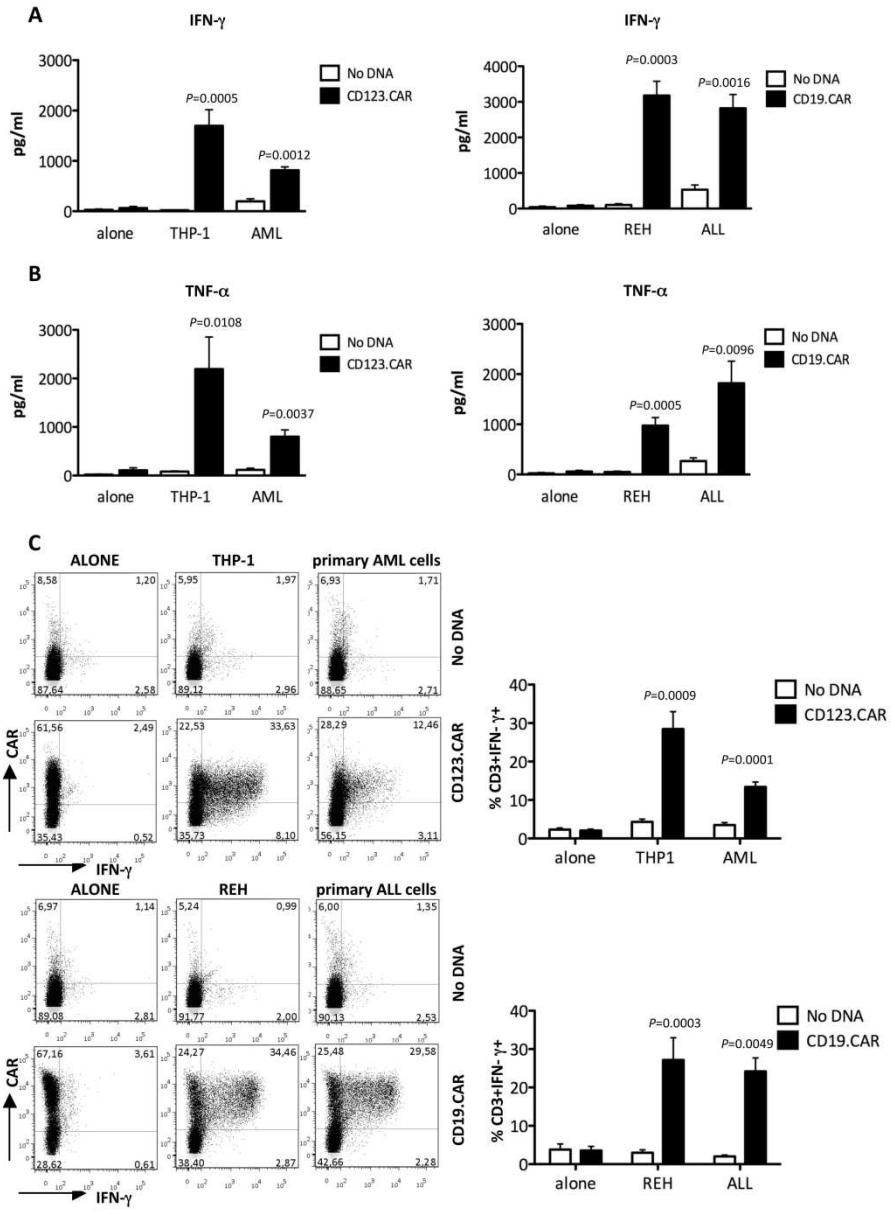
A
IFN-γ
pg/ml
3000
2000
1000
0
P=0.0005
P=0.0012
No DNA
CD123.CAR
alone
THP-1
AML
IFN-γ
pg/ml
4000
3000
2000
1000
0
P=0.0003
P=0.0016
No DNA
CD19.CAR
alone
REH
ALL
B
TNF-α
pg/ml
3000
2000
1000
0
P=0.0108
P=0.0037
No DNA
CD123.CAR
alone
THP-1
AML
TNF-α
pg/ml
3000
2000
1000
0
P=0.0005
P=0.0096
No DNA
CD19.CAR
alone
REH
ALL
C
ALONE
THP-1
primary AML cells
No DNA
CD123.CAR
CAR
IFN-γ
8,58
1,20
87,64
2,58
5,95
1,97
89,12
2,96
6,93
1,71
88,65
2,71
61,56
2,49
35,43
0,52
22,53
33,63
35,73
8,10
28,29
12,46
56,15
3,11
% CD3+IFN- γ+
40
30
20
10
0
P=0.0009
P=0.0001
No DNA
CD123.CAR
alone
THP1
AML
ALONE
REH
primary ALL cells
No DNA
CD19.CAR
CAR
IFN-γ
6,97
1,14
89,08
2,81
5,24
0,99
91,77
2,00
6,00
1,35
90,13
2,53
67,16
3,61
28,62
0,61
24,27
34,46
38,40
2,87
25,48
29,58
42,66
2,28
% CD3+IFN- γ+
40
30
20
10
0
P=0.0003
P=0.0049
No DNA
CD19.CAR
alone
REH
ALL

Figure 4. Specific cytokine production of CD123.CAR and CD19.CAR CIK cells. A-B. The IFN-γ (**A**) and TNF-α (**B**) production was determined by ELISA upon stimulation of CD123.CAR CIK cells with THP1 and primary AML cells and CD19.CAR CIK cells with REH or primary ALL cells. Mean±SEM of THP-1 (n=10) and REH (n=8), and of primary AML and ALL cells (n=7) are shown. **C.** In parallel, IFN-γ expression was determined by intracytoplasmic staining. Representative results for one donor out of 9, for CD123.CAR, and 8, for CD19.CAR, are shown. Numbers represent the percentages of positive cells. Mean±SEM values are plotted alongside. P-values of the Paired t test are indicated.

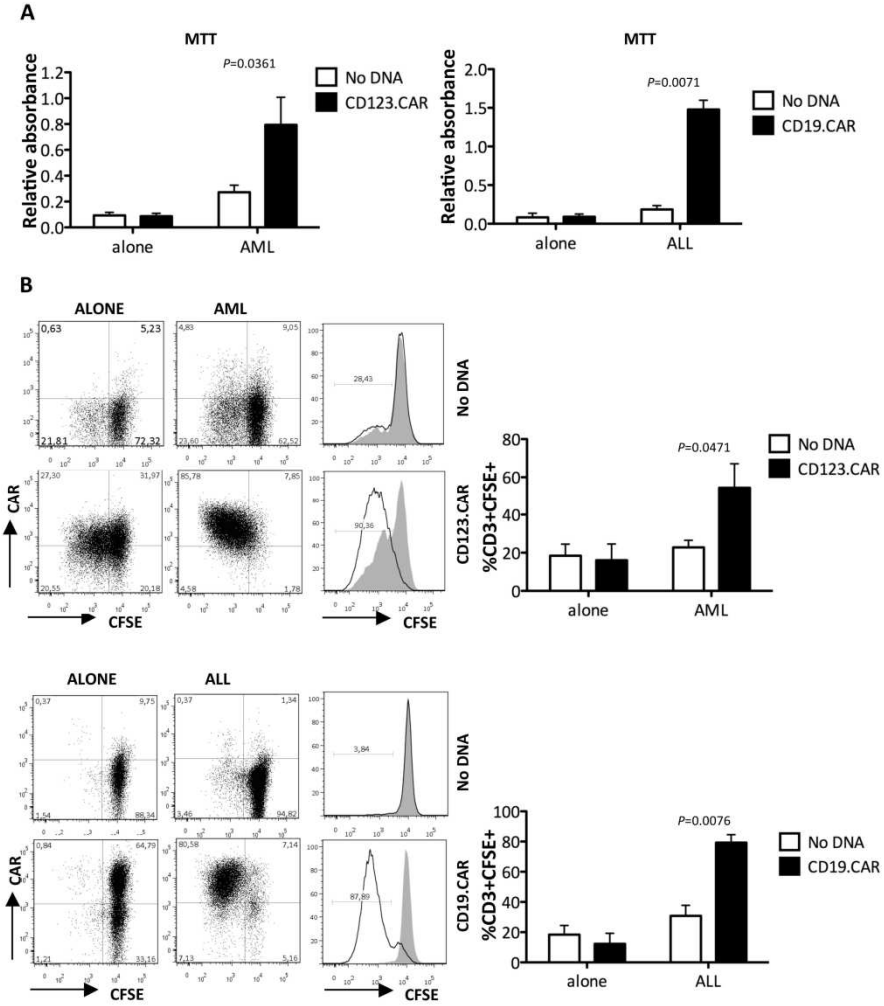
A
MTT
P=0.0361
No DNA
CD123.CAR
Relative absorbance
1.2
1.0
0.8
0.6
0.4
0.2
0.0
alone
AML
MTT
P=0.0071
No DNA
CD19.CAR
Relative absorbance
2.0
1.5
1.0
0.5
0.0
alone
ALL
B
ALONE
AML
No DNA
CD123.CAR
CAR
CFSE
%CD3+CFSE+
P=0.0471
No DNA
CD123.CAR
alone
AML
ALONE
ALL
No DNA
CD19.CAR
CAR
CFSE
%CD3+CFSE+
P=0.0076
No DNA
CD19.CAR
alone
ALL

Figure 5. CD123.CAR and CD19.CAR CIK cells proliferate in response to CD123+ and CD19+ blasts. A. Proliferation of No DNA, CD123.CAR and CD19.CAR CIK cells after stimulation with AML or ALL cell lines was determined by MTT assay. Mean±SEM of CD123.CAR (n=8) and CD19.CAR (n=5) are shown. **B.** Proliferation was determined by CFSE standard assay. Representative results from one out of 5 donors are shown. Numbers represent the percentages of positive cells. Mean±SEM values are plotted alongside. P-values of the Paired t test are indicated.

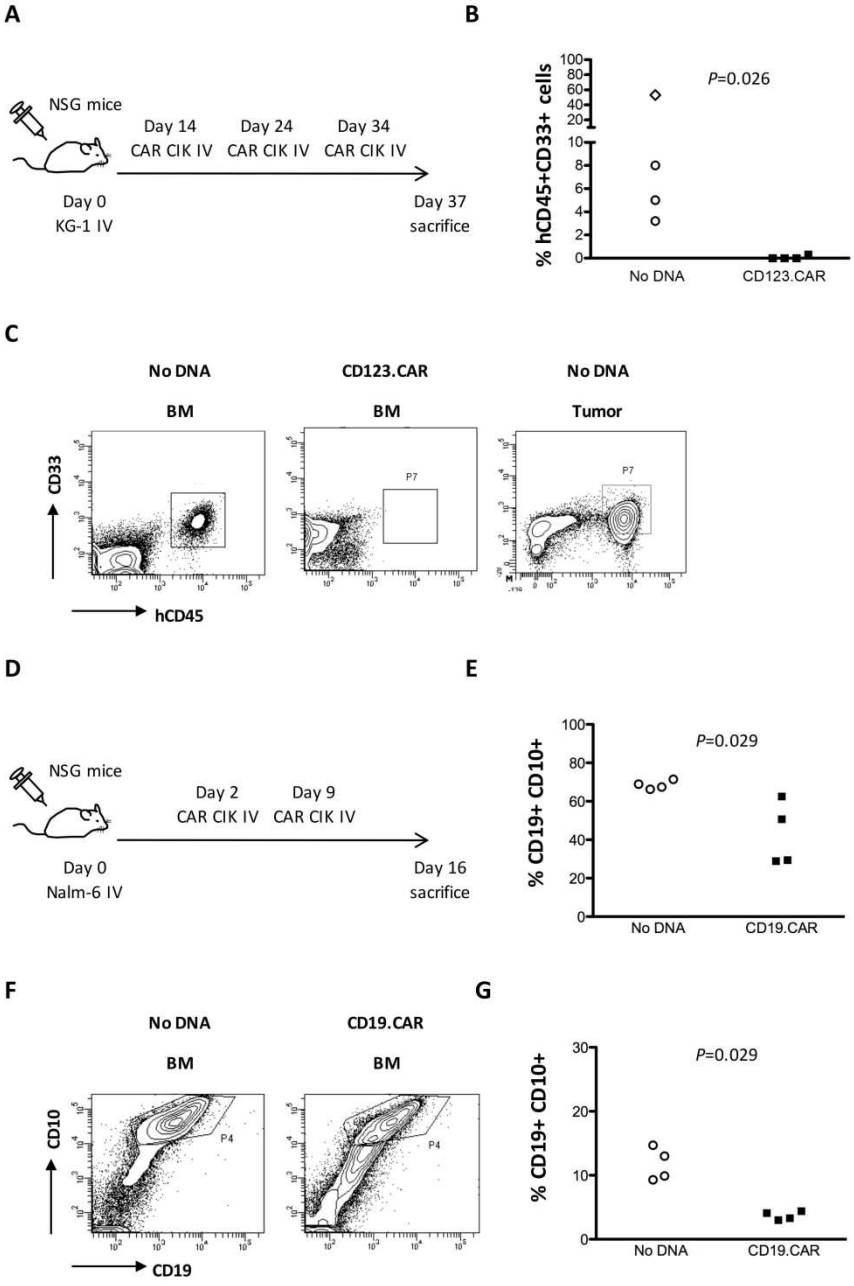
A
NSG mice
Day 14
CAR CIK IV
Day 24
CAR CIK IV
Day 34
CAR CIK IV
Day 0
KG-1 IV
Day 37
sacrifice
B
% hCD45+CD33+ cells
P=0.026
No DNA
CD123.CAR
C
No DNA
BM
CD123.CAR
BM
No DNA
Tumor
CD33
hCD45
P7
D
NSG mice
Day 2
CAR CIK IV
Day 9
CAR CIK IV
Day 0
Nalm-6 IV
Day 16
sacrifice
E
% CD19+ CD10+
P=0.029
No DNA
CD19.CAR
F
No DNA
BM
CD19.CAR
BM
CD10
CD19
P4
G
% CD19+ CD10+
P=0.029
No DNA
CD19.CAR

Figure 6. *In vivo* anti-tumor activity of CD123.CAR and CD19.CAR CIK cells. A. Schematic representation of the AML experiment. Engraftment was measured based on the presence of mouse $CD45^-$ human $CD45^{dim}$ $CD33^+$ cells by BM puncture. Infusion of CIK cells was performed on days 14, 24 and 34 after transplantation. Mice were sacrificed after 37 days. **B-C.** KG-1 engraftment in the BM or in extramedullary tumors (rhombus). Each dot represents a mouse. Representative results from one CD123.CAR donor and one No DNA donor are shown. **D.** Schematic representation of the ALL experiment. Engraftment was measured based on the presence of mouse $CD45^-$ $CD10^+$ $CD19^+$ cells by BM puncture. Infusion of CIK cells was performed on days 2 and 9 after transplantation. **E-G.** Mice were sacrificed after 16 days. Nalm-6 engraftment in the BM (**E-F**) and spleen (**G**). Each dot represents a mouse. Representative results from one CD19.CAR donor and one No DNA donor are shown. P-values of the Mann Whitney test are indicated.

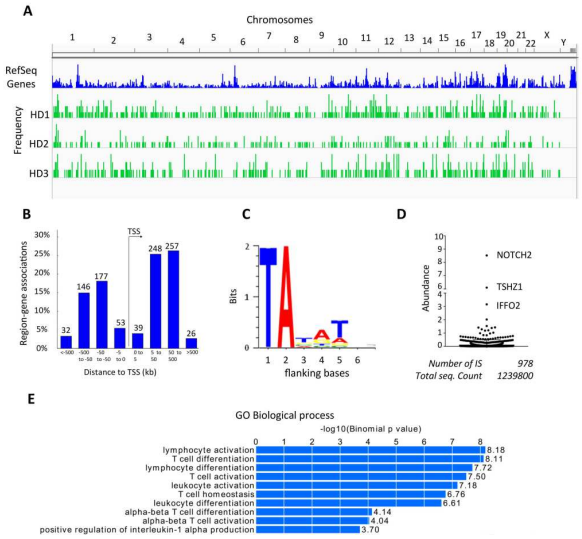

Figure 7. Integration site analysis in transduced CIK-cell cultures. A. Graphic representation of the distribution of integrations at chromosome level in the genome of each HDs. **B.** Frequency distribution of SB integrations around the Transcription Start Site (TSS) (intervals in Kb, x-axis) of the nearest target gene (in %, y-axis). The number of integrations mapping in each genomic interval is indicated above each bar. **C.** logo-plot representation of the bases flanking the SB integration sites - the positions of the bases after the SB integration site are indicated in the X-axis - showing the characteristic TA motif present at each SB integration. **D.** Relative clonal abundance of clones harboring specific ISs; y-axis, % of sequencing reads with respect to the total sequencing reads found for HD1, HD2 and HD3 pooled together. The name of the nearest target gene is indicated for clones with abundance >3%. **E.** Overrepresented gene classes of the Gene Ontology (GO) Biological process targeted by SB integrations.

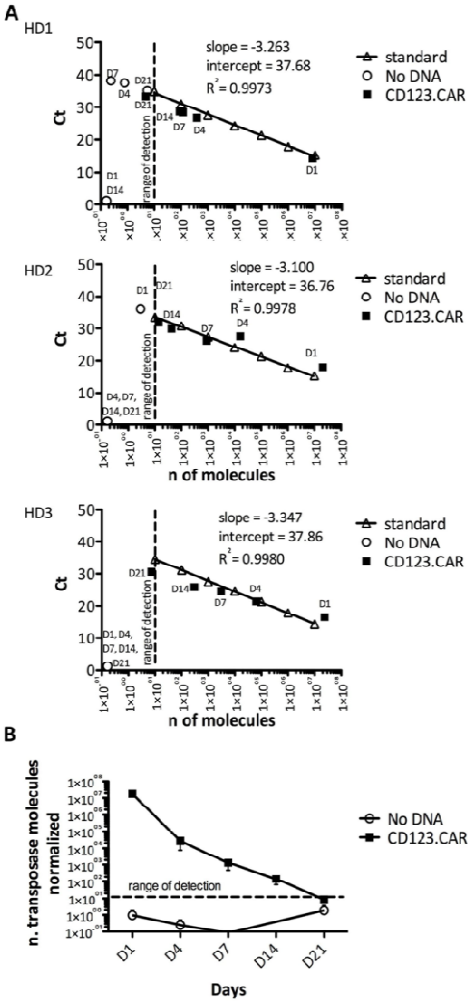

Figure 8. Transposase clearance in transduced CIK cells. A. Expression analysis of transposase by quantitative real time PCR (Q-RT-PCR) in No DNA control cells and CD123.CAR cells on days 1, 4, 7, 14, 21 during differentiation (n=3). Slope, coefficient of determination (R2), and intercept of the standard curve are shown. **B.** Evaluation of the transposon expression in CIK cell cultures over time by Q-RT-PCR, as number of transposase molecules normalized to 10^4 GUS copies. Mean±SEM from 3 donors are shown.

References:

1. Grupp SA, Kalos M, Barrett D, Aplenc R, Porter DL, Rheingold SR, Teachey DT, Chew A, Hauck B, Wright JF, Milone MC, Levine BL and June CH. Chimeric antigen receptor-modified T cells for acute lymphoid leukemia. N Engl J Med. 2013; 368(16):1509-1518.

2. Lee DW, Kochenderfer JN, Stetler-Stevenson M, Cui YK, Delbrook C, Feldman SA, Fry TJ, Orentas R, Sabatino M, Shah NN, Steinberg SM, Stroncek D, Tschernia N, Yuan C, Zhang H, Zhang L, et al. T cells expressing CD19 chimeric antigen receptors for acute lymphoblastic leukaemia in children and young adults: a phase 1 dose-escalation trial. Lancet. 2015; 385(9967):517-528.

3. Maude SL, Frey N, Shaw PA, Aplenc R, Barrett DM, Bunin NJ, Chew A, Gonzalez VE, Zheng Z, Lacey SF, Mahnke YD, Melenhorst JJ, Rheingold SR, Shen A, Teachey DT, Levine BL, et al. Chimeric antigen receptor T cells for sustained remissions in leukemia. N Engl J Med. 2014; 371(16):1507-1517.

4. Kochenderfer JN, Dudley ME, Kassim SH, Somerville RP, Carpenter RO, Stetler-Stevenson M, Yang JC, Phan GQ, Hughes MS, Sherry RM, Raffeld M, Feldman S, Lu L, Li YF, Ngo LT, Goy A, et al. Chemotherapy-refractory diffuse large B-cell lymphoma and indolent B-cell malignancies can be effectively treated with autologous T cells expressing an anti-CD19 chimeric antigen receptor. J Clin Oncol. 2015; 33(6):540-549.

5. Kalos M, Levine BL, Porter DL, Katz S, Grupp SA, Bagg A and June CH. T cells with chimeric antigen receptors have potent

antitumor effects and can establish memory in patients with advanced leukemia. Sci Transl Med. 2011; 3(95):95ra73.

6. Garfall AL, Maus MV, Hwang W-T, Lacey SF, Mahnke YD, Melenhorst JJ, Zheng Z, Vogl DT, Cohen AD, Weiss BM, Dengel K, Kerr NDS, Bagg A, Levine BL, June CH and Stadtmauer EA. Chimeric Antigen Receptor T Cells against CD19 for Multiple Myeloma doi:10.1056/NEJMoa1504542. New England Journal of Medicine. 2015; 373(11):1040-1047.

7. Zhang T, Cao L, Xie J, Shi N, Zhang Z, Luo Z, Yue D, Zhang Z, Wang L, Han W, Xu Z, Chen H and Zhang Y. Efficiency of CD19 chimeric antigen receptor-modified T cells for treatment of B cell malignancies in phase I clinical trials: a meta-analysis. Oncotarget. 2015; 6(32):33961-33971.

8. Davila ML, Riviere I, Wang X, Bartido S, Park J, Curran K, Chung SS, Stefanski J, Borquez-Ojeda O, Olszewska M, Qu J, Wasielewska T, He Q, Fink M, Shinglot H, Youssif M, et al. Efficacy and toxicity management of 19-28z CAR T cell therapy in B cell acute lymphoblastic leukemia. Sci Transl Med. 2014; 6(224):224ra225.

9. Gross G, Waks T and Eshhar Z. Expression of immunoglobulin-T-cell receptor chimeric molecules as functional receptors with antibody-type specificity. Proc Natl Acad Sci U S A. 1989; 86(24):10024-10028.

10. Kay MA, Glorioso JC and Naldini L. Viral vectors for gene therapy: the art of turning infectious agents into vehicles of therapeutics. Nat Med. 2001; 7(1):33-40.

11. Chira S, Jackson CS, Oprea I, Ozturk F, Pepper MS, Diaconu I, Braicu C, Raduly LZ, Calin GA and Berindan-Neagoe I. Progresses towards safe and efficient gene therapy vectors. Oncotarget. 2015; 6(31):30675-30703.

12. Scholler J, Brady TL, Binder-Scholl G, Hwang WT, Plesa G, Hege KM, Vogel AN, Kalos M, Riley JL, Deeks SG, Mitsuyasu RT, Bernstein WB, Aronson NE, Levine BL, Bushman FD and June CH. Decade-long safety and function of retroviral-modified chimeric antigen receptor T cells. Sci Transl Med. 2012; 4(132):132ra153.

13. Magnani CF, Tettamanti S, Maltese F, Turazzi N, Biondi A and Biagi E. Advanced targeted, cell and gene-therapy approaches for pediatric hematological malignancies: results and future perspectives. Front Oncol. 2013; 3:106.

14. Schutsky K, Song DG, Lynn R, Smith JB, Poussin M, Figini M, Zhao Y and Powell DJ, Jr. Rigorous optimization and validation of potent RNA CAR T cell therapy for the treatment of common epithelial cancers expressing folate receptor. Oncotarget. 2015; 6(30):28911-28928.

15. Zhao Y, Moon E, Carpenito C, Paulos CM, Liu X, Brennan AL, Chew A, Carroll RG, Scholler J, Levine BL, Albelda SM and June CH. Multiple injections of electroporated autologous T cells expressing a chimeric antigen receptor mediate regression of human disseminated tumor. Cancer Res. 2010; 70(22):9053-9061.

16. Ivics Z, Hackett PB, Plasterk RH and Izsvak Z. Molecular reconstruction of Sleeping Beauty, a Tc1-like transposon from fish, and its transposition in human cells. Cell. 1997; 91(4):501-510.

17. Yant SR, Wu X, Huang Y, Garrison B, Burgess SM and Kay MA. High-resolution genome-wide mapping of transposon integration in mammals. Mol Cell Biol. 2005; 25(6):2085-2094.

18. Vigdal TJ, Kaufman CD, Izsvak Z, Voytas DF and Ivics Z. Common physical properties of DNA affecting target site selection of sleeping beauty and other Tc1/mariner transposable elements. J Mol Biol. 2002; 323(3):441-452.

19. Huang X, Guo H, Tammana S, Jung YC, Mellgren E, Bassi P, Cao Q, Tu ZJ, Kim YC, Ekker SC, Wu X, Wang SM and Zhou X. Gene transfer efficiency and genome-wide integration profiling of Sleeping Beauty, Tol2, and piggyBac transposons in human primary T cells. Mol Ther. 2010; 18(10):1803-1813.

20. Montini E, Cesana D, Schmidt M, Sanvito F, Bartholomae CC, Ranzani M, Benedicenti F, Sergi LS, Ambrosi A, Ponzoni M, Doglioni C, Di Serio C, von Kalle C and Naldini L. The genotoxic potential of retroviral vectors is strongly modulated by vector design and integration site selection in a mouse model of HSC gene therapy. J Clin Invest. 2009; 119(4):964-975.

21. Huang X, Wilber AC, Bao L, Tuong D, Tolar J, Orchard PJ, Levine BL, June CH, McIvor RS, Blazar BR and Zhou X. Stable gene transfer and expression in human primary T cells by the Sleeping Beauty transposon system. Blood. 2006; 107(2):483-491.

22. Singh H, Figliola MJ, Dawson MJ, Olivares S, Zhang L, Yang G, Maiti S, Manuri P, Senyukov V, Jena B, Kebriaei P, Champlin RE, Huls H and Cooper LJ. Manufacture of clinical-grade CD19-specific T cells stably expressing chimeric antigen receptor using Sleeping Beauty

system and artificial antigen presenting cells. PLoS One. 2013; 8(5):e64138.

23. Singh H, Manuri PR, Olivares S, Dara N, Dawson MJ, Huls H, Hackett PB, Kohn DB, Shpall EJ, Champlin RE and Cooper LJ. Redirecting specificity of T-cell populations for CD19 using the Sleeping Beauty system. Cancer Res. 2008; 68(8):2961-2971.

24. Schmidt-Wolf IG, Negrin RS, Kiem HP, Blume KG and Weissman IL. Use of a SCID mouse/human lymphoma model to evaluate cytokine-induced killer cells with potent antitumor cell activity. J Exp Med. 1991; 174(1):139-149.

25. Marin V, Dander E, Biagi E, Introna M, Fazio G, Biondi A and D'Amico G. Characterization of in vitro migratory properties of anti-CD19 chimeric receptor-redirected CIK cells for their potential use in B-ALL immunotherapy. Exp Hematol. 2006; 34(9):1219-1229.

26. Tettamanti S, Marin V, Pizzitola I, Magnani CF, Giordano Attianese GM, Cribioli E, Maltese F, Galimberti S, Lopez AF, Biondi A, Bonnet D and Biagi E. Targeting of acute myeloid leukaemia by cytokine-induced killer cells redirected with a novel CD123-specific chimeric antigen receptor. Br J Haematol. 2013; 161(3):389-401.

27. Pizzitola I, Anjos-Afonso F, Rouault-Pierre K, Lassailly F, Tettamanti S, Spinelli O, Biondi A, Biagi E and Bonnet D. Chimeric antigen receptors against CD33/CD123 antigens efficiently target primary acute myeloid leukemia cells in vivo. Leukemia. 2014; 28(8):1596-1605.

28. Nishimura R, Baker J, Beilhack A, Zeiser R, Olson JA, Sega EI, Karimi M and Negrin RS. In vivo trafficking and survival of cytokine-

induced killer cells resulting in minimal GVHD with retention of antitumor activity. Blood. 2008; 112(6):2563-2574.

29. Introna M, Borleri G, Conti E, Franceschetti M, Barbui AM, Broady R, Dander E, Gaipa G, D'Amico G, Biagi E, Parma M, Pogliani EM, Spinelli O, Baronciani D, Grassi A, Golay J, et al. Repeated infusions of donor-derived cytokine-induced killer cells in patients relapsing after allogeneic stem cell transplantation: a phase I study. Haematologica. 2007; 92(7):952-959.

30. Field AC, Vink C, Gabriel R, Al-Subki R, Schmidt M, Goulden N, Stauss H, Thrasher A, Morris E and Qasim W. Comparison of lentiviral and sleeping beauty mediated alphabeta T cell receptor gene transfer. PLoS One. 2013; 8(6):e68201.

31. Peng PD, Cohen CJ, Yang S, Hsu C, Jones S, Zhao Y, Zheng Z, Rosenberg SA and Morgan RA. Efficient nonviral Sleeping Beauty transposon-based TCR gene transfer to peripheral blood lymphocytes confers antigen-specific antitumor reactivity. Gene Ther. 2009; 16(8):1042-1049.

32. Huang X, Guo H, Kang J, Choi S, Zhou TC, Tammana S, Lees CJ, Li ZZ, Milone M, Levine BL, Tolar J, June CH, Scott McIvor R, Wagner JE, Blazar BR and Zhou X. Sleeping Beauty transposon-mediated engineering of human primary T cells for therapy of CD19+ lymphoid malignancies. Mol Ther. 2008; 16(3):580-589.

33. Gagliani N, Magnani CF, Huber S, Gianolini ME, Pala M, Licona-Limon P, Guo B, Herbert DR, Bulfone A, Trentini F, Di Serio C, Bacchetta R, Andreani M, Brockmann L, Gregori S, Flavell RA, et al.

Coexpression of CD49b and LAG-3 identifies human and mouse T regulatory type 1 cells. Nat Med. 2013; 19(6):739-746.

34. Aiuti A, Biasco L, Scaramuzza S, Ferrua F, Cicalese MP, Baricordi C, Dionisio F, Calabria A, Giannelli S, Castiello MC, Bosticardo M, Evangelio C, Assanelli A, Casiraghi M, Di Nunzio S, Callegaro L, et al. Lentiviral hematopoietic stem cell gene therapy in patients with Wiskott-Aldrich syndrome. Science. 2013; 341(6148):1233151.

35. Biffi A, Montini E, Lorioli L, Cesani M, Fumagalli F, Plati T, Baldoli C, Martino S, Calabria A, Canale S, Benedicenti F, Vallanti G, Biasco L, Leo S, Kabbara N, Zanetti G, et al. Lentiviral hematopoietic stem cell gene therapy benefits metachromatic leukodystrophy. Science. 2013; 341(6148):1233158.

36. de Jong J, Akhtar W, Badhai J, Rust AG, Rad R, Hilkens J, Berns A, van Lohuizen M, Wessels LF and de Ridder J. Chromatin landscapes of retroviral and transposon integration profiles. PLoS Genet. 2014; 10(4):e1004250.

37. Gogol-Doring A, Ammar I, Gupta S, Bunse M, Miskey C, Chen W, Uckert W, Schulz TF, Izsvak Z and Ivics Z. Genome-wide Profiling Reveals Remarkable Parallels Between Insertion Site Selection Properties of the MLV Retrovirus and the piggyBac Transposon in Primary Human CD4(+) T Cells. Mol Ther. 2016; 24(3):592-606.

38. McLean CY, Bristor D, Hiller M, Clarke SL, Schaar BT, Lowe CB, Wenger AM and Bejerano G. GREAT improves functional interpretation of cis-regulatory regions. Nat Biotechnol. 2010; 28(5):495-501.

39. Nakazawa Y, Huye LE, Salsman VS, Leen AM, Ahmed N, Rollins L, Dotti G, Gottschalk SM, Wilson MH and Rooney CM. PiggyBac-mediated cancer immunotherapy using EBV-specific cytotoxic T-cells expressing HER2-specific chimeric antigen receptor. Mol Ther. 2011; 19(12):2133-2143.

40. Magnani CF, Biondi A and Biagi E. Donor-derived CD19-targeted T cells in allogeneic transplants. Curr Opin Hematol. 2015; 22(6):497-502.

41. Schmeel LC, Schmeel FC, Coch C and Schmidt-Wolf IG. Cytokine-induced killer (CIK) cells in cancer immunotherapy: report of the international registry on CIK cells (IRCC). J Cancer Res Clin Oncol. 2014; 141:839-849.

42. Gattinoni L, Lugli E, Ji Y, Pos Z, Paulos CM, Quigley MF, Almeida JR, Gostick E, Yu Z, Carpenito C, Wang E, Douek DC, Price DA, June CH, Marincola FM, Roederer M, et al. A human memory T cell subset with stem cell-like properties. Nat Med. 2011; 17(10):1290-1297.

43. Xu Y, Zhang M, Ramos CA, Durett A, Liu E, Dakhova O, Liu H, Creighton CJ, Gee AP, Heslop HE, Rooney CM, Savoldo B and Dotti G. Closely related T-memory stem cells correlate with in vivo expansion of CAR.CD19-T cells and are preserved by IL-7 and IL-15. Blood. 2014; 123(24):3750-3759.

44. Pule MA, Straathof KC, Dotti G, Heslop HE, Rooney CM and Brenner MK. A chimeric T cell antigen receptor that augments cytokine release and supports clonal expansion of primary human T cells. Mol Ther. 2005; 12(5):933-941.

45. Hombach AA, Heiders J, Foppe M, Chmielewski M and Abken H. OX40 costimulation by a chimeric antigen receptor abrogates CD28 and IL-2 induced IL-10 secretion by redirected CD4(+) T cells. Oncoimmunology. 2012; 1(4):458-466.

46. Hombach AA, Rappl G and Abken H. Arming cytokine-induced killer cells with chimeric antigen receptors: CD28 outperforms combined CD28-OX40 "super-stimulation". Mol Ther. 2013; 21(12):2268-2277.

47. Singh H, Figliola MJ, Dawson MJ, Huls H, Olivares S, Switzer K, Mi T, Maiti S, Kebriaei P, Lee DA, Champlin RE and Cooper LJ. Reprogramming CD19-specific T cells with IL-21 signaling can improve adoptive immunotherapy of B-lineage malignancies. Cancer Res. 2011; 71(10):3516-3527.

48. Sun Q, Woodcock JM, Rapoport A, Stomski FC, Korpelainen EI, Bagley CJ, Goodall GJ, Smith WB, Gamble JR, Vadas MA and Lopez AF. Monoclonal antibody 7G3 recognizes the N-terminal domain of the human interleukin-3 (IL-3) receptor alpha-chain and functions as a specific IL-3 receptor antagonist. Blood. 1996; 87(1):83-92.

49. Marin V, Pizzitola I, Agostoni V, Attianese GM, Finney H, Lawson A, Pule M, Rousseau R, Biondi A and Biagi E. Cytokine-induced killer cells for cell therapy of acute myeloid leukemia: improvement of their immune activity by expression of CD33-specific chimeric receptors. Haematologica. 2010; 95(12):2144-2152.

50. Nicholson IC, Lenton KA, Little DJ, Decorso T, Lee FT, Scott AM, Zola H and Hohmann AW. Construction and characterisation of a functional CD19 specific single chain Fv fragment for immunotherapy

of B lineage leukaemia and lymphoma. Mol Immunol. 1997; 34(16-17):1157-1165.

51. Schmidt M, Schwarzwaelder K, Bartholomae C, Zaoui K, Ball C, Pilz I, Braun S, Glimm H and von Kalle C. High-resolution insertion-site analysis by linear amplification-mediated PCR (LAM-PCR). Nat Methods. 2007; 4(12):1051-1057.

52. Bene MC, Castoldi G, Knapp W, Ludwig WD, Matutes E, Orfao A and van't Veer MB. Proposals for the immunological classification of acute leukemias. European Group for the Immunological Characterization of Leukemias (EGIL). Leukemia. 1995; 9(10):1783-1786.

Chapter 5

Summary, conclusions and future perspectives

B-cell Acute lymphoblastic leukemia is the most common type of leukemia in children and, although the outcome has greatly improved over the past decades reaching an overall survival rate of 85%, a significative number of patient sill relapse or become refractory to the therapies[34]. Moreover, adult patients are still difficult to cure with standard chemotherapies demonstrating the poorest prognosis with an overall survival of 30-40% [1]. In this context, the use of immunotherapeutic approaches such as CAR expressing T cells, could represent a valid therapeutic alternative. CARs are artificial receptors that are able to redirect T-cell specificity and killing/effector activity towards virtually any surface tumor-associated antigen combining an antigen-binding moiety derived from a monoclonal antibody with an intracellular signaling domain obtained from T-cells [35]. The role of immunotherapy is well established by now. Indeed, among the therapeutic options for cancer treatment, conventional chemotherapy is now flanked by immunotherapy. In particular, in B-ALL context anti-CD19 CAR T-cell therapy has been granted as "breakthrough therapy" by the United States Food and Drug Administration in 2013 [36]. This event opened a new era in the field of cancer therapy. Despite the initial success, various adverse events were evident in the clinical translation including the risk of "on-target-off-tumor" toxicity, risk of cytokine release syndrome and the establishment of an antigen escape mechanism [37,38]. The downregulation of the target antigen is the latest side effect described in CAR context [22]. CD19 represent an ideal target for immunotherapeutic treatment of B-cell neoplasms because of its

pattern of expression and because the “on-target-off-tumor” toxicity is limited to a B-cell aplasia easily manageable with periodic intravenous administration of immunoglobulins [39]. However, recent data supports the idea that B-ALL leukemic blasts do not depend on CD19 for survival and proliferation [9]. For this reason the selective pressure exerted by CD19-specific therapies leads to the establishment of CD19-negative relapses in about 60% of treated patients [8]. Hence, the need of finding more effective therapeutic strategies become urgent. To date several studies have described the expression of BAFF-R in various B-cell malignancies, including B-ALL, and its fundamental role in maturation and survival of mature B cells and in survival and chemoresistance of B-ALL blasts [15–18]. Furthermore, BAFF-R is undetectable on pro-B and pre-B cells it begins to be expressed from immature B cells [40]. Recently, our collaborators reported interesting observations about the preservation of BAFF-R expression during early drug treatment and the recovery of BAFF physiological threshold after leukemic bulk reduction (Fazio G. *et al.*, *manuscript in preparation*).

Being BAFF-BAFF-R axis so essential both in normal and pathological conditions we hypothesized that the downregulation of the antigen, as reported for CD19, will be unlikely upon treatment with CAR approach. Moreover, the more restricted expression pattern compared to CD19, allows to reduce the impact of B-cell aplasia and consequential side effects.

In this study we confirmed a B-cell restricted distribution of BAFF-R mRNA transcript in primary B-ALL samples and in B-cells containing

organs but not in other healthy tissues. At the same time we found that surface expression of this receptor has been preserved and significantly increased in relapsed samples compared to diagnostic one.

In our work we described the development of the first anti-BAFFR CAR, to our knowledge, and the feasibility of targeting BAFF-R antigen. We designed and constructed variants of the same chimeric receptor where we modified the orientation of variable regions and/or the length of the spacer moiety. An initial screening of these anti-BAFFR CAR variants allowed us to test the effect of spacer modification on CAR expression and functionality. Thanks to the obtained information we were able to identify the optimal configuration for our anti-BAFFR CAR which resulted in best antitumor performances. We found that spacer truncation in some cases heavily impaired CAR expression and the best interaction with the antigen and more efficient cytokine production were obtained in absence of the CH2CH3 moiety and with the single chain in the inverted orientation. We then further demonstrated the capability of the selected INVsh.CAR variant to produce a specific anti-tumor activity against NALM-6 cell line. An inferior cytotoxic activity has been observed towards REH cell line and primary B-ALL blasts which become more evident prolonging the co-incubation period. However, our INVsh.CAR was not able to satisfactory trigger cytokine production and proliferation towards REH and primary cells. Indeed, we noted that the target antigen density showed by REH and primary cells was likely not sufficient to activate these later effector functions,

according to our recent unpublished observations. To address the problem of CD19-negative relapse we propose to improve CAR therapy targeting multiple antigens. We found that a simultaneous treatment with both CD19.CAR and INVsh.CAR lead to a superior cytotoxic effect compared to each single effector subset. The same effect has been observed towards CD19-negative B-ALL blasts.

Altogether our data confirm the feasibility to develop a CAR strategy against BAFF-R. In our setting the inversion of the variable regions within the scFv and the removal of the spacer moiety resulted in a winning strategy in order to obtain the best antigen recognition. Finally, targeting more antigens at the same time resulted in a more efficacious strategy to obtain the complete leukemia eradication and to avoid escape mechanisms such as antigen downregulation.

The modest activity exerted by INVsh.CAR may be overcome in future by CAR platform optimization. Altogether these data establish a starting point in developing an effective CAR strategy for the targeting of BAFF-R on B-ALL blasts. In order to improve our platform we would be interested in screening other moAb clones to find the one that will show optimal antitumor activity once translated into CAR format. Once obtained a completely *in vitro* functional anti-BAFFR CAR it will be fundamental to test it in an *in vivo* mouse model. We will also evaluate the possibility of developing a TanCAR strategy connecting CD19 and BAFF-R scFv regions. Indeed, it has been demonstrated that this approach showed more potent antitumor activity than single CAR expressing T cells or pooled CART [8,41].

1. Paul, S., Kantarjian, H. & Jabbour, E. J. Adult Acute Lymphoblastic Leukemia. *Mayo Clin Proc* **91,** 1645–1666 (2016).
2. Luo, Y. *et al.* First-in-Man CD123-Specific Chimeric Antigen Receptor-Modified T Cells for the Treatment of Refractory Acute Myeloid Leukemia. *Blood* **126,** 3778 (2015).
3. Ali, S. A. *et al.* T cells expressing an anti-B-cell maturation antigen chimeric antigen receptor cause remissions of multiple myeloma. *Blood* **128,** 1688–1700 (2016).
4. Louis, C. U. *et al.* Antitumor activity and long-term fate of chimeric antigen receptor – positive T cells in patients with neuroblastoma. *Mol. Ther. J. Am. Soc. Gene Ther.* **14,** 1324–1334 (2011).
5. Ruella, M. & Gill, S. How to train your T cell: genetically engineered chimeric antigen receptor T cells versus bispecific T-cell engagers to target CD19 in B acute lymphoblastic leukemia. *Expert Opin. Biol. Ther.* **15,** 761–766 (2015).
6. Bassan, R. Toward victory in adult ALL: Blinatumomab joins in. *Blood* **120,** 5094–5095 (2012).
7. Maude, S. L. *et al.* Chimeric Antigen Receptor T Cells for Sustained Remissions in Leukemia. *N. Engl. J. Med.* **371,** 1507–1517 (2014).
8. Ruella, M. *et al.* Dual CD19 and CD123 targeting prevents antigen-loss relapses after CD19-directed immunotherapies. *J. Clin. Invest.* **126,** 3814–3826 (2016).
9. Weiland, J. *et al.* BCP-ALL blasts are not dependent on CD19 expression for leukaemic maintenance. *Leukemia* **30,** 1920–

1923 (2016).

10. le Viseur, C. *et al.* In Childhood Acute Lymphoblastic Leukemia, Blasts at Different Stages of Immunophenotypic Maturation Have Stem Cell Properties. *Cancer Cell* **14,** 47–58 (2008).
11. Day, E. S. *et al.* Selectivity of BAFF/BLyS and APRIL for binding to the TNF family receptors BAFFR/BR3 and BCMA. *Biochemistry* **44,** 1919–1931 (2005).
12. Mihalcik, S. a, Huddleston, P. M., Wu, X. & Jelinek, D. F. The structure of the TNFRSF13C promoter enables differential expression of BAFF-R during B cell ontogeny and terminal differentiation. *J. Immunol.* **185,** 1045–54 (2010).
13. Gross, J. A. *et al.* TACI-Ig neutralizes molecules critical for B cell development and autoimmune disease: Impaired B cell maturation in mice lacking BLyS. *Immunity* **15,** 289–302 (2001).
14. Thompson, J. S. *et al.* BAFF-R, a newly identified TNF receptor that specifically interacts with BAFF. *Science (80-.).* **293,** 2108–2111 (2001).
15. Parameswaran, R., Muschen, M., Kim, Y. M., Groffen, J. & Heisterkamp, N. A functional receptor for B-cell-activating factor is expressed on human acute lymphoblastic leukemias. *Cancer Res.* **70,** 4346–4356 (2010).
16. Rodig, S. J., Shahsafaei, A., Li, B., Mackay, C. R. & Dorfman, D. M. BAFF-R, the major B cell-activating factor receptor, is expressed on most mature B cells and B-cell lymphoproliferative disorders. *Hum. Pathol.* **36,** 1113–1119 (2005).

17. Maia, S. *et al.* Aberrant expression of functional baff-system receptors by malignant b-cell precursors impacts leukemia cell survival. *PLoS One* **6,** (2011).

18. Parameswaran, R. *et al.* Effector-Mediated Eradication of Precursor B Acute Lymphoblastic Leukemia with a Novel Fc-Engineered Monoclonal Antibody Targeting the BAFF-R. *Mol. Cancer Ther.* **13,** 1567–77 (2014).

19. Parameswaran, R. *et al.* Treatment of acute lymphoblastic leukemia with an rGel/BLyS fusion toxin. *Leukemia* **26,** 1786–96 (2012).

20. Magnani, C. F. *et al.* Immunotherapy of acute leukemia by chimeric antigen receptor-modified lymphocytes using an improved Sleeping Beauty transposon platform. *Oncotarget* **5,** (2016).

21. Guest, R. D. *et al.* The role of extracellular spacer regions in the optimal design of chimeric immune receptors: evaluation of four different scFvs and antigens. *J Immunother* **28,** 203–211 (2005).

22. Sotillo, E. *et al.* Convergence of acquired mutations and alternative splicing of CD19 enables resistance to CART-19 immunotherapy. *Cancer Discov.* **5,** 1282–1295 (2015).

23. Braig, F. *et al.* Resistance to anti-CD19/CD3 BiTE in acute lymphoblastic leukemia may be mediated by disrupted CD19 membrane trafficking. *Blood* (2016). doi:10.1182/blood-2016-05-718395

24. Gardner, R. *et al.* Acquisition of a CD19-negative myeloid

phenotype allows immune escape of MLL-rearranged B-ALL from CD19 CAR-T-cell therapy. *Blood* **127,** 2406–2410 (2016).

25. Rayes, A., Mcmasters, R. L. & O'Brien, M. M. Lineage Switch in MLL-Rearranged Infant Leukemia Following CD19-Directed Therapy. *Pediatr. Blood Cancer* **63,** 1113–1115 (2016).
26. Jacoby, E. *et al.* CD19 CAR immune pressure induces B-precursor acute lymphoblastic leukaemia lineage switch exposing inherent leukaemic plasticity. *Nat. Commun.* **7,** 12320 (2016).
27. Qin, H. *et al.* Eradication of B-ALL using chimeric antigen receptor-expressing T cells targeting the TSLPR oncoprotein. *Blood* **126,** 629–639 (2015).
28. Zhang, W. *et al.* Treatment of CD20-directed Chimeric Antigen Receptor-modified T cells in patients with relapsed or refractory B-cell non-Hodgkin lymphoma: an early phase IIa trial report. *Signal Transduct. Target. Ther.* **1,** 1–9 (2016).
29. Haso, W. *et al.* Anti-CD22-chimeric antigen receptors targeting B-cell precursor acute lymphoblastic leukemia. *Blood* **121,** 1165–1171 (2013).
30. Bühler, P. *et al.* Influence of structural variations on biological activity of anti-PSMA scFv and immunotoxins targeting prostate cancer. *Anticancer Res.* **30,** 3373–3379 (2010).
31. Ye, Q. *et al.* BAFF binding to T cell-expressed BAFF-R costimulates T cell proliferation and alloresponses. *Eur. J. Immunol.* **34,** 2750–2759 (2004).
32. Sommermeyer, D. *et al.* Chimeric antigen receptor-modified T

cells derived from defined CD8+ and CD4+ subsets confer superior antitumor reactivity in vivo. *Leukemia* **30,** 492–500 (2016).

33. Anurathapan, U. *et al.* Kinetics of tumor destruction by chimeric antigen receptor-modified T cells. *Mol Ther* **22,** 623–633 (2014).
34. Chiarini, F. *et al.* Advances in understanding the acute lymphoblastic leukemia bone marrow microenvironment: From biology to therapeutic targeting. *Biochim. Biophys. Acta* **1863,** 449–463 (2015).
35. Pule, M., Finney, H. & Lawson, A. Artificial T-cell receptors. *Cytotherapy* **5,** 211–226 (2003).
36. Couzin-Frankel, J. Breakthrough of the year 2013. Cancer immunotherapy. *Science* **342,** 1432–3 (2013).
37. Morgan, R. a *et al.* Case report of a serious adverse event following the administration of T cells transduced with a chimeric antigen receptor recognizing ERBB2. *Mol. Ther.* **18,** 843–851 (2010).
38. Brentjens, R. J. *et al.* Safety and persistence of adoptively transferred autologous CD19-targeted T cells in patients with relapsed or chemotherapy refractory B-cell leukemias. *Blood* **118,** 4817–4828 (2011).
39. Davila, M. L., Kloss, C. C., Gunset, G. & Sadelain, M. CD19 CAR-Targeted T Cells Induce Long-Term Remission and B Cell Aplasia in an Immunocompetent Mouse Model of B Cell Acute Lymphoblastic Leukemia. *PLoS One* **8,** 1–14 (2013).

40. Tussiwand, R., Rauch, M., Flück, L. A. & Rolink, A. G. BAFF-R expression correlates with positive selection of immature B cells. *Eur. J. Immunol.* **42,** 206–216 (2012).

41. Grada, Z. *et al.* TanCAR: A Novel Bispecific Chimeric Antigen Receptor for Cancer Immunotherapy. *Mol. Ther. Nucleic Acids* **2,** e105 (2013).